

Analytische Chemie

**CHARACTERIZATION OF HIGH MOLECULAR WEIGHT
SULFUR AROMATIC COMPOUNDS IN VACUUM RESIDUES**

Inaugural-Dissertation
zur Erlangung des Doktorgrades
der Naturwissenschaften im Fachbereich Chemie und Pharmazie
der Mathematisch-Naturwissenschaftlichen Fakultät
der Westfälischen Wilhelms-Universität Münster

vorgelegt von
HENDRIK MÜLLER
aus Freiburg im Breisgau

-2004-

Dekan:

Prof. Dr. J. Leker

Erster Gutachter:

Prof. Dr. J. T. Andersson

Zweiter Gutachter:

Prof. Dr. U. Karst

Tag der mündlichen Prüfungen:

.....

Tag der Promotion:

.....

Meinen Eltern

Vielen Dank!

Ich möchte mich bedanken bei

Prof. Dr. Jan T. Andersson für die interessante Themenstellung, die Unterstützung die er mir bei der Bearbeitung des Themas gab, sowie für sein großes Interesse an dieser Arbeit und die stete Diskussionsbereitschaft,

Dr. Wolfgang Schrader vom Max Planck Institut in Mülheim sei gedankt für die Messungen am FT-ICR-MS, ohne die diese Arbeit nicht in dieser Form möglich gewesen wäre und für viele hilfreiche Gespräche über Massenspektrometrie im Allgemeinen und häufig auch im Besonderen,

Dr. Stephane Kressmann and Dr. François Xavier vom Institut Français du Pétrole für die Preparation und Überlassung der Aromatenfraktionen der Vakuumrückstandsproben sowie für die Daten von Elementaranalysen und ^{13}C NMR Spektroskopie,

Herman Rabeneck danke ich für die Aufnahme der MALDI-TOF-MS Spektren,

Carsten Engelhard und Karin Weißenhorn sei gedankt für die Hilfe bei der Sulfatbestimmung,

Susanne Angelow und Thomas Schade für das Korrekturlesen dieser Arbeit,

allen Laborkollegen: Thomas Schade, Benedikte Roberz, Frank Wasinski, Kishore Sripada, Saroj Panda, Nina Kolbe, Markus Penassa, Ansgar Japes, Claudia Sill, Dr. Abdelrahman Hegazi und Sebastian Kortz möchte ich für die gute Zusammenarbeit und die schöne Zeit im Labor danken. Besonders danken möchte ich Thomas Schade für sein bereitwilliges Überlassen der Pd(II)-Säulen, seinen Teil zur Synthese von Oskar und für viele hilfreiche Diskussionen,

allen Analytikern der zweiten Etage für das freundliche Arbeitsklima.

Meinen Freunden Thomas und Diana, Felix und Anja und allen vom Chiisai Mori danke ich für die Möglichkeit, auch außerhalb des Labors eine wunderbare Zeit zu verbringen und „mal den Kopf frei zu kriegen“,

meinen Eltern, die mich jederzeit in allem unterstützt haben,

und ganz besonders bei meiner lieben Freundin Susanne.

<u>I</u>	<u>Fossil Fuels & Sulfur</u>	<u>1</u>
1	Crude Oil Composition	1
1.1	Sulfur Compounds in Heavy Oil Fractions	4
1.2	Legislation on Sulfur Limits and Economic Consequence	4
2	Refining Process	6
3	Desulfurization	10
<u>II</u>	<u>Analysis of High-Molecular-Weight Fossil Fuel Fractions</u>	<u>16</u>
1	Liquid Chromatography	16
1.1	Group Separation into Saturates, Aromatics, Resins and Asphaltenes (SARA)	17
1.2	High Performance Liquid Chromatography (HPLC)	17
1.2.1	Gel Permeation Chromatography (GPC)	17
1.2.2	Charge Transfer Stationary Phases	17
1.2.3	Reversed Phase Separations	18
2	Bulk Analytical Methods	18
2.1	Chemical Approaches of Degradation and Derivatization	18
2.1.1	Chemical (Degradation) Reactions	18
2.1.2	Pyrolysis	19
2.2	Spectroscopic Techniques	20
3	Mass Spectrometry (MS)	20
3.1	High Resolution Mass Spectrometry of Vacuum Residues and Related Samples	21
<u>III</u>	<u>Objectives</u>	<u>23</u>
<u>IV</u>	<u>Vacuum Residue Sample Investigated in This Work</u>	<u>25</u>
1	Average Composition of the Vacuum Residues	25
2	Synthesis of an Highly Alkylated PASH	28
<u>V</u>	<u>Liquid Chromatography of Vacuum Residues</u>	<u>30</u>

1	Detection of Polycyclic Aromatic Compounds (PACs)	31
1.1	UV– Vis Spectroscopic Detection of Polycyclic Aromatic Compounds with Diode Array Detector	31
1.2	UV Spectroscopy of the Aromatics Contained in Feed and Effluent Vacuum Residue Fractions	34
1.3	Matrix Assisted Laser Desorption Ionization Time of Flight Mass Spectrometry (MALDI-TOF-MS) as Off Line Mass Selective Detector	35
2	Charge Transfer Chromatography	35
2.1	Influence of Alkyl Substituents and Hetero Atoms on Retention Order	36
2.2	Charge Transfer Chromatography of the Vacuum Residue Sample	36
2.2.1	DNAP as Stationary Phase	37
2.2.2	TCPP-Silica Used as Stationary Phase	41
3	Reversed Phase Partition Chromatography	43
4	Ligand Exchange Chromatography	44
5	Gel Permeation Chromatography	46
5.1	Influence of the Mobile Phase Composition	46
5.2	Influence of Temperature	47
5.3	Chromatographic Workflow	48
5.4	GPC of the Vacuum Residue Sample to Produce Fractions with Narrow Mass Distribution	50
5.4.1	GPC with Strongly Solvating Solvent	51
5.4.2	GPC with a Weakly Solvating Solvent	53
5.4.3	Combination of GPC With “Weakly” and “Strongly” Solvating Solvent	54
6	Summary of Liquid Chromatography Applied on High Molecular Weight Aromatics	55
VI	Mass Spectrometry of Vacuum Residues	57
1	Matrix Assisted Laser Desorption and Ionization (MALDI)	57
1.1	Time of Flight (TOF) Mass Analyzer	58

2	MALDI-TOF-MS of the Complete Vacuum Residues Aromatic Fraction	59
3	MALDI-TOF-MS of Chromatographically Cut Fractions	61
3.1	MALDI-TOF-MS of GPC Fractions Obtained with Weak Solvent	61
3.2	MALDI-TOF-MS of GPC Fractions Obtained with Strong Solvent	64
VII	High Resolution Mass Spectrometry	68
1	Ionization Techniques	68
1.1	Electrospray Ionization (ESI)	69
1.2	Atmospheric Pressure Chemical Ionization (APCI)	70
2	Mass Analyzer	70
2.1	Ion Cyclotron Resonance (ICR) Mass Spectrometer	72
2.1.1	Principal of Operation: ICR	72
2.1.2	Fourier Transform Ion Cyclotron Resonance (FT-ICR) Mass Spectrometer	73
3	High Accuracy Data Interpretation	75
3.1	Kendrick Mass Scale	77
3.2	Software Aided Data Analysis	78
3.2.1	First Step: Establishing Preliminary Elemental Compositions	81
3.2.2	Second Step: Tabled KMD to Assign Elemental Compositions	82
3.2.3	Third Step: Use of Homologue Series for Extended Assignments	84
4	MALDI FT-ICR-MS Analysis of the Vacuum Residue Aromatics	84
5	APCI FT-ICR-MS Analysis of the Vacuum Residue Aromatics	86
5.1	Recalibration	86
6	ESI FT-ICR-MS Analysis of the Vacuum Residue Aromatics	89
6.1	Methylation Reaction of Sulfur Compounds	90
6.1.1	Standard Molecules	91
6.1.2	Vacuum Residue Samples	91
6.2	Mass Range, Multiply Charged Ions and Clusters in the Mass Spectra	96
6.3	Vacuum Residue Analysis by Combination of FT-ICR-MS with LEC	97
6.3.1	Vacuum Residue before HDS: Feed	98

6.3.2 Vacuum Residue after HDS: “Effluent”	102
6.4 Changes in the Vacuum Residue during HDS	103
6.4.1 Selected S1 Series Obtained from Processed Data Before and After HDS	105
7 High Abundance of the $[M+1]^+$ Signals in Mass Spectra of PACs	107
8 Summary of High-Resolution Mass Spectrometry of Vacuum Residues	109
<u>VIII Summary</u>	<u>111</u>

IX Appendix **114**

1 Procedure & Parameters for Preliminary Elemental Composition Assignment by “Molecular Weight Calculator”	114
1.1 Raw Data	114
1.2 Molecular Weight Calculator	114
1.3 Decision-Scheme of Spreadsheet “MWCsort.xls”	115
2 Elemental Composition Identification Based on Tabled Kendrick Mass Defects	116
2.1 Settings and Parameters	117
2.2 Initial Identification and Assignment of Class and Type	117
2.3 Secondary Assignments to Fill Gaps of Unassigned Signals in the Mass List	118
3 Sulfur Quantification.	119
3.1 Oxidation to Sulfate by Combustion of the Sample	119
3.2 Sulfate Quantification by Inductively Coupled Plasma – Optical Emission Spectroscopy (ICP-OES)	119
4 Supporting Material: Initial Data (Provided by IFP, Vernaison, France)	119
5 Materials and Devices	120
6 Instrumental Parameters	122
7 Abbreviations	124
8 Calculated “Mass Spectra” of S1 Class Homologue Series	127

9 Code for Data Processing Makros	131
10 Spreadsheet Code “HP2000”	142

I FOSSIL FUELS & SULFUR

Fossil fuels are the world's unrivaled energy supplier, as they combine high energy density with convenient physical properties. Petroleum products are massively used as transportation fuels and coal is a common feedstock for energy in power plants and industry. This use of fossil fuels continues to grow several ecological threats at alarming rates. The consequences for the world climate of the greenhouse gas carbon dioxide is undisputed. Combustion fuels directly pollute the environment with acidic oxides (e.g. SO_x , NO_x), particulates, trace elements and unsaturated hydrocarbons. A key factor for environmental protection is the control of SO_x in exhaust gases since they cause acid rain, poison catalysts in catalytic processes, are a major contributor to particulates, and promote the formation of smog. Widespread combustion of heteroatom rich "sour" fuels directly leads to acid rain and causes damage to forests and increased weathering of building materials. Improvement of catalytic converters, e.g. in cars, directed against SO_x is limited with respect to space and costs. The major part of pollution control is therefore forced onto refineries, but cleaner fuels with a low sulfur content, down to trace levels of sulfur, still poison catalytic converters. Those converters are used in cars and elsewhere to clean the combustion exhausts from particulates, CO and NO_x . Thus sulfur, even in low levels, is indirectly responsible for higher emission of other pollutants [1].

1 Crude Oil Composition

Petroleum is possibly the world's most complex organic mixture [2], containing chemically distinct constituents over a wide range of polarity and molecular size in a mass range from below 100 up to 100,000 Da. Aliphatic and aromatic hydrocarbons constitute the largest part of most oils, followed by hetero atom containing structures with e.g. nitrogen, sulfur and oxygen (N, S, O) and in trace amounts metals (Ni, V). Crude oils can further vary greatly in composition and physical properties in a range from light liquids to heavy tar like materials.

In some crude oils aromatic compounds even represent the major part. The abundance of heteroatoms and the aromatic character usually increase with the average molecular weight of the sample, so that paraffinic and aromatic structures containing heteroatoms dominate heavier fractions. The molecular weight range of heavier fractions ranges from ~300 up to several thousand Da. The aliphatically bound heteroatoms on the other hand are readily removed in technical desulfurization processes, so that heterocycles of aromatic character dominate in heavy fractions after processing. Some examples for organic sulfur compounds (OSC) are presented in Figure I-1.

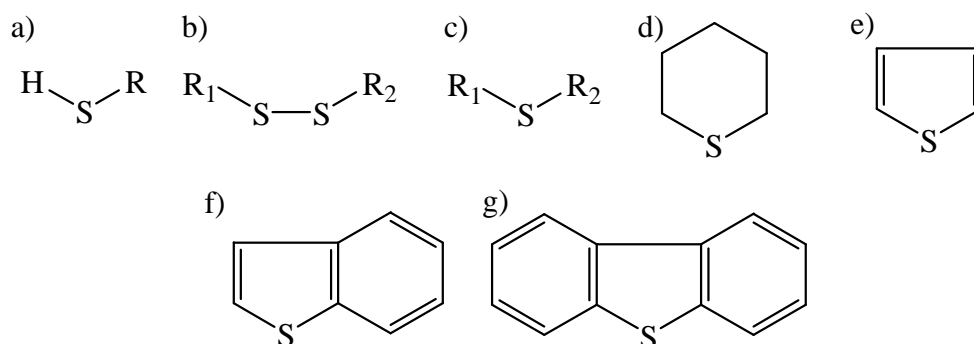


Figure I-1. Sulfur containing structural elements in petroleum crudes. From the left in ascending recalcitrance against desulfurization processes: a) thiol, b) disulfide, c) thioether, d) thiarane, e) thiophene, f) benzothiophene (BT) and g) dibenzothiophene (DBT). The latter two are polycyclic aromatic heterocycles (PASH).

Sulfur contents in crude oils range from 0.05 to 13.95 %wt [3], typical amount of sulfur for economically interesting oils vary from 0.1 to 3 %wt with contents above 1 %wt considered as sulfur rich oils.

The origin of such high amounts of sulfur in crude oils cannot be explained entirely by sulfur from biota since it is not present in such high levels in living organisms. Today the origin of sulfur is believed to lie in sulfate ions in seawater. Microorganisms like *Desulfovibrio* reduce sulfate to sulfide. This reduced sulfur (e.g. HS_x^-) can be oxidized by other microbes, e.g. *Thiobacillus*, to elemental sulfur which then undergoes anaerobic incorporation into plant or animal derived organic material [4]. Several hundred OSC have been identified in sulfur rich kerogenes and immature oils [5]. Mono- and dialkylated thiophenes, benzo- and dibenzothiophenes have been found. Strong evidence for isoprenoid thiophenes (alkylthiophenes with an isoprenoid carbon skeleton) in the

“aromatic” fraction in sulfur rich oils¹ with 15, 20, 30, and 35 carbon atoms in side chains has been found [6]. Some OSC present in lesser amounts have a structural resemblance to hydrocarbons known as geochemical markers or their biochemical precursors. Sulfur containing geochemical markers, e.g. steranes and hopanes have been identified. The sulfur incorporation process is strongly discussed and presently three pathways are considered:

Biosynthesis formation of OSC was suggested by Cyr and Payzant [7, 8]. Site selectivity in biosynthetic pathways was believed to determine the position of sulfur. However, neither any of the investigated OSC nor functionalized precursors have been reported in biota.

Reaction of elemental sulfur with hydrocarbons early in the diagenesis process has been investigated by Schmid et al. [9]. Heating of alkanes with elemental sulfur produced mixtures of 2,5-dialkylthiophenes. Cholestane with elemental sulfur yielded sulfur containing steranes, but of different isomeric composition compared to those identified in crude oils. Sinninghe Damste et al. studied the reaction of early sulfur incorporation by comparison between hydrocarbon structure obtained from OSC via desulfurization (on Raney-Ni) and the hydrocarbon structures originally present. Sulfur incorporation takes place intramolecularly as well as intermolecularly, which might explain the high amount of sulfur in high molecular weight petroleum fractions, e.g. in asphaltenes and kerogenes. This “intermolecular sulfur cross-linking mechanism” [10, 11] connects building blocks consisting of n-alkanes, saturated and monounsaturated 2-alkylthiophenes and -thiolanes as well as hopanes and steranes.

Formation during early diagenesis was considered by Brassel et al. [10]. Some examples of chiral derivatives of thiophene have been reported and accounted to incorporation of inorganic sulfur species (HS-, HS_x-,...) into chlorophyll derivatives. Sinninghe Damsté et al. suggested incorporation of sulfur in thiophene rings at an early diagenetic stage [11]. Early incorporation of sulfur in kerogen structures is also discussed by Barakat [12]. Sulfur-containing moieties present in macromolecular substances, i.e. kerogen, asphaltenes and high molecular weight fractions of crude oils have been reported to form OSC in a similar way in lighter fractions [13].

¹ Rozel Point oil field, Utah, USA and oil from Northern Apennines, Italy

The initially formed aliphatic sulfides then undergo various cyclization and aromatization reactions leading to a very complex mixture of sulfur compounds in mature oils. A common structural element of sulfur is the thiophene ring shown in Figure I-1e), but thiols a), sulfides b) and disulfides c) are also present [14]. Thiophene is frequently condensed to benzene rings or additional heteroaromatic rings. A great number of parent sulfur structures in fossil fuels, and especially those of petroleum origin are reviewed by Czogalla and Boberg. [3].

1.1 Sulfur Compounds in Heavy Oil Fractions

Thiophenes are the dominant sulfur species in fractions boiling over 250 °C. Fractions boiling higher than 540 °C (residues) contain approximately half of the sulfur of a crude oil. The sulfur was estimated to be mostly thiophenic (~80 %) and exists in polycyclic systems with aromatic and naphthenoaromatic rings. Substitutions with alkyl chains and other heteroatoms (N, O) or additional sulfur are common. Linkage to other aromatic systems has also been described.

Asphaltenes

Asphaltenes consist of polymeric polyaromatic structures, which form micelles in the oil and can clog pipelines by precipitation. Asphaltene bottom cracking (ABC) is connected to removal of vanadium and to desulfurization [15]. During the cracking process macromolecules are broken up at connecting inter-unit structures where sulfur is often located. The ABC process does not change the overall sulfur content present in feedstock materials, but redistributes this sulfur into the outgoing streams and thus is a major source of sulfur in refined streams.

1.2 Legislation on Sulfur Limits and Economic Consequence

Europe, the United States of America, and other developed countries worldwide lowered sulfur limits for transportation fuels continuously in the last 30 years and this trend is still continuing. In 1998 the European directive on transportation fuels set limits of sulfur in gasoline and diesel fuel to 150 ppm and 350 ppm, respectively. For 2005 the limit will be reduced to 50 ppm for all transportation fuels. In 2003 German legislation went even further by rising taxes on transportation fuels by 1.53 cents per liter for gasolines exceeding 10 ppm sulfur.

Similar trends are observed in the USA, where legislation limited diesel fuels to 50 ppm S by the Clean Air Act in 1994 and in 2000 the Environmental Protection Agency (EPA) proposed sulfur limits of 15 ppm for 2006. Japan decided in 1993 on 200 ppm and in 1997 on 50 ppm S [1, 16], respectively.

For these reasons, during the past decade refining efforts focused on “deep refining” to very low sulfur levels in middle distillates, which mainly serve as transportation fuels. Improvement of desulfurization processes, but also the inexpensive availability of low sulfur crude feedstocks helped meeting those standards. This situation may change in future as low sulfur crudes are eventually limited and restrictions on transportation fuels become stricter. Gas oils and heavier fractions which are converted into lighter fractions pose their own problems as present means of desulfurization cannot reach the required low sulfur levels at economically viable conditions and maintain product quality [16].

Crude oil production is expected to continue to become more dependent on heavy oils with higher sulfur contents while environmental restrictions continue to significantly reduce the demand for high-sulfur residual fuel oil. Although light “sweet” crudes will be available, there will be an even greater demand than there is today. To reduce the production of high-sulfur residual fuel oil and to increase the production of low-sulfur distillate transportation fuels refineries will be faced with the choice of purchasing light sweet crudes at elevated price, or increasing heavy residue upgrading capacity. There are several pressures that are expected to push refineries towards increased upgrading. These include [16]:

- Increasing low-sulfur distillate fuel demand, which will require increased refining capacity.
- Heavier crudes feedstocks, which will result in a greater high-sulfur residual fuel oil production, if conversion is not added.
- Environmental restrictions, which will result in reduced demand for high-sulfur residual fuel oil.
- A major unknown factor in this equation is the effect of legislation directed at "greenhouse gases" such as CO₂.

The economics of residue upgrading are driven by the difference in price between transportation fuels and high-sulfur residual fuel oil. This differential between residual fuel oil as refining output and transportation fuels in Rotterdam and New York (NY) Harbor has averaged about \$6/BBL in Rotterdam and \$7/BBL in NY Harbor, respectively, over the last 5 years ². Natural gas has an impact on this differential, but in general residual fuel oil containing 1 wt% sulfur can be expected to remain in this range. Table I-A shows the recent average differential prices in NY Harbor for some sulfur levels compared to 1 wt% sulfur residual fuel oil

Table I-A. Residual fuel oil price differential for various sulfur levels.

% wt Sulfur	Price Differential, \$/BBL
0.3	+3.16
0.7	+0.34
1	Base
3.0	-1.79

A continuing tightening on sulfur limits of residual fuel oils is expected and the requirement for 0.5 %wt or even 0.3 %wt will become more prevalent. As the margin for refineries fades the extended desulfurization will be intensified.

2 Refining Process

Crude petroleum cannot be used directly; all raw material is treated in refineries. The refining process is essentially a separation by distillation, followed by complex process

² as reported by the Oil & Gas Journal "Statistics"

patterns including hydrodesulfurization (HDS), fluid catalytic conversion (FCC), and blending. A flow diagram of a schematic refining process is given in Figure I-2.

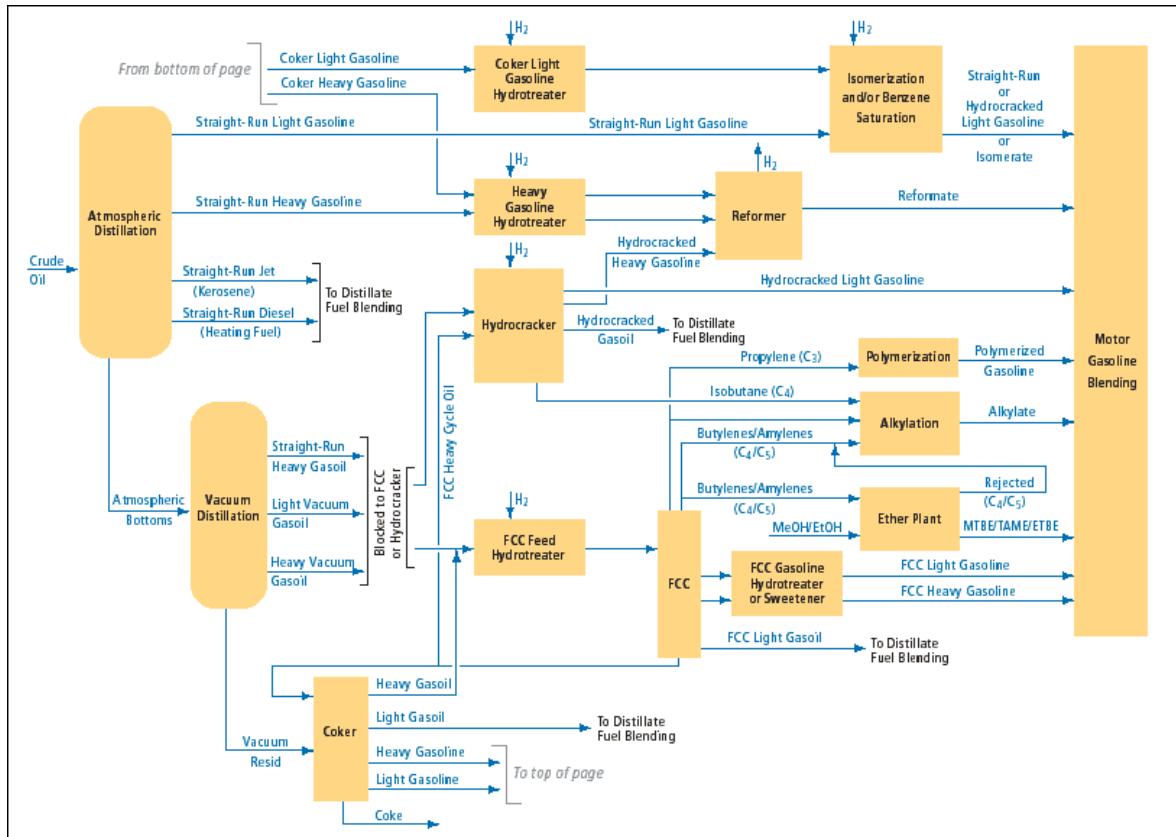


Figure I-2. Scheme of refining process.

The amount of distillation residue material ranges from 14 up to ~55 %wt of the crude oil feedstock [16, 17]. This residue is further fractionated under reduced pressure. In this way heavy and vacuum gas oils are obtained. Vacuum distillation residues, in contrast to most lighter fractions, cannot be economically used after distillation, but are rather converted into lighter fractions. This process is shown at the bottom of Figure I-2 as “coker” unit. Refineries primarily apply three strategies:

- residue catalytic cracking
- residue hydroprocessing
- delayed coking

Typical characteristics for refining products are provided in Table I-B.

Table I-B. Boiling ranges for classification of refinery products³. Typical maximal and minimal values are listed in column 3 and 4.

	Boiling range	Average			C-range
		[%v]	High [%v]	Low [%v]	
Sulfur, %wt		1.1	4.3	0.1	
Light Ends		3.27	6.75	0.5	C ₂ -C ₅
Light Naphtha	< 65 °C	5.5	9.0	1.5	C ₆ -C ₁₀
Medium Naphtha	65-105 °C	7.0	11.8	3.6	
Heavy Naphtha	105-175 °C	13.3	18.2	8.5	
Kerosene	175-330 °C	17.1	28.7	11.5	C ₁₀ -C ₁₂
Light Gas Oil	260-330 °C	12.7	18.2	8.9	C ₁₂ -C ₂₀
Vacuum Gas Oil	330-550 °C	29.2	37.6	19.2	C ₂₀ -C ₄₀
Residual Oil	> 550 °C	13.8	37	1.4	>C ₄₀

Residue hydrotreating is a well-established method for reducing high-sulfur residual fuel oil yields. This technology was originally developed to reduce the sulfur content of atmospheric residues to produce low sulfur residual fuel oil.

Residue fluidized catalytic cracking (RFCC) is another approach for converting a significant portion of the heavier fractions into gasoline blending components. In addition to high gasoline yields, the RFCC unit also produces gaseous, distillate and fuel oil-range products. The RFCC unit's product quality, however, is directly affected by its feedstock quality. In particular, unlike hydrotreating, RFCC redistributes sulfur, but does not remove it from the products [18]. Consequently, tightening product specifications have forced refiners to hydrotreat some, or all, of the products obtained by RFCC.

Coking has been selected by many refiners as their preferred choice for heavy fraction upgrading, because of the process' inherent flexibility to handle even the heaviest residues. The process provides essentially complete rejection of metals and coke while providing partial or complete conversion to naphtha and diesel. Most recent cokers have been designed to minimize coke and produce a heavy coker gas oil that is then catalytically

³Environmental Protection Agency (EPA), USA, <http://www.epa.gov/earth1r6/6en/xp/lppapp6a.pdf>. Accessed June 27th, 2004

upgraded to lighter products of higher value. The conversion is accomplished by heating the feed material to a high temperature of about 550 °C at controllable residence time for the reactions to take place.

Changes in crude oil quality and product demand have changed this technology to include pretreating of conversion feedstocks to minimize catalyst replacement and coker feedstocks and to increase the quality and reduce the yield of the by-product coke fraction.

Unfortunately, the FCC catalysts used to cleave the heavy fractions (hydrocracking) can be poisoned by heteroatoms, especially nitrogen and sulfur, and the abundance of those elements increases with increasing molecular weight. Characteristic values for atmospheric residue fractions for two exemplary crude oil atmospheric residues are given in Table I-C [19]. Fractions 10 to 12 belong to the class of asphaltenes and have been obtained by precipitation from the solvent given in the table.

Table I-C. Characteristic data for average molecular weight, degree of saturation, and heteroatom content of the atmospheric residues (>350 °C) of two exemplary crude oils⁴.

Kern River					Av. no. atoms/molecule		
Fraction	50% AEBP ^a °C	%wt ^b	Av. mol. weight ^c	Hydrogen deficiency "Z"	S	N	O
1	369	21.6	337	-8.9	0.104	0.075	0.088
2	426	32.8	420	-12.0	0.134	0.156	0.118
3	461	42.8	471	-14.7	0.163	0.215	0.177
4	499	51.4	527	-16.9	0.196	0.293	0.198
5	536	58.3	594	-19.7	0.249	0.378	0.264
6	574	64.3	682	-23.6	0.296	0.492	0.349
7	611	68.9	755	-27.0	0.316	0.615	0.235
8	656	74.3	876	-31.5	0.356	0.745	0.515
9	726	90.3	1464	-57.9	0.608	1.464	0.873
10	pentane ^c	96.1	3064	-170.5	1.388	4.815	2.298
11	cyclohexane	99.1	5625	-334.6	2.514	9.643	4.641
12	toluene	99.6					

⁴ Source: M. M. Boduszynski, Energy & Fuels, (1988) **2**(5), 597-613.

Offshore California

Fraction	50% AEBP ^a °C	%wt ^b	Av. mol. weight ^c	Hydrogen deficiency "Z"	S	N	O
1	355	18.9	329	-7.6	0.282	0.056	0.062
2	415	30.4	399	-10.1	0.353	0.108	0.09
3	461	38.4	469	-11.7	0.462	0.141	0.117
4	499	45.4	549	-13.8	0.624	0.188	0.137
5	538	49.4	609	-16.8	0.807	0.239	0.164
6	579	54.2	704	-21.3	0.99	0.332	0.189
7	609	57.0	785	-25.6	1.185	0.387	0.235
8	659	62.7	955	-30.8	1.611	0.532	0.31
9	730	78.4	2254	-79.3	4.12	1.481	0.873
10	pentane ^c	87.9	5697	-278.2	11.358	7.121	2.991
11	cyclohexane	98.6	16348	-908.9	34.739	23.938	12.261
12	toluene	99.7					

a) Atmospheric equivalent boiling point (AEBP). b) Cumulated %wt starting from atmospheric residue. c) Determined by vapor pressure osmosis (VPO) in toluene. c) Matter insoluble in pentane, cyclohexane, or toluene.

The heaviest matter boiling at an equivalent of above 650 °C contains the highest content of heteroatoms; on the average each molecule in the vacuum residues contains one or more sulfur, nitrogen and oxygen atoms. This high average sulfur content is also true for the coking products, which largely contribute to sulfur in blended product streams. Refineries therefore must apply hydrotreating steps for desulfurization. Those are placed after coking, as depicted in Figure I-2.

3 Desulfurization

The goal of hydrodesulfurization (HDS) is the removal of sulfur without affecting non-sulfur compounds, e.g. in terms of saturation. Although HDS is considered to be one of the most mature technologies in the petroleum refining industry, on-going studies examine the HDS process to keep track with increasingly stricter fuel specifications. As can be seen in Figure I-2, p. 7 all refinery streams are hydrotreated at least once. Frequently used catalysts are bimetal systems of CoMo/Al₂O₃ or NiMo/Al₂O₃ at moderate temperatures (340-360

°C) and hydrogen pressures of 3.0-5.0 MPa [1]. In light boiling diesel fuels only few organic sulfur compounds remain after deep desulfurization, mainly of the type 4-alkyl- and 4,6-dialkydibenzothiophenes.

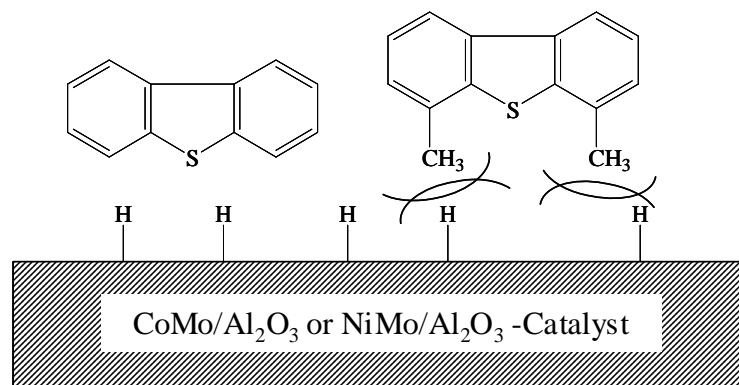



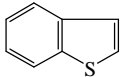
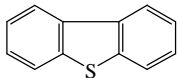
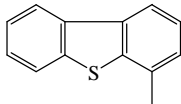
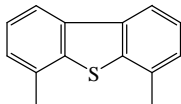
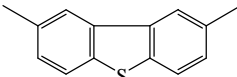
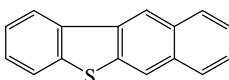
Figure I-3. Desulfurization scheme of dibenzothiophene (DBT) and 4,6-dimethyldibenzothiophene on catalyst site. Steric hindrance for 4- or 4,6-alkylated dibenzothiophene hampers bonding of the sulfur atom to a free catalyst site.

The same is true for atmospheric gas oils [20] where a relatively low number of persistent species was found after conventional hydrotreating which could be identified as polycyclic aromatic sulfur heterocycles [21]. Dibenzothiophene and derivatives containing alkyl substitution in adjacent positions to the sulfur were the only major sulfur structures found [20-23]. Reactivity of PASH could be classified into four groups according to HDS. Investigated were typical HDS conditions, e.g. CoMo and NiMo as catalysts on carbon or Al_2O_3 at 360 °C and ~3 MPa hydrogen pressure, the reactivity decreases as follows:

- (1) AlkylBTs lacking substituents in 2- and 7-positions.
- (2) 2,7-Substituted BTs, DBTs and alkylDBTs lacking substituents in 4- and 6-positions.
- (3) AlkylDBTs containing only one substituent in 4- or 6-positions.
- (4) AlkylDBT containing two of the alkyl substituents in the 4- and 6-positions.

Parameters for the desulfurization of model compounds were representative for refining operations as alkyldibenzothiophenes listed under (4) were the only sulfur

Table I-D. HDS reactivity of thiophene derivatives⁵.

Structure	Relative constants ^d	rate
		2250 ^a
		1330 ^a
		100 ^{a, b, c}
		9 ^b or 38 ^c
		6.7 ^b or 11 ^c
		91 ^b
		260 ^a

Relative reaction rate constants for a) CoMo/Al₂O₃, 300 °C, 7-10 MPa, b) CoMo/Al₂O₃, 300, 10.2 MPa, c) NiMo/Al₂O₃, 320 °C, 2.5 MPa. d) Relative to DBT = 100.

moieties observed in deeply desulfurized fuels. Sterically constrained access of the sulfur atom is therefore the main reason to reduced reactivity [21], substitution in any position other than adjacent to the sulfur atom is of minor influence [20, 23]. Thus structures with terminal thiophene rings showed similar behavior as benzothiophene. Standardized reaction rates for the problematic PASH are given in Table I-D. Although values originate from different authors and have been obtained with different catalyst systems, data are in agreement with the reaction order described above. Thiophene derivatives with more than three condensed aromatic rings are more readily desulfurized than dibenzothiophene [20].

Two major pathways have been described for desulfurization of PASH on bimetal catalysts. The direct desulfurization (DDS) pathway competes with the hydrogenation of one adjacent

benzene ring followed by eased reduction of the sulfur atom (HYD). Both pathways are shown in Figure I-4 a) and b) for two common bimetal catalyst systems. The second path (HYD) consumes four times more hydrogen than direct reductive removal of the sulfur atom. The hydrogenation route facilitates the higher reactivity of benzonaphthothiophenes

⁵ Source: D. D. Whitehurst, T. Isoda, and I. Mochinda, Adv. Catal., (1998) **42**, 345-471.

compared to dibenzothiophene since the higher electron density in the larger systems facilitates reduction of an aromatic ring [23, 24].

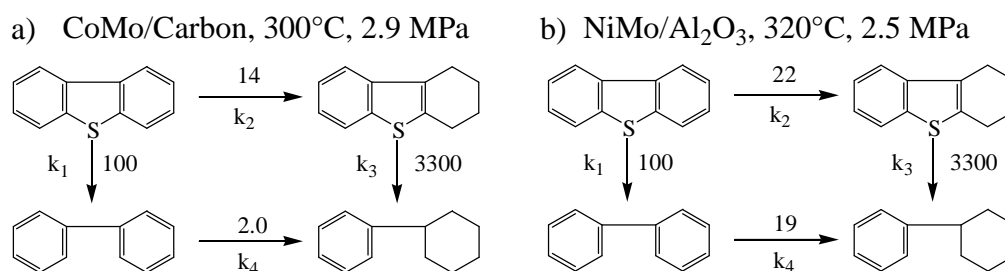


Figure I-4. Major reaction pathways of desulfurization. a) Reaction rates on CoMo/carbon; the left side arrow (k₁) shows the direct pathway (DDS), upper (k₂) and right (k₃) arrows show hydrogenation of an adjacent benzene ring followed by desulfurization (HYD). b) Shows the reaction rates for dibenzothiophene on NiMo/Al₂O₃⁷.

In case of low sulfur feedstocks these bimetal catalysts work well for the desulfurization of lighter fractions down to 0.05 %wt of sulfur [1]. Lower concentrations like the 10 ppm demanded by German legislation, which means technically sulfur free fuel, can be achieved by lowering the distillation cutoff for fuel fractions. Otherwise such sulfur levels are hardly achieved by conventional HDS even for diesel fractions while maintaining other fuel specifications like boiling range, oxygen content, vapor pressure, and overall aromatic content [16]. This cutoff additionally adds to a higher amount of heavier -less valuable- products. Hydrotreating process conditions typical for various refinery streams are shown in Table I-E.

Resistance to hydrodesulfurization increases with molecular weight [1, 19, 23, 25], more drastic conditions are necessary as the target fraction boiling ranges increase. Higher temperature and hydrogen pressure, though necessary, lead to side reactions, e.g. hydrogenation, cracking reactions, and also formation of larger condensed aromatic structures have been reported [19]. Under too severe conditions, like temperatures above ~400 °C, product quality declines and consumption of hydrogen rises tremendously due to conversion of all matter in the sample. The resulting decrease in cetane⁶ number, formation of fluorescence dyes and other side products limit the brute application of temperature and

⁶ Cetane number: Flammability of fuels in comparison to a mixture of n-hexadecane (value = 100; highly flammable) and 1-methylnaphthalin (value = 0; less flammable).

hydrogen pressure for high boiling fractions. Recent studies showed that the complex molecules present in heavy feed adversely affect removal of heteroatoms [25].

Table I-E. Typical hydrotreating process conditions for various boiling range fractions ⁷.

Feed	Process	Temperature [°C]	H ₂ Pressure [MPa]	H ₂ Consumption [Nm ³ /m ³]
Naphtha	HDT	320	1-2	2-10
Kerosine	HDT	330	2-3	5-10
Atm. Gas Oil	HDT	340	2.5-4	20-40
Vac. Gas Oil	HDT	360	5-9	50-80
Atm. Residue	HDS	370-410	8-13	100-175
Vac. Gas Oil	HDC	380-410	9-14	150-300
Vac. Residue	HDC	400-440	10-15	150-300

Those side reactions results in a cost of raised hydrogen consumption as can be seen in the fifth column in Table I-E. The improvement of desulfurization of heavy fractions therefore must concentrate on the catalysts involved, but directed development for residue processing is not possible due to lack of information on recalcitrant sulfur species. Development of catalysts takes place on a more or less empirical base, hence much of the sulfur remains in the residues even after costly hydrogen and energy is spent. Furthermore refineries are forced by ongoing increase in demand and overconsumption of better feedstocks to exploit more and more oils of lower quality [1, 16]. For economical processing, structural knowledge of critical compounds, such as the persisting sulfur structures, is highly desirable.

The final determination of the offending sulfur species in heavier fractions starting with atmospheric gas oils was believed to be impossible with present analytical procedures (1998 Whitehurst) [1]. General features of naphtha and gas oils and the relative reactivity in the conventional hydrodesulfurization process have been studied. The aliphatic and monoaromatic fractions after HDS were found to be almost free of sulfur, which was

⁷ Source: D. D. Whitehurst, T. Isoda, and I. Mochida, *Adv. Catal.*, (1998) **42**, 345-471.

present almost exclusively in multiring aromatic structures. Benzothiophenes and dibenzothiophenes with up to 16 carbon atoms in alkyl chains have been reported to account for the largest part of the sulfur in atmospheric gas oils. Higher condensed PASH with four rings have been described in gas oil samples [23], but seem to be more readily desulfurized than dibenzothiophenes [24].

Summary

The catalytic conversion of heavy fractions is often hampered by heteroatoms present in the feedstock, especially nitrogen and sulfur. Necessary desulfurization is difficult and not always possible due to recalcitrance of some sulfur species. Analysis of lighter petroleum fractions revealed PASH, especially those with alkyl substitution that sterically shields the sulfur in the molecule, to be the major sulfur contributors. For heaviest fractions, less structural knowledge of the recalcitrant species is available. Consequently, for rational development of efficient desulfurization procedures and new catalysts, structural knowledge of the relevant sulfur species is needed.

II ANALYSIS OF HIGH-MOLECULAR-WEIGHT FOSSIL FUEL FRACTIONS

Fossil fuels are a major source of environmental pollution and therefore in the focus of numerous studies of pollution control. Ecologically driven legal limitations of sulfur and other pollution precursors naturally bring about the analysis of sulfur in those materials. Due to the enormous importance of this topic a great number of methods and techniques for sulfur analysis are presented in literature. Numerous authors investigated sulfur in fossil fuel materials (oils, shale oils, tar sands, or coal) and various kinds of products and intermediates of the refining process. Analytical techniques have also been applied for heavy petroleum fractions as presented in detail in this chapter. Many studies combine various analytical methods, those studies are reported according to the most significant method. Since heavier refinery streams are not directly used, the analysis of sulfur is not directly driven by limiting legislation. Process demands and the high sulfur contribution to blended fuels propelled the interest in this field in the past. A major obstacle to heavy fraction analysis is the difficulty of the task, as the complexity in composition and the number of possible isomers increase tremendously with rising average molecular weight. Due to their non-volatile nature heavier fractions additionally defy common powerful analytical techniques like gas chromatography or some ionization techniques for mass spectrometry.

1 Liquid Chromatography

Spectroscopic, chemical and pyrolytic methods described below yield only bulk parameters and cannot give information on single structures or narrowly defined classes. To gather such information, separation into chemical classes by all kinds of methods is therefore undertaken in the literature [26, 27]. A detailed description of liquid chromatography (LC) applied in this thesis for the separation of vacuum residue samples is given in the chapter “Liquid Chromatography of Vacuum Residues” (p. 30). The most important separation techniques and most widely spread chromatographic systems applied for petroleum samples in the literature shall now be summarized.

1.1 Group Separation into Saturates, Aromatics, Resins and Asphaltenes (SARA)

The initial and most common step in petroleum analysis of distilled fractions is the group separation into saturated and aromatic compounds, resins and asphaltenes. Resins are polar components usually of high molecular weight, and asphaltenes are a solubility class of highest molecular weight matter insoluble in saturated alkanes. For SARA first the asphaltenes are removed by precipitation, then column chromatography on silica or alumina separates saturates, aromatics and resins by stepwise elution with solvent of increasing polarity [28, 29].

1.2 High Performance Liquid Chromatography (HPLC)

For better separation characteristics high performance liquid chromatography (HPLC), (see also Chapter V, p. 30) is used rather than simple LC instrumentation. The main effort after SARA separation is the isolation of chemically and procedurally well defined compound classes. Especially the separation of the “aromatic” class according to number of fused aromatic rings is of great aid for further analysis, e.g. mass spectrometry. Three classes of stationary phases have been frequently applied for chromatographic analysis of polycyclic aromatic compounds (PAC).

1.2.1 Gel Permeation Chromatography (GPC)

Molecular weight distribution of several vacuum residues by gel permeation chromatography (GPC) in combination with matrix assisted laser desorption and ionization (MALDI) mass spectrometry (MS) [30-33] or laser desorption ionization (LDI) MS [34] has been the subject of investigations in some depth. The retention of heavy materials in GPC was sought to be predicted by comparison with their mobility in thin layer chromatography [35-37]. Herod stresses the use of 1-methyl-2-pyrrolidone as mobile phase [38], but all efforts focused on the whole residues or the insoluble asphaltenes and not specifically on the aromatic fraction, with focus on compounds of much higher molecular weight than those studied in this work.

1.2.2 Charge Transfer Stationary Phases

Charge transfer stationary phases have been applied for isolation of aromatic moieties according to the number of annealed aromatic rings [39]. Usually electron pair acceptors

are loaded on silica or chemically bound to the stationary phase. Many phases have been used for the separation of PAC in coal liquefaction products and petroleum pitches [40-44] and for the class separation and preparation of petroleum aromatics [45-49]. However, the influence of substituents and heteroatoms limits the applicability of the method. Charge transfer LC applied for the separation of vacuum residue samples in this thesis is further discussed in detail in chapter V1.3 (page 35).

1.2.3 Reversed Phase Separations

The shape selectivity of bonded alkyl stationary phases has been described for PAC analysis [50, 51]. Length to breadth ratio, planarity and alkyl substitution of aromatic molecules greatly influence the interactions with the stationary phase and allows for separation of isomers that co-elute in normal phase chromatography.

2 Bulk Analytical Methods

A wide variety of analytical techniques have been applied to the study of petroleum fraction structures. Bulk structural characterization methods, e.g. elemental analysis, ultra violet (UV) and visible light spectroscopy, infrared spectroscopy, nuclear magnetic resonance (NMR) spectroscopy, and X-ray spectroscopic methods [52], give useful overall information, particularly with respect to the determination of functional groups and degree of “aromaticity”. Mass spectrometry is used to provide molecular weight distributions. Degradation techniques, which include chemical degradation and pyrolysis, also give a better insight into petroleum structure.

2.1 Chemical Approaches of Degradation and Derivatization

The aim of degradation studies is to make the degradation yield a maximum of identifiable products, which still retain their structural relationship to the crude material, but are more suitable for analytical methods (fingerprint).

2.1.1 Chemical (Degradation) Reactions

Oxidative degradation of sulfur rich kerogens by sodium dichromate ($\text{Na}_2\text{Cr}_2\text{O}_7$) in glacial acetic acid cleaves off alkyl substituents from the aromatic system at the benzylic positions [53, 54], leaving aromatic carboxylic acids for analysis behind. Ruthenium

tetroxide is reported to degrade aromatic rings [55, 56] to carboxylic acid functions and thus preserve the alkyl substituents for analysis. Both reactions (and various others) have been used for the study of alkylated polycyclic aromatic compounds in petroleum and coal samples [53-58].

Hydrogenation. Other authors determine overall sulfur content in petroleum products by hydrogenation [59, 60].

Derivatization. The derivatization of compound classes in petroleum samples has been used to improve separation characteristics and detectability. Sulfides and thiols in petroleum distillates are differentiated by derivatization with pentafluorobenzoyl chloride, which forms thiol esters [61]. The subsequent gas chromatographic separation is supported by increased thiol elution times, separating them from sulfides. Characteristic fragment ions aid in mass selective detection. Structural characterization of sulfur compounds in petroleum by ^{13}C NMR was improved by sulfur methylation [62].

Desulfurization with Raney-Ni. Mass spectrometric analysis of sulfur rich oils and shale oils is supported by desulfurization of OSC with Raney-Ni [63]. The resulting hydrocarbons are compared with the hydrocarbons initially present in aromatic fractions to determine the OSC formation process [5, 6].

Reagent selectivity and the possible formation of new compounds not representative for the sample are always problematic for reaction approaches. Even small differences in reactivity, e.g. due to steric hindrance make quantification difficult. This is particularly important for complex mixtures of mostly unknown composition.

2.1.2 Pyrolysis

Pyrolysis thermally fragments the sample in an inert atmosphere. Heavy petroleum fractions and related materials yield small structural units volatile enough for gas chromatographic analysis during pyrolysis [64]. Generally, the fragments are separated and analyzed by gas chromatographic systems that allow for the use of powerful detectors like mass selective, pulsed flame photometric, and atomic emission detector. However, similar problems as discussed in 2.1.1 arise. While some pyrolysis products may be representative for moieties originally present in the sample, others might also be produced during pyrolysis.

2.2 Spectroscopic Techniques

Compositional information is obtained to some degree from elemental analysis. Infrared or nuclear magnetic resonance (NMR) spectroscopy have been applied to the study of functional groups or quantification of carbon species (e.g. degree of aromaticity). Several publications contribute to the determination and quantification of organic sulfur compounds in petroleum samples by spectroscopic techniques like X-ray absorption near edge structure (XANES) spectroscopy and X-ray photoelectron spectroscopy (XPS) [65-67]. A quantitative response to inorganic and organic sulfur, e.g. thiolic, thiophenic and sulfonic sulfur is obtained. Structural characterization of an asphaltene fraction from vacuum residues of an Arabian crude mixture has been done by a combination of spectroscopic and pyrolytic methods [68].

3 Mass Spectrometry (MS)

In numerous studies heavy petroleum fractions have been investigated by mass spectrometric methods. Depending on analyte polarity various ionization techniques can be applied. For the ionization of aromatics in high boiling fractions several methods have been developed and shall now be described.

Boduszynski [19] reported on field ionization (FI)-MS of heavy petroleum fractions, however, reliance on thermal introduction limits application to samples within a certain boiling range. Non-volatile components of vacuum residues are thus discriminated. The analysis of nonvolatile residue components with field desorption ionization (FD)-MS of nonvolatile petroleum components has been reported by Larsen [69], but the sample loading procedure on a fragile emitter proved impractical for routine analysis. Thermospray ionization (TSP) has been applied to interface HPLC to MS for analysis of high boiling polycyclic aromatic compounds (PAC) as shown by Hsu [70] but has not been used extensively due to sensitivity limitations and inaccessibility of more polar compounds including some heterocycles. Particle beam ionization (PB) is another interface device capable of ionizing heavy aromatic compounds [71], but recent PB interface designs suffer from sensitivity and linearity limitations [72]. Matrix assisted laser desorption and ionization (MALDI) is extensively used for molecular weight distribution determination of heavy petroleum fractions. Atmospheric pressure chemical ionization (APCI) has been developed as interface between HPLC and MS as well and has been applied for ionization

of heavy PAH by various authors [72-74]. APCI-MS spectra have the disadvantage of arising from various ionization mechanisms, depending on analyte structure and size, leading to the formation of several possible ions [75]. This can hinder interpretation of the mass spectra. So are PASHs reported to yield $[M]^{\bullet+}$ as well as $[M+1]^+$ ions in weak correlation with molecular size, which complicates the spectra and possibly interfere with signals from nitrogen or ^{13}C containing species.

Electrospray ionization (ESI) of polar crude oil fractions has been reported to be superior to APCI in sensitivity and ease of interpretation of the resulting spectra. Direct ionization of aromatic compounds with ESI techniques is not very efficient [76-78] so that pre-ionized compounds are desirable. Electrospray ionization of aromatic hydrocarbons in heavy petroleum fractions has been investigated by Roussis [79], who use silver nitrate as ionization aid. Other studies employed trifluoroacetic acid, 2,3-dichloro-5,6-dicyano-1,4-benzoquinone, and antimony pentafluoride as chemical electron-transfer reagents for the ESI ionization of neutral PAC [80]. For PASHs, palladium(II) has recently been used as a sensitivity enhancing reagent in standard resolution experiments with an ESI ion trap MS [76, 81].

3.1 High Resolution Mass Spectrometry of Vacuum Residues and Related Samples

In 1954 Lumpkin and Johnson reported the identification of sulfur compound types in a petroleum gas oil and presented strong evidence for benzothiophenes and dibenzothiophenes on a double focusing instrument with a resolution of 10,000 [82-85]. Recently Marshall et al. showed the capability of mass spectrometry of highest resolution power by Fourier transform ion cyclotron resonance mass spectrometry (FT-ICR-MS or FT-MS) for identification of elemental compositions of polar compounds in diesel fractions [86, 87]. Unrivalled resolution of this spectrometer-type allows identification of thousands of signals, each representing a distinct elemental composition, in a single spectrum of a sample. The use of FT-MS instruments has been expanded to crude oil [88], middle [89] and heavy petroleum fractions [90], and coal extracts [91], extending the upper mass limit to approximately 1,000 Da. Nonetheless the focus remains on polar compounds and on advancing the instrumentation used. Various ion sources, like low energy electron impact (EI) [87], ESI [92] and FD [89] have been utilized in combination with high resolution FT-MS for petroleum analysis. Aromatic components in petroleum vacuum

residues are ionized by in-beam EI [93] and characterized by FT-ICR-MS. It shows that all aromatics, both hydrocarbons and heterocycles, are unselectively ionized.

III OBJECTIVES

For the refining operation in the past, meeting higher sulfur levels than today, exact knowledge of the structures of individual fuel compounds was not necessary for their removal. Rising prices for low sulfur crude oil feedstocks and decreased legal sulfur limits in transportation fuels enforce the increased refining of oils and heavy petroleum fractions with lesser quality while at the same time lowering the sulfur content in product streams. Even with modern hydrotreatment procedures low quality feedstocks cannot be converted to meet the desired specifications under economic conditions.

Characterization of petroleum cuts is a necessary stage to a better understanding of the desulfurization reaction mechanisms and to describe the kinetics of certain refining processes such as hydrotreating or catalytic cracking. This knowledge is essential to get a deeper insight into reactivities of sulfur compounds in the heavy ends of refining and for development of improved desulfurization processes for crude oils. So far, despite great technical progress, no satisfying method has been reported for the characterization of recalcitrant sulfur aromatics in vacuum residues.

For analysis, crude and distilled oils are often separated into aliphatic, aromatic, and polar compounds (resins) and insoluble asphaltenes. The aromatic fraction is the hardest one to desulfurize [19, 25, 94] and is therefore the fraction of interest in this work. As a major target, a simple method that provides structural information on recalcitrant aromatic vacuum residue compounds should be established.

In the first part of this work a representative PASH structure should be defined, based on preliminary bulk analysis, and synthesized for use as a standard to test analytical procedures, e.g. retention on various chromatographic systems or ionization and fragmentation behavior with various ion sources for mass spectrometric analysis.

Secondly, a chromatographic method should be developed to separate chemically well-defined fractions of the aromatic compound class contained in the vacuum residue samples. The fractionation into classes according to the number of fused aromatic rings per molecule should be investigated. Other structural elements, which characterize certain groups of structures, should also be exploited for their use as separation criteria. Special

focus of the investigated chromatographic methods should be directed on the distinct separation of sulfur compounds.

After establishing a successful chromatographic fractionation procedure the obtained fractions should be analyzed by spectrometric and spectroscopic methods to advance knowledge of the molecular structures present in the aromatic fraction, again with major focus on organic sulfur structures. The applicability of the established method should then be demonstrated on the aromatic fraction of two vacuum residue samples before and after a partial hydrodesulfurization (HDS) procedure. Finally, information on the effect of HDS on high molecular weight sulfur structures present in heavy petroleum fractions should be gathered.

IV VACUUM RESIDUE SAMPLE INVESTIGATED IN THIS WORK

The vacuum residues investigated in this thesis have been obtained from a Safania (Saudi Arabia) crude oil. Boiling ranges of the samples have been determined by simulated distillation and range from 466 °C to above 720 °C, with 10 % of the material remaining at highest temperature. One fraction used for investigations was untreated material (“feed”); the other fraction has been hydrotreated with metal catalysts for partial desulfurization (“effluent”). The aromatic fraction of the “feed” and “effluent” has been prepared according to the SARA⁸ [95] method. Asphaltenes have been removed by precipitation with n-heptane and the aromatic fractions have been isolated from saturates and polar compounds by liquid chromatography on silica [28]. These aromatic residue fractions and the data mentioned have been provided by the Institute Français du Pétrole, Vernaison, France [77, 96].

1 Average Composition of the Vacuum Residues

The elemental compositions are given in Figure IV-1 a) on the left the “feed” of the hydrodesulfurization process, the data given on the right b) refer to the “effluent” of partially processed stock.

Heteroatoms are enriched in fractions with increasing boiling point, but oxygen and nitrogen containing species are expected to be found mainly in more polar fractions. Therefore the relatively high amount of sulfur of 4.7 %wt along with low concentrations of oxygen and nitrogen is consistent with the heavy fraction compositions discussed before. The amount of carbon and hydrogen remained nearly unchanged during HDS, the content of sulfur in the aromatic fraction is decreased from 4.7 to 2.9 %wt. This remaining high amount of sulfur illustrates the problem of recalcitrant sulfur species in such heavy petroleum samples [96].

⁸Precipitation of asphaltenes with nonpolar solvent followed by liquid chromatographic separation of the soluble part into saturated, aromatic, and resin compounds: Saturated, aromatics, resins and asphaltenes (SARA).

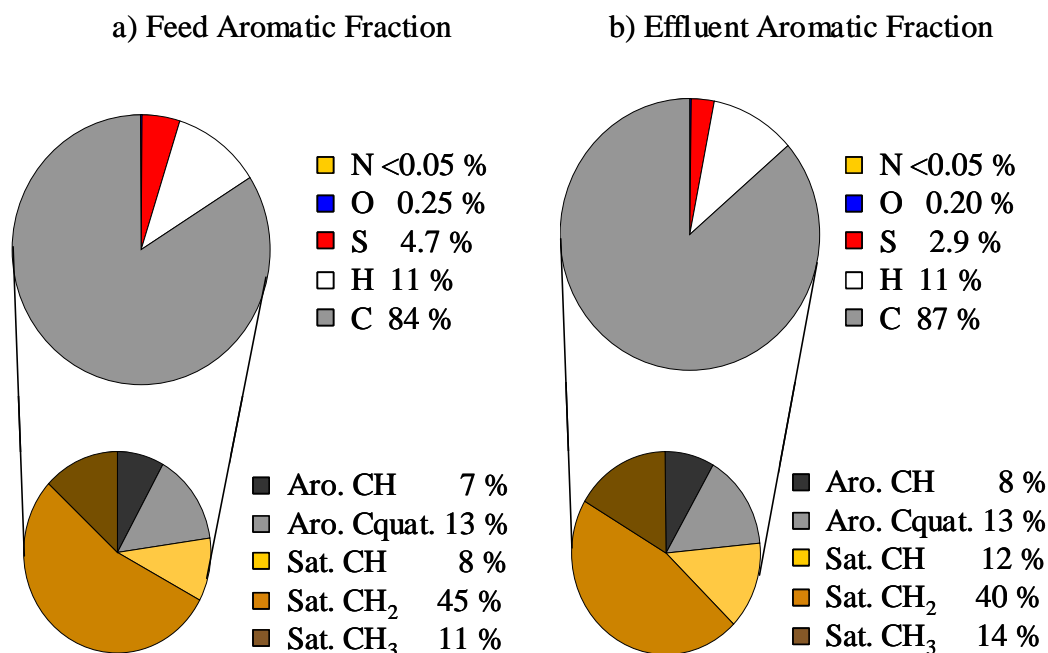


Figure IV-1. Elemental composition and ¹³C NMR data describing fractions of the aromatic compounds of the Safania vacuum residue investigated in this thesis a) before (feed) and b) after (effluent) partial HDS.

Elemental analysis, quantitative ¹³C NMR experiments and molecular weight distribution determination by GPC were provided with the sample. Data to support this work are given in Appendix IX4.

The data presented in combination with UV spectroscopy and molecular weight distribution determination by use of mass spectrometry of the vacuum residue samples indicated highly alkylated PASHs as major sulfur containing species. A standard compound is necessary to predict such a molecule's analytical properties, e.g. retention behavior or ion stability in mass spectrometric analysis. Such highly alkylated structures are not commercially available and thus had to be synthesized. The following data serve as a basis for defining such a molecule.

The UV spectra of the vacuum residue before and after HDS indicate that 2 to 3 condensed aromatic rings might account for the average molecular structure. Elemental analysis led to an average elemental composition of C₄₈H₇₆S₁ for the feed and C₇₉H₁₁₆S₁ for the effluent fraction. The latter elemental composition has a molecular weight about twice that of the average weight determined by GPC and MS. If half of the compounds after the HDS process are approximated to contain organic sulfur, the elemental

composition for the effluent would divide into $C_{39}H_{58}S$ for an average PASH and $C_{40}H_{58}$ for PAHs. The corresponding molecular weight of 530 Da is in good agreement with the maximum of the molecular weight distribution determination by GPC and MALDI-TOF-MS. Remaining sulfur structures in the effluent fraction should contain sulfur in thiophenic rings analogous to HDS recalcitrant structures in lighter refining fractions. Combining this with the result from UV spectroscopy indicates benzothiophenes or dibenzothiophenes. Such molecules of 530 Da would have side chains made up of $C_{29}H_{48}$ or $C_{30}H_{36}$ (feed) for a benzothiophene (BT), a dibenzothiophene (DBT) would comprise $C_{25}H_{46}$ or $C_{26}H_{34}$, respectively. This substituents cannot be unbranched, but must contain a number of rings (R) given by:

$$C_cH_h = 2c+2-2R \text{ or } R = c+1-\frac{h}{2} \quad (\text{eq. 1.})$$

c : total number of carbon atoms in all side chains

h : number of hydrogen atoms in all side chains

The number of naphthenic rings in an average molecule is given in Table IV-A for BT and DBT assumed as parent structures. The calculated distribution of aromatic and aliphatic carbon atoms was compared to the value obtained with quantitative ^{13}C NMR spectroscopy⁹.

Table IV-A. Naphthenic rings depending on parent structure in comparison to data provided by quantitative ^{13}C NMR spectroscopy.⁹

Parent structure	Alkyl groups	Naphthenic rings		^{13}C NMR	$C_{29}H_{48}$
$C_{37}H_{56}S$					
BT	$C_{29}H_{48}$	5	arom. C%	21.6	22.9
	$C_{30}H_{36}$	12	aliph. C%	78.4	77.1
					$C_{26}H_{34}$
DBT	$C_{25}H_{46}$	1	arom. C%	21.6	32.4
	$C_{26}H_{34}$	9	aliph. C%	78.4	67.6

⁹ Data for ^{13}C NMR has been provided by the Institute Français du Pétrole, Vernaison, France.

From quantitative ^{13}C NMR spectroscopy (given in Appendix IX4) the average amounts of carbon hybridization, quarternary, secondary and tertiary carbon atoms and the number of aromatic carbons can be estimated. A BT aromatic structure with 29 C atoms in side chains can be deduced together with an average number of five rings in aliphatic side chains.

2 Synthesis of an Highly Alkylated PASH

The assumption of a BT with substituents of the formula $\text{C}_{29}\text{H}_{48}$ implies five aliphatic rings and thus fits with all above mentioned criteria and can thus be represented by the molecules displayed in Figure IV-2.

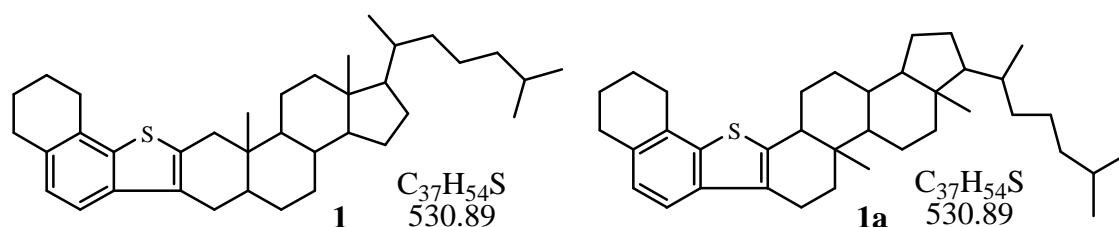


Figure IV-2. Structure of cholestano[2,3-*b*]-5,6,7,8-tetrahydronaphtho[2,1-*d*]-thiophene **1** (CHNT) as a representative molecule for average properties and the isomer **1a** obtained as side product by bromination of 3-cholestanone in 4-position.

Cholestano[2,3-*b*]-5,6,7,8-tetrahydronaphtho[2,1-*d*]thiophene (CHNT) $\text{C}_{37}\text{H}_{54}\text{S}$ **1**, which is shown in Figure IV-2, has been prepared from 3-cholestanone and 1-mercapto-5,6,7,8-tetrahydronaphthalene **2** according to previously described methods [97]. This reaction pathway is depicted in Figure IV-3. For this synthesis, 2-bromo-3-cholestanone **3** is required and is reported to be the major product of bromination of 3-cholestanone [98].

Presumably some 4-bromo-3-cholestanone was also formed, leading to a mixture of two isomers **1** and **1a** of the final product. MALDI mass spectrometry showed no other signals than a base signal at m/z 531 ($\text{M}+\text{H}^+$), 532 (67 %), 533 (23 %) and 534 (6 %). The signal for $\text{M}+1$ is considerably higher than theoretically calculated (67 % vs. 42 %). This may be due to protonation as observed elsewhere, even without obvious proton source [99, 100].

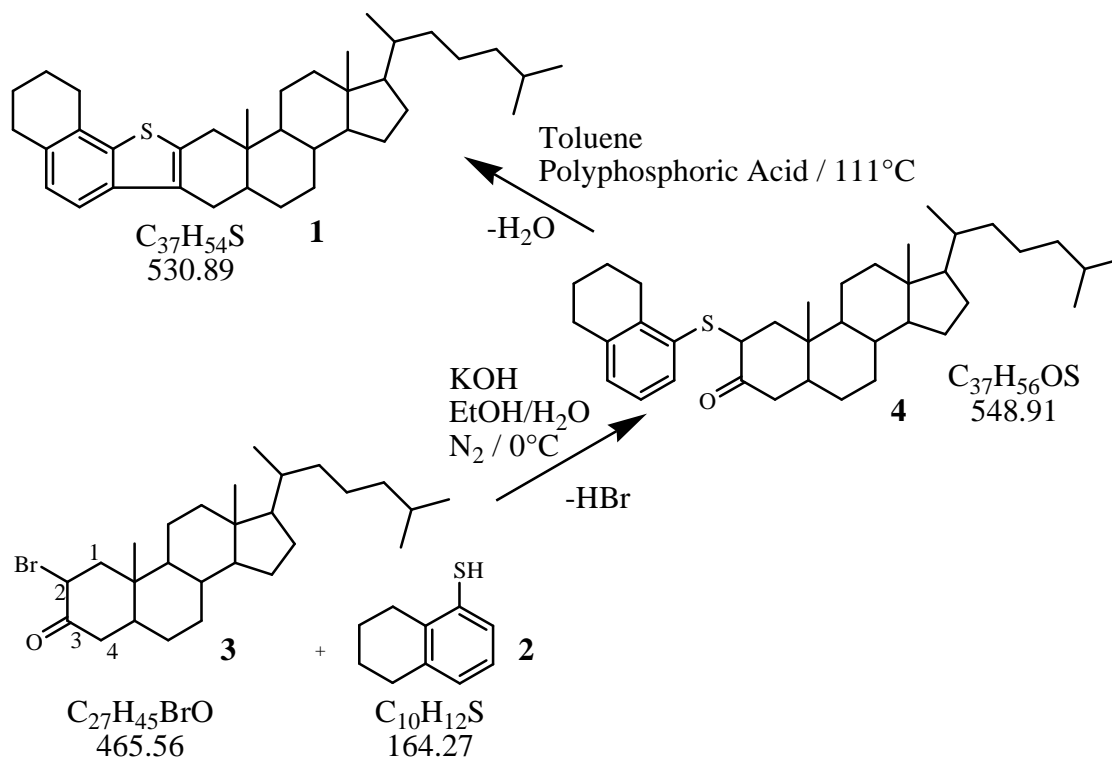


Figure IV-3. Reaction path for the synthesis of cholestano[2,3-*b*]-5,6,7,8-tetrahydronaphtho[2,1-*d*]thiophene **1** (CHNT) from 2-bromo-3-cholestanone **3**.

In 1H NMR only two doublets at 7.48 and 6.90 ppm are seen in the aromatic region. These doublet signals agree with the [2,1-*d*] attachment of the tetrahydronaphtho substructure to the thiophene ring true for both isomers **1** and **1a**. The ^{13}C NMR spectrum is more complex, showing more than 37 signals, indicating the presence of a second isomer **1a** of CHNT.

1H -NMR: (360 MHz, $CDCl_3$):

δ = 7.48 (d, 3J = 8.1 Hz, 1H C1-*H*); 6.90 (d, 3J = 8.1 Hz, 1H C2-*H*); 2.90 to 0.60 (m, 52-*H*) ppm.

V LIQUID CHROMATOGRAPHY OF VACUUM RESIDUES

Many preparative and semi-preparative chromatographic methods used for group separation of petroleum have been developed over the years. Apart from separating aliphatic, aromatic, polar compounds and asphaltenes, the further fractionation of the aromatic class has received much attention.

Some applications of HPLC separation on heavy petroleum samples have been presented earlier in Chapter III. Generally, different types of interactions have been used in liquid chromatography to separate mixtures of solutes. A possible classification of separating mechanisms is based on the following principles: Surface adsorption, solute partitioning, ion exchange and relative solute size, to name the major categories. In surface adsorption chromatography analytes with different degree of attraction to the stationary phase are separated through a series of adsorption/desorption steps. In partition chromatography different solubility of the analytes is utilized which results in repeated partition between mobile and stationary phase and finally in separation. These two basic principles have been widely used; normal phase chromatography combines a polar stationary phase with relatively non-polar solvent whereas in reversed phase chromatography a non-polar stationary phase with polar solvent is used. For ion chromatography the desired interactions are of an electrostatic nature. Stationary phases are weak cationic or anionic exchange resins. In the fourth major category of chromatographic methods, namely size exclusion chromatography, a porous gel separates analytes according to molecular size. Interactions between analyte and stationary phase are not desired and usually suppressed by solvent with strong solubility. The smaller the hydrodynamic volume of an analyte, the more pore volume is accessible and the longer is its path through the stationary phase.

In an ideal chromatographic separation, only one of the four mentioned separation mechanisms is operating, but in practical work an overlap of different mechanisms is found. This can be exploited for better separation performance (e.g. silanol groups in addition to alkyl chains bound to the silica can strongly influence the retention order in

reversed phase partition chromatography). The overlap of mechanisms can also be suppressed, e.g. by altering temperature, solvent strength or by modification of free silanol groups on silica stationary phases.

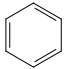
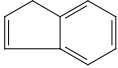
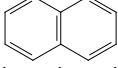
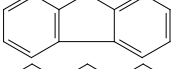
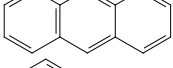
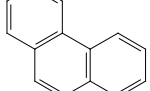
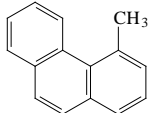
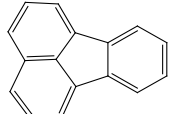
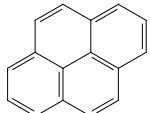
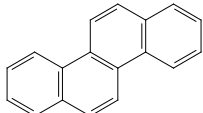
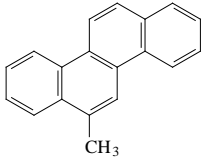
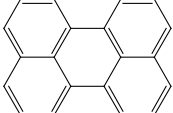
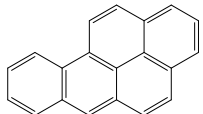
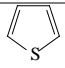
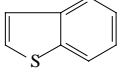
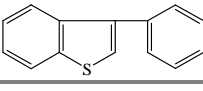
1 Detection of Polycyclic Aromatic Compounds (PACs)

Several principles can be applied for signal detection. In this thesis a diode array detector was utilized for online recording of UV/vis absorbance spectra. The main advantages and drawbacks of this detection method will now be described. Additionally employed for the offline mass spectrometric characterization of chromatographic fractions was matrix assisted laser desorption ionization time of flight mass spectrometry (MALDI-TOF-MS).

1.1 UV– Vis Spectroscopic Detection of Polycyclic Aromatic Compounds with Diode Array Detector

It is well known that UV light absorption of an aromatic molecule strongly depends on the number and structure of rings. Spectral properties of aromatic systems with one to four fused rings are listed in Table V-A. The influence of aliphatic substituents on the spectral properties of a compound must be considered, because a high degree of alkylation is to be expected for heavy petroleum samples [19]. Judged from the tabled values, methyl groups shift the absorption maxima only a few nanometers. The length of alkyl chains has a negligible effect as can be seen for 4-methyl-, 4-ethyl- and 4-octyl-substituted dibenzothiophene. Multiple substituents have slightly more influence on spectral data, however the shift of UV absorption maxima is small (below 10 nm). To minimize the effect of the solvent on the UV absorbance characteristics isocratic elution was used in the chromatographic experiments. Identification of separated parent structures by online UV spectroscopic detection thus is a simple tool to follow the desired separation of a HPLC system.

Table V-A. UV spectra characteristics for some aromatic parent compounds.

Structure	Name	Aromatic rings	Aro. π - electrons	Major maxima [nm/abs. ^b]	Side maxima [nm/abs. ^b]
	Benzene ^c	1	6	254/2.5; 260/1.7	243/1.0
	Indene ^c	1½ ^a	8	209/22.0; 221/10.8	252/9.6; 262sh/5.3; 280; 290
	Naphthalene ^d	2	10	225	265; 275; 285
	Fluorene ^d	2½ ^a	12	215	253; 258; 265; 273; 302
	Anthracene ^d	3	14	246/10.0; 252/20.8	339/0.6; 356/0.9; 374/0.9
	Phenanthrene ^d	3	14	246sh/5.0; 252/6.4	213/3.5; 221/2.2; 275/1.43; 282/1.1; 294/1.4
	4-Methylphenanthrene ^d	3	14	251/7.1	211/1.7; 224/1.4; 276/1.0; 386/1.0; 298/1.3
	Fluoranthene ^c	3½ ^a	16	236/52; 276/24; 287/45;	342/7.9; 358/8.3
	Pyrene ^d	4	16	238/5.7; 273/5.4; 335/5.6	232/4.5; 263/2.5; 320/3.2; 332sh/3.2
	Chrysene ^d	4	18	259/7.6; 269/15.2	218/2.9; 223/2.9; 283/1.1; 295/1.2; 307/1.3; 320/1.2
	6-Methylchrysene ^d	4	18	261/7.5 270/14.6;	218/3.4; 223/3.3; 286/1.2; 298/1.3; 310/1.5; 324/1.5
	Perylene ^d	5	20	206/6.4; 253/4.8	227sh/2.0; 246/3.3; 387/1.23; 408/2.72; 436/3.8
	Benzo[a]pyrene ^d	5	20	297/6.4	266/4.9; 385/3.1
	Thiophene ^c	1	6	227/6.8; 231/7.1; 237/6.6	243/3.8
	Benzo[b]thiophene ^{e,f}	2	10	227; 255sh; 262	268; 290
	3-Phenylbenzo[b]- thiophene ^f	2+1	14	233 ;255	300

	<i>Cholestano[2,3-b]-5,6,7,8-tetrahydronaphtho[2,1-d]-thiophene^e</i>	2	10	255sh; 262	268
	<i>Dibenzothiophene^d</i>	3	14	236/5.7	211/1.8; 254/1.6; 263/1.0; 286/1.4
	<i>R₁: 4-Methyl^d- ; 4-Ethyl- ; 4-Octyl-dibenzothiophene^e</i>	3	14	235/3.6; 239/3.8	233/1.0; 256/1.1; 264/0.7; 285/0.9
	<i>R: 4,6-Dimethyl- ; 1,4,8-Trimethyl- ; 2,4,6,8-Tetramethyl-dibenzothiophene^e</i>	3	14	236/3.6; 238/3.8	233/1.0; 256/1.1; 264/0.7; 285/0.9
	<i>Naphtho[2,3-b]-thiophen^e</i>	3	14	250; 233	335; 350
	<i>Benzo[b]naphtho-[2,1-d]-thiophene^d</i>	4	18	265/5.4	223/2.2; 235/2.9; 257/4.5; 294/1.0; 308/1.4; 321/1.6
	<i>Benzo[b]naphtho-[1,2-d]-thiophene^d</i>	4	18	254/5.4	245/4.8; 267/2.5; 276/4.2; 292/1.5; 303/1.8
	<i>Benzo[b]naphtho-[2,3-d]-thiophene^d</i>	4	18	245/5.8; 265/5.0; 275/9.3	211/1.6; 288/3.0; 268/4.8; 282/3.2

a) Aromatic systems with bridged methylene groups are denoted by 1/2; e.g. those with conjugated double bonds. Experimental findings also suggest that their “aromaticity” is between two aromatic ring classes. b) Molar Absorption Coefficient [$\text{mol}^{-1} \text{cm}^{-1} 10^{-4}$]. c) UV Atlas of Organic Compounds, Weinheim, Butherworks, London 1962. d) Spectral Atlas of Polycyclic Aromatic Compounds, D. Reidel publishing company, Dordrecht, Boston, Lancaster, 1985. e) Own measurements. f) Schuetz, R. and Ciporin, L., J. Org. Chem. (1958), **23**(2), p. 209-211.

A general tendency exists among PAHs of a shift of the major absorption maxima towards higher wavelengths with increasing number of fused rings. The maxima of UV absorption for benzolog PAHs are: (2-rings) $225 < (3\text{-rings}) 246$ and $252 < (4\text{-rings}) 238, 273$ and 335 nm . This tendency is more or less unaltered for alkylated structures. Diode array detectors consequently have been used to identify the aromatic structures in petroleum samples [19, 101] or coal liquefaction products [102]. However, the data in Table V-A reveal that the identification of PACs is complicated by the presence of PASH. The absorption maxima of PASHs are not as simply correlated to the number of fused aromatic rings. BT has a side absorption maximum at higher wavelengths than the absorption maximum of its three-ring benzolog DBT. The influence of structural isomers has an additional influence on the UV absorbance. Benzo[*b*]naphtho[2,1-*d*]thiophene

exhibits a maximum absorbance at 254 nm similar to benzothiophene, but its isomer benzo[*b*]naphtho[2,3-*d*]thiophene absorbs at 275 nm.

Identification is further complicated or even impossible if several unknown analytes co-elute. Nevertheless UV spectroscopy allows a check of the chromatographic separation and is therefore used for online HPLC detection in this thesis.

1.2 UV Spectroscopy of the Aromatics Contained in Feed and Effluent Vacuum Residue Fractions

The UV spectra of a) untreated and b) partially desulfurized vacuum residue aromatics dissolved in cyclohexane (CH) are displayed in Figure V-1. With reference to the data listed in Table V-A, some general information might be deduced of average structure characteristics.

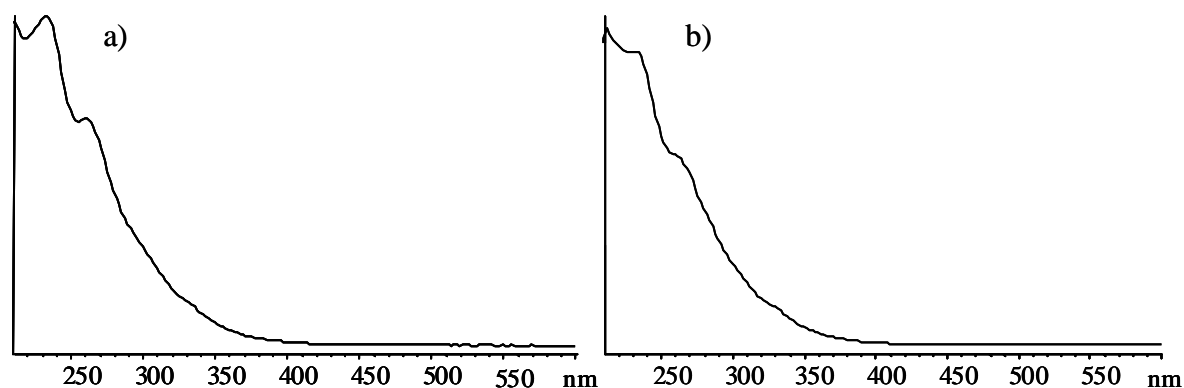


Figure V-1. UV spectra of a) feed and b) effluent fraction. The samples were dissolved in cyclohexane.

The main absorbance is from 235 to 240 nm, which would agree with dibenzothiophenes. Both spectra also show a flanking maximum, a) quite distinct at slightly below 270 nm which agrees with benzothiophenes, but as well with chrysenes, and b) less pronounced at 280 nm. Absorbance is detectable up to ~360 nm for both spectra which excludes many structures with five or more condensed aromatic rings, which still absorb UV light at 385 nm and longer wavelengths.

The main absorbance ranges from 235 to 240 nm, which agrees with dibenzothiophenes or thiophenes. Both spectra also show a flanking maximum, Figure V-1 a) quite distinct at 270 nm. This also matches with the absorption of benzothiophenes, but as well with that of chrysenes. The UV spectrum in b) shows a less pronounced shoulder at

280 nm. Absorbance extends up to ~360 nm for both spectra, so most structures containing five or more condensed aromatic rings. The distinction between PASHs and PAHs from the UV spectra of not further chromatographically simplified samples is impossible.

1.3 Matrix Assisted Laser Desorption Ionization Time of Flight Mass Spectrometry (MALDI-TOF-MS) as Off Line Mass Selective Detector

From the UV data discussed in the previous chapters it is obvious that additional and more sophisticated means of detection must be utilized to support UV spectroscopy. Mass spectrometric detection can offer supplementary information about the sample, but considering the complexity of the samples, simplification by chromatographic fractionation and an ionization technique providing unfragmented molecular ions are highly favorable. In this thesis Matrix assisted laser desorption and ionization (MALDI) was applied for soft ionization of aromatic species and was therefore used to support the chromatographic system as an off line detection system. Chapter VII, p. 57 deals in detail with the instrumental setup of a MALDI-TOF-MS and its use for the investigation of aromatics in heavy fractions and the interpretation of the resulting mass spectra.

2 Charge Transfer Chromatography

Formation of molecular complexes by association of aromatic compounds is well documented [40-49]. It is known that polynitroaromatic compounds form more or less stable complexes with aromatic hydrocarbons. Herein charge transfer interactions between electron rich π -electron pair donors (*EPD*) and electron pair acceptors (*EPA*) are involved. Based on this interactions, Godlewicz [103] used dinitrobenzene deposited on silica as *EPA* to isolate aromatic fractions from lubrication oils by liquid chromatography. Picric acid and picric ether, 2,4,6-trinitrobenzene, 2,4,7-trinitrofluorenone, and other nitroaromatic compounds have been used deposited on silica gel. Later chemically bound stationary phases like 3-(2,4-dinitroanilino)propano (DNAP), tetrachlorophthalimidopropano (TCPP) and other species have been used as *EPA* stationary phases for the separation and isolation of PAC in coal liquefaction products and petroleum pitches and other fractions [40-44]. Retention was described to depend on the solvent, number of π -electrons in the analyte aromatic system, spatial arrangement of aromatic rings (length/breadth ratio, planarity), and substituents (electron donating/withdrawing)

[104]. Molecules with isolated aromatic structures are retained similarly to the parent structure. Biphenyl, for example elutes with monoaromatics. Principally, the separation according to number of fused aromatic rings is possible, but the effect of alkyl substituents must be further discussed.

2.1 Influence of Alkyl Substituents and Hetero Atoms on Retention Order

The strength of a charge transfer complex employed for charge transfer chromatography depends strongly on electron density of the analytes' aromatic systems. Substituents on the aromatic system, in petroleum samples predominantly alkyl chains, give an inductive effect (+I) that increases the electron density of the π -electron system. However, alkyl chains also provide steric hindrance and hence reduce the strength of the charge transfer complex [104, 105]. As a result the greatest increase of retention is observed for methyl substituted PACs while longer chains shorten retention times. Furthermore, higher methylation increases electron density since PAH retention is reported to increase with the number of methyl groups [105]. Number and structure of alkyl and naphthenic substituents therefore influence retention in an opposite way and thus limit the predictability and applicability of the separation method.

In addition to the discussed influence of alkyl substituents heteroatoms contribute to electron density in the aromatic π -systems. Stronger donor-acceptor complexes have been observed for heterocyclic aromatic compounds. They were retained longer and even interfered with PAH elution [105]. For petroleum fractions heteroatom content and the bulk of alkyl substituents increase with molecular weight. As vacuum residues feature highest sulfur content and a tremendous bulk of alkyl chains, a poor efficiency for separation into ring-size classes based on aromatic cores is to be expected.

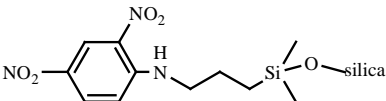
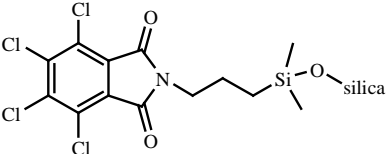
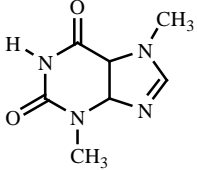
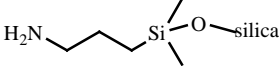
However, in a comparison between various charge transfer phases DNAP-silica [106, 107] and TCPP-silica [47] have been reported to show the smallest influence of substituents and have been exploited for this investigations presented in this thesis.

2.2 Charge Transfer Chromatography of the Vacuum Residue Sample

Aromatic nitrogen heterocycles (PANH) have been reported to be especially problematic for charge transfer separations. Even small PANH can undergo strong interactions with the stationary phase and thus elute together with PAH and PASH

containing a larger number of fused rings, interfering with a group separation according to the number of fused aromatic rings. However, by elemental analysis of the investigated aromatic fractions no nitrogen was detected, so that co-elution of polycyclic aromatic nitrogen heterocycles (PANH) with PAH and PASH needs not to be considered. The retention behavior of alkylated PASH, however, was studied for some reference compounds.

Table V-B. Stationary phases investigated for the separation of vacuum residue samples according to aromatic parent structure.

Stationary Phase	Name
	Dinitroanilinopropano (DNAP) - silica
	Tetrachlorophthal-imidopropano (TCPP) - silica
	Theobromine (TB)
	Aminopropano (AP) - silica

A DNAP stationary phase was successfully employed for the isolation of aromatics containing three fused rings for lighter diesel and crude oil fractions [108]. DBTs containing up to eight carbon atoms in aliphatic side chains have been isolated from mono-, di- and tetracyclic aromatic systems with higher or lower numbers of aromatic rings. DNAP-silica was the first choice used to investigate the residue sample with related PASH structures. For this work also a TCPP bound stationary phase was synthesized and investigated. Theobromine (TB) deposited on silica and an aminopropano-silica were used for comparison. The four stationary phases listed in Table V-B were tested for the group separation of standard PACs. TCPP and DNAP bonded to silica showed the best group separation according to number of aromatic rings.

2.2.1 DNAP as Stationary Phase

Retention data for some non-substituted or alkylated standard compounds are listed in Table V-C. For methylated PACs retention strictly according to ring-size classes is maintained, although methylated compounds show slightly stronger retention than their parent compounds.

Table V-C. Retention factors of PACs on DNAP-silica ^a.

Compound	k	Signal in Figure V-2
Toluene	0.17	1
Naphthalene	0.55	2
1-Methylnaphthalene	0.67	2
2-Methylnaphthalene	0.67	2
<i>1,2,3,4-Tetrahydro- dibenzothiophene</i>	0.79	3
Fluorene	0.87	4
Acenaphthalene	0.87	4
<i>4-Octyldibenzothiophene</i> ^b	1.03	-
<i>Dibenzothiophene</i>	1.41	5
Anthracene	1.63	6
Phenanthrene	1.68	7
1-Methylphenanthrene	2.07	8
Fluoranthene	3.51	9
Pyrene	3.75	10
Chrysene	5.87	11
Perylene ^b	16.92	-

a) Chromatographic parameters: 150x4.0 mm ID column, 10 µm, isocratic elution with cyclohexane/dichloromethane 19:1 (v/v). b) Not shown in Figure V-2.

In comparison to hydrocarbons, PASHs were retained more weakly, but were eluted in their PAH-analog ring-size class. The two higher alkylated PASHs, namely tetrahydrodibenzothiophene and octyldibenzothiophene, were less retained than the parent structures BT and DBT, respectively. This is in agreement with earlier studies on PAHs and might be explained by steric hindrance caused by the alkyl substituents. The

chromatogram of the aromatic compounds contained in the vacuum residue sample prior to HDS is shown in Figure V-2.

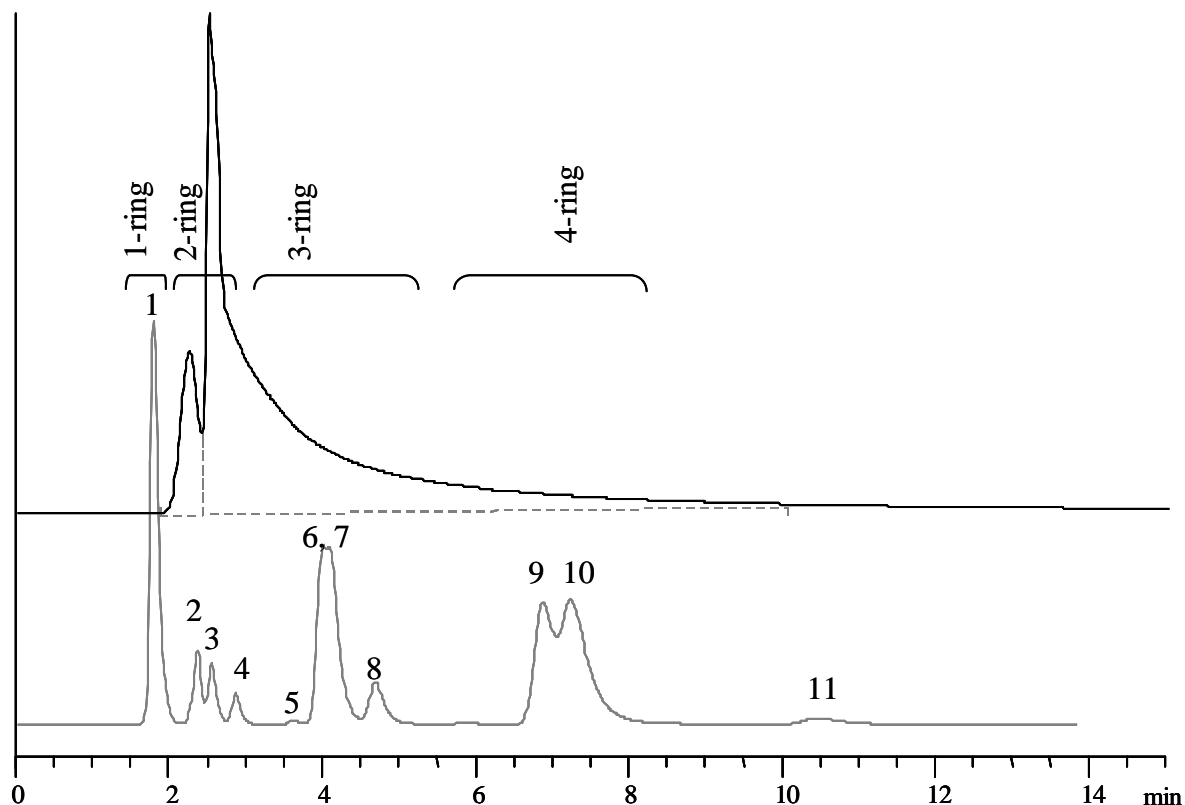


Figure V-2. Chromatogram of the aromatics of the vacuum residue after HDS on a DNAP stationary phase. The lighter chromatogram shows aromatic standard compounds listed in Table V-C. DNAP-Silica, 10 μm , 150x4 mm ID column, isocratic elution with cyclohexane/dichloromethane (CH/DCM) 19:1 (v/v) at 1.0 mL/min, detection at 236 nm (40.1 μg AE PAC).

In the lower gray chromatogram the compounds listed in Table V-C are shown for better comparison. The standards elute according to number of aromatic rings in agreement with the literature [19]. The chromatogram of the vacuum residue fraction shows a partially resolved peak at a retention time ranging from 2 to 2.5 min followed by the unresolved bulk of the sample eluting from 2.5 min in one tailing signal to 10 min.

Obviously, strict separation into ring classes was not achieved for the sample. Nonetheless UV spectra have been recorded over the course of the chromatogram and are presented in Figure V-3. They show a weak tendency of a continuous shift towards higher absorption wavelengths with longer retention time. The first UV spectrum taken after 2.24 min shows the maximum at shortest wavelengths (215 to 220 nm) that allows the

conclusion of isolated or two fused aromatic rings being the major moieties present at that time. In a time interval ranging from 2.5 to 3 minutes the absorption maximum of the eluted main bulk is from 225 to 237 nm indicating that naphthalene, benzothiophene and/or dibenzothiophene structures might be present. Minor absorption bands at 260 to 265 nm and an even lesser one at ~285 nm agree with this assumption. Considering the elution behavior of octyldibenzothiophene (RT: 3.02 min) even higher alkylated dibenzothiophenes are assumed to be present in the sample. After three minutes the absorption slowly fades with a very weak shift towards higher wavelengths and an absorption maximum at 335 nm.

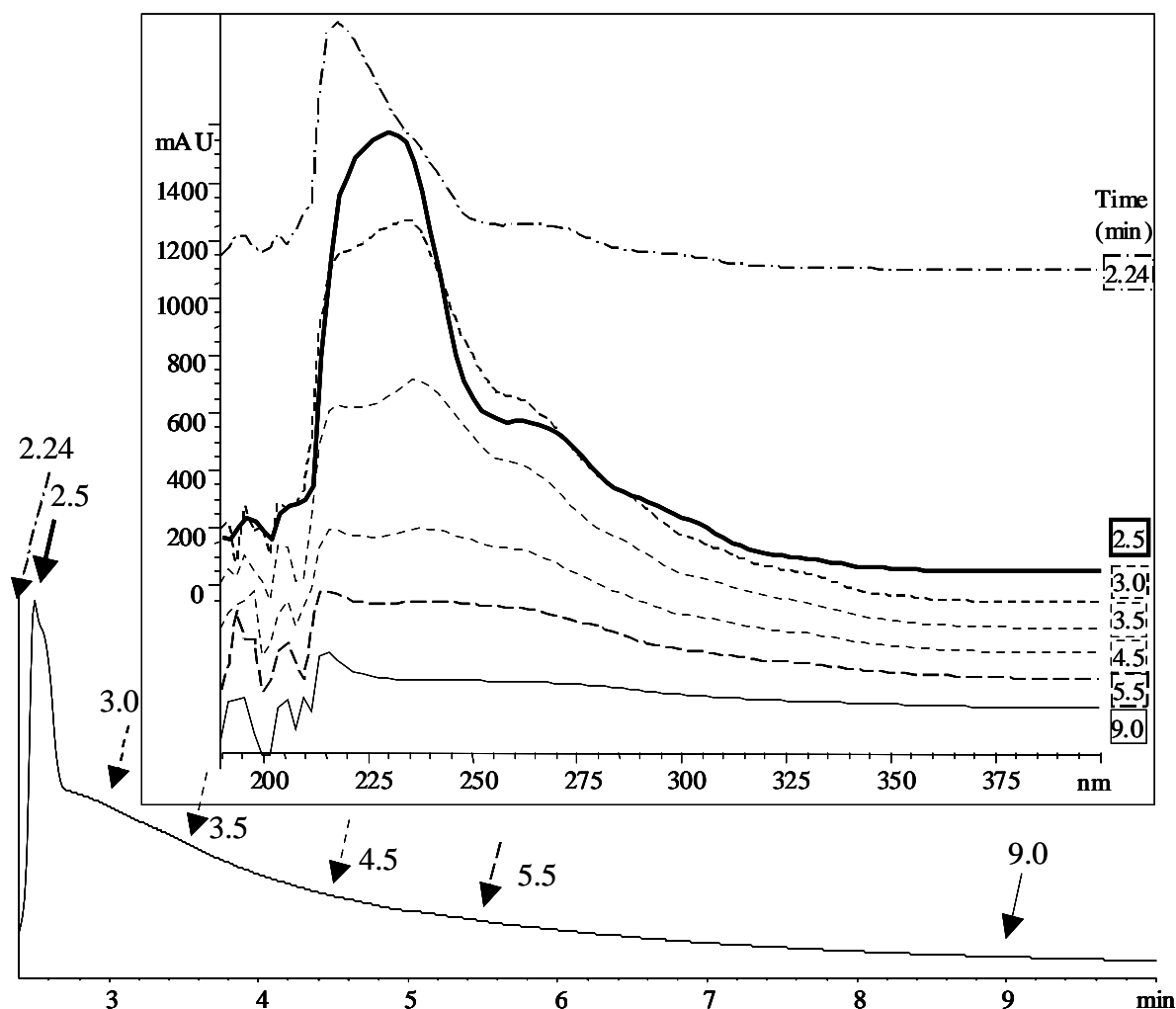


Figure V-3. UV spectra over the course of the vacuum residue sample's main bulk shown in Figure V-2. The arrows in the section of the chromatogram indicate the time when the corresponding spectra were recorded.

This shift of the maxima may correspond roughly to an increase in number of aromatic rings. Large amounts of structures with four or more fused rings can be excluded. However, as the spectral data for a great number of parent structures fit the obtained UV data, no additional conclusion on the nature of the parent structures can be drawn.

2.2.2 TCPP-Silica Used as Stationary Phase

Retention data for standard compounds on TCPP bound stationary phase are given in Table V-D. Similar to the “separation” on the DNAP-phase parent compounds and standards with low degree of alkylation elute in order of aromatic rings in agreement with literature findings [47]. The residue samples were eluted without distinct class separation, although three standard analytical size columns were consecutively coupled for better performance. Figure V-4 displays the chromatograms of feed and effluent of a partial HDS process, yet no distinct difference between both fractions can be observed. Both chromatograms feature a sharp peak at the beginning (RT: 5.6 min) which is not completely resolved from the main bulk of the sample that is eluted in one tailing peak from 6.0 to ~25 min.

Table V-D. Retention data for the TCPP stationary phase ^a.

Compound	k
Toluene	0.17
<i>Benzo</i> thiophene	1.31
<i>1,2,3,4-Tetrahydro</i> dibenzo- <i>thiophene</i>	3.06
<i>Dibenzo</i> thiophene	7.60
Phenanthrene	11.52

a) Chromatographic parameters: 120x4.6 mm ID, 10 µm, isocratic elution with cyclohexane/dichloromethane 19:1 (v/v) at 0.5 mL/min.

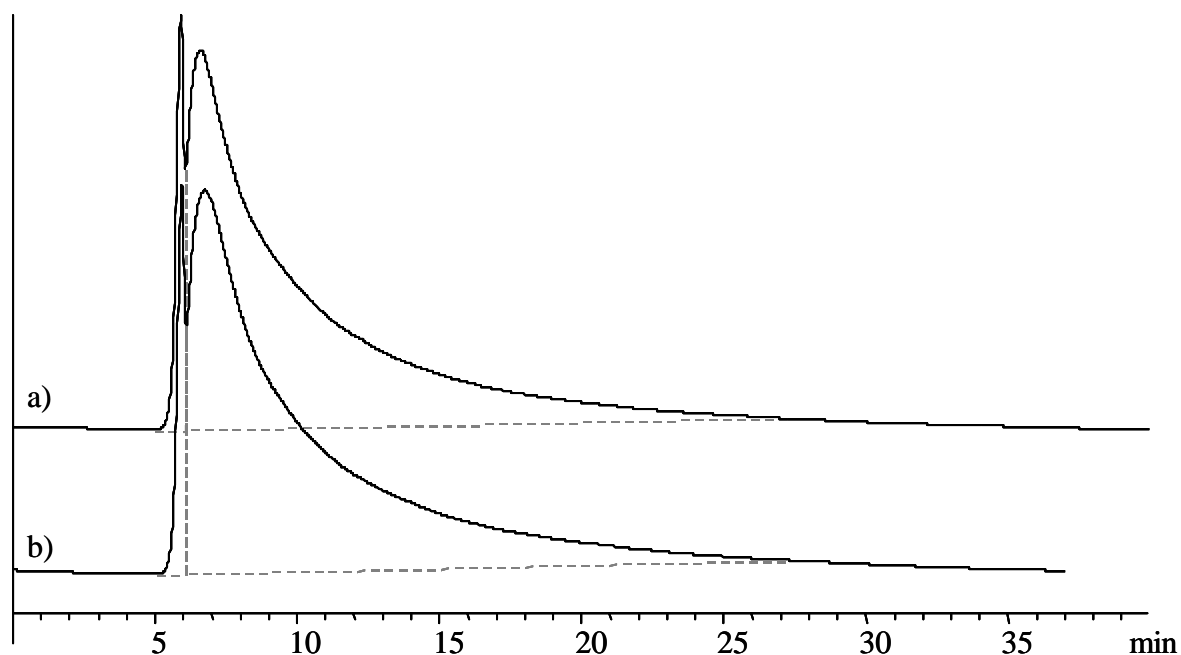


Figure V-4. UV chromatograms of aromatic compounds a) of the feed (upper) and b) effluent (lower) on three serially coupled TCPP columns. 3 x 125x4.6 mm ID, 10 μ m, detection at 236 nm, isocratic elution with 0.8 mL cyclohexane/isopropanol 7:3 (v/v).

The UV spectra (not shown) are indistinguishable from those obtained before when DNAP-silica was used as stationary phase and thus lead to the same conclusions.

Summary

Four stationary phases, with electron pair donator properties, that have been applied in the literature for chromatographic workup of heavy petroleum fractions or for the separation of PACs have been selected. The influence of alkyl substitution on retention has been investigated by the use of standard PAHs and PASHs. Standard compounds showed best group separation on the TCPP and DNAP bonded stationary phases. These two stationary phases have been tested for their separation ability of vacuum residue aromatics. LEC fractions 1 and 2 of the vacuum residue samples are analyzed. The influence of alkyl chains in the residue samples, as discussed above, is proven to clearly dominate over the desired selectivity in case of both investigated stationary phases. A separation of these complex samples according to the parent structures is not possible. Based on this, one can conclude that charge transfer chromatography cannot cope with the complex composition of the investigated samples and does not yield well defined sub-fractions

3 Reversed Phase Partition Chromatography

The investigated monomeric octadecyl (ODS) stationary phase has a high selectivity towards alkyl substitution. Solubility in polar solvents of the aromatic matter of the vacuum residues is poor. The investigated fractions could not be fully dissolved and the insoluble part could neither be dissolved in fresh solvent, or by heating (35 °C) nor by ultrasonication (30 min). Studies on the solubility with DBT revealed a solubility of ~100 ng DBT per μL acetonitrile (ACN) that significantly exceeds the solubility of DBT in distilled water and methanol. Those solvents are therefore regarded as unpractical for the desired semi-preparative chromatography. Using ACN as mobile phase, mixtures of DBTs containing various numbers of ethyl substituents and methylated DBT were easily separated.

When the soluble parts of the residue samples were tested on the ODS column it turned out they eluted without the slightest UV observable separation. The selectivity towards alkylation seems to counterbalance the separation according to the parent aromatic structures. Another explanation can be seen in the number of isomers present in the sample being too high for reversed phase chromatographic resolution. For this reason, mixtures containing various aromatic parent structures with heavy alkylation could not be separated by reversed phase partition chromatography.

Summary

Serious drawbacks for reversed phase fractionation of vacuum residues have been found in this work: the solubility of the sample limits the applicability, and additionally interfere the selectivities towards alkyl substituents and towards parent structures. Therefore prior to application of reversed mode a separation according to parent structures should be achieved to utilize the influence of alkyl groups in a second step for further chromatographic simplification.

4 Ligand Exchange Chromatography

A larger number of parent systems must be expected among PASHs than among PAHs since the sulfur atom introduces an element of asymmetry into the molecule [109]. The presence of a sulfur atom can be exploited with a chromatographic phase of suitable

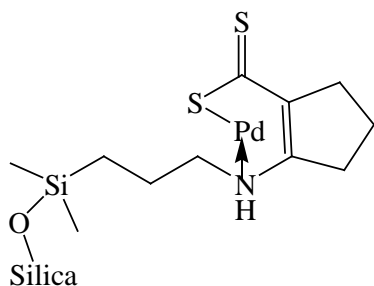


Figure V-5. The complex Pd(II)-ACDA bonded to silica as stationary phase in LEC.¹⁰

selectivity. Previous studies found that some sulfur aromatics are retained on a stationary phase containing palladium ions in normal-phase liquid chromatography [110]. This principle was improved using a bonded stationary phase which prevents slow loss (“bleeding”) of the Pd-metal center by complexation with silica-bonded 2-aminocyclopentene-1-dithiocarboxylic acid (ACDA) depicted in Figure V-5 [111]. Using gas chromatography with a sulfur-selective detector it

has been shown previously that this method can be applied to the aromatic compounds in low boiling materials like diesel fuel. They are completely separated into a fraction 1 which only contains hydrocarbons and, after an increase in eluent polarity, a fraction 2 that only contains PASHs [112-114].

Therefore, after the isolation of a fraction containing the non-polar polycyclic aromatic compounds, the next important step in the strategy for analyzing organic sulfur species in fossil material is further fractionation on a stationary phase containing Pd(II) ions [112].

When this ligand exchange chromatography (LEC) fractionating step was employed for separating the much larger aromatics in the vacuum residue two distinct peaks were clearly distinguishable in the chromatograms a) of the feed and b) of the effluent presented in Figure V-6. In the insets c) and d) the black line shows the UV spectra of fraction 1 and the gray line that of fraction 2. Those two fractions of the feed and those of the effluent do not differ in their UV absorbance spectra. The main absorbance ranges from 235 to 240 nm with a shoulder at 275 nm.

¹⁰ Andersson, J.T., Schade, T., and Muller, H., Abstracts of Papers of the American Chemical Society, 2002. 224: p. U574-U575.

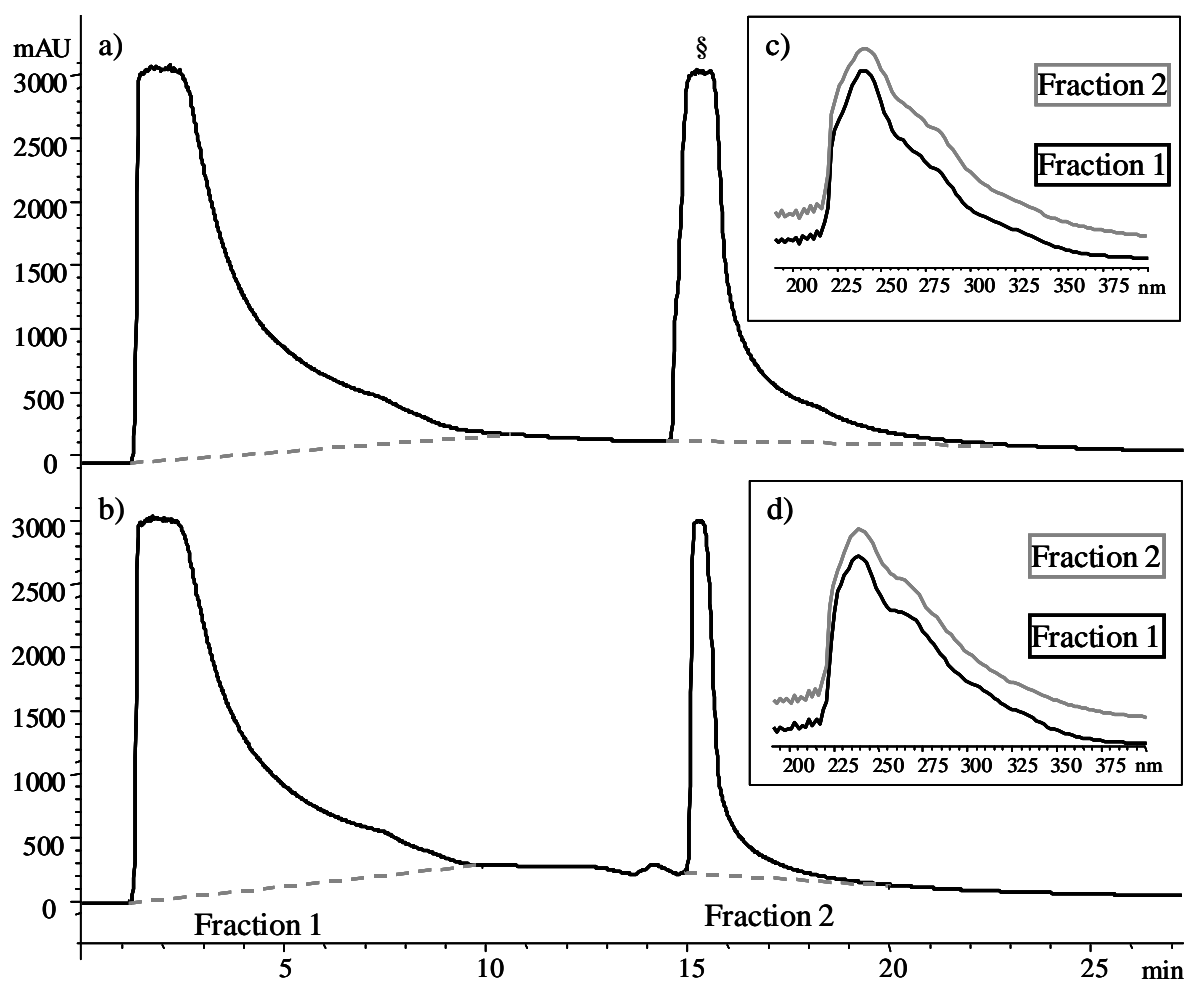


Figure V-6. Ligand Exchange Chromatogram of a) Aromatics of the Feed and b) Aromatics of the Effluent on Pd(II)-ACDA-Silica, 120x4.6 mm ID, 10 μm 100 Å, cyclohexane/dichloromethane 7:3 (v/v), from 15th min add. 0.5 %v isopropanol, detection at 236 nm. The insets show the UV spectra of fractions 1 and 2 c) feed and d) effluent.

When these two fractions were investigated separately it was found that the strict separation of sulfur species from pure aromatic hydrocarbons had not been achieved. Total sulfur determination with inductively coupled plasma optical emission spectroscopy (ICP-OES) showed similar sulfur contents in both fractions of the effluent: 2.0 %wt sulfur in fraction 1 and 2.8 %wt for fraction 2. For details of the procedure see also Appendix IX3, p. 119.

In a separate study¹¹ it was found that some sulfur compounds, e.g. those containing an isolated or terminal thiophenic ring, are not strongly retained by the Pd(II)-ACDA complex and therefore can be separated from PASHs. Those classes of non- retained sulfur species includes indenothiophenes, diindenothiophene and indanylthiophenes, which can now be analyzed separately from PASHs. This fact will greatly support interpretation of the accurate mass data described in Chapter VI-4, p.84.

5 Gel Permeation Chromatography

In gel permeation chromatography (GPC) retention of analytes supposedly occurs according to their size or, more precisely, to their hydrodynamic volume, which is usually the desired criteria of retention. For molecules smaller than a few hundred Dalton, shape has an impact on retention as well. A material commonly used for the stationary phase is highly porous polystyrene-divinylbenzene (PSDVB) copolymer with aromatic structures that can act as electron pair acceptors or donators [32]. It is known that in weakly solvating solvents aromatic compounds can undergo electron donor-acceptor interactions with the gel leading to mixed retention mechanisms and therefore a less clear-cut elution sequence [38]. This *EPA-EPD* interaction has some similarity to charge transfer chromatography described above in chapter V1.3 and has been described for PAHs [115] and PASHs [108]. In the diploma thesis of the author GPC was exploited using weakly solvating solvent for the chromatographic separation of alkylated dibenzothiophenes containing up to 20 carbon atoms in crude and diesel oil samples [108].

5.1 Influence of the Mobile Phase Composition

In preliminary experiments the influence of the mobile phase composition on retention of aromatic compounds was investigated using two test solutes of comparable size but of different degree of aromaticity, namely dibenzothiophene and 1,2,3,4-tetrahydrodibenzothiophene, containing three and two aromatic rings, respectively [108]. Figure V-7 shows the retention data of the tested compounds as a function of the percentage of tetrahydrofuran (THF) in cyclohexane (CH) used as the mobile phase.

¹¹ Unpublished results, K. Sripada. T. Schade, 2004, University of Münster.

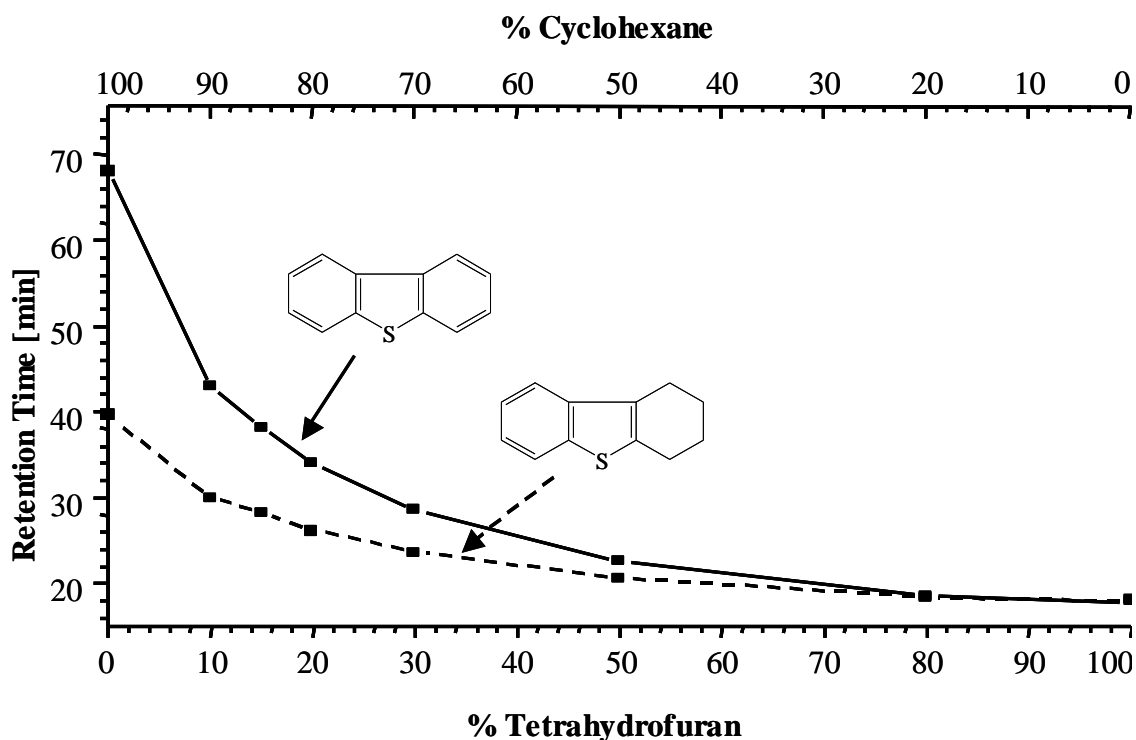


Figure V-7. GPC retention time of dibenzothiophene and 1,2,3,4-tetrahydrodibenzothiophene depending on solvent strength.¹²

Using the strongly solvating solvent tetrahydrofuran:cyclohexane 85:15(v/v), the retention times of the two solutes were identical at 18 min with peak widths of 15 s. However, with pure cyclohexane the retention times differed considerably and were 39 and 68 min, showing the much stronger interaction of the more extended π -electron system of dibenzothiophene with the stationary phase. The retention volume can become larger than the volume of total permeation due to such interactions. However, the peak width reduces the performance of the system drastically since less than 15 % (v/v) tetrahydrofuran causes very broad peaks (elution times up to 15 min). The best resolution was achieved with approximately 15 % (v/v) tetrahydrofuran in the mobile phase [108]. The achieved large differences in retention times were exploited for the best possible separation of compounds of similar size, according to their degree of aromaticity.

5.2 Influence of Temperature

The existence of more than one single retention mechanism responsible for a separation can be identified by plotting the logarithm of the retention factor (k) against the inverse

¹² Source: Müller, H. Diploma Thesis, Münster, Germany, Nov. 2000.

temperature. In the so-called van't Hoff plot the equilibrium constant (K_{eq}) is replaced by k divided by phase ratio (β). $\Delta G^o = -RT \ln K_{eq}$ with $K = k/\beta$ is transformed into:

$$\ln k = -\frac{\Delta G^o}{R} \frac{1}{T} \quad (\text{eq. 2.})$$

The plot appears as a straight line if separation is based on a single mechanism, while a changing slope indicates competing retention mechanisms, which differ in temperature dependency. GPC retention of dibenzothiophene was studied at 0, 25, and 45 °C using a weak and a strong solvating mobile phase. Figure V-8 shows the corresponding plots that display a bent line for both compounds with temperature variation.

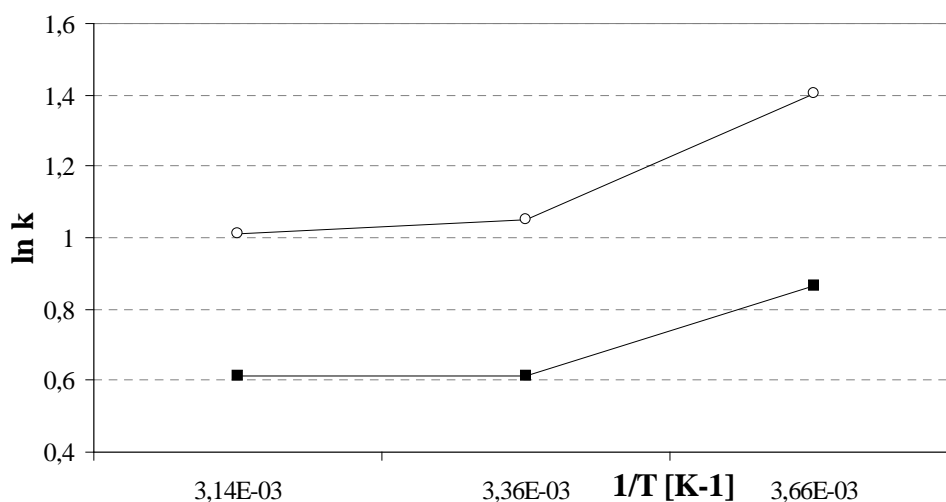


Figure V-8. Van't Hoff plot of PASH retention in GPC with 15/85 (v/v) THF/CH. (○) refers to DBT and (■) to THDBT.

These data strengthen the assumption that separation is based on the superimposition of more than one retention mechanism in GPC of PASHs. Two mechanisms, the retention according to size and the interaction between aromatic analytes and the stationary phase were addressed by investigating the preparation of fractions with a narrow molecular weight distribution, Chapter 5.4, p. 50.

5.3 Chromatographic Workflow

In this thesis the aromatic fractions of the vacuum residues were first separated by LEC as described above. The PASH containing fraction 2 is a highly complex sample containing several thousand compounds as can be seen in the mass spectra (Chapter VI,

p. 61). Since a number of isomers hide behind each exact mass, a tremendous multitude of individual compounds must be expected even for defined subclasses of a petroleum sample. If any kind of useful information is sought on the aromatic compounds, an additional simplification of the sample is highly desirable. In this chapter the simplification of the fraction of aromatic compounds by GPC and the PASH fraction by LEC for subsequent mass spectrometric studies is described. A scheme of the consecutive separation steps is illustrated in Figure V-9.

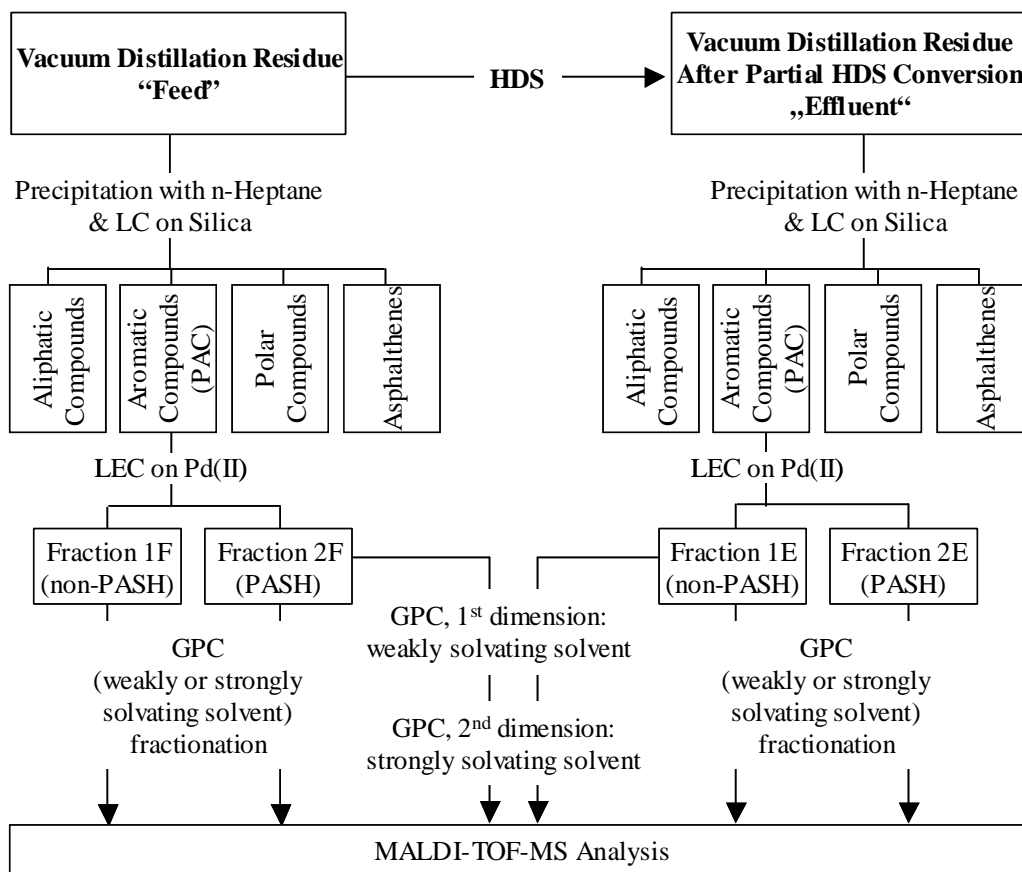


Figure V-9. Scheme of the chromatographic fractionation before mass spectrometric analysis of the vacuum residue samples “feed” and “effluent”.

Furthermore, the influence of solvent strength on the chromatographic behavior of PASHs on a GPC column was investigated by variation of the composition of the mobile phase. Different retention mechanisms were investigated for their use in achieving fractions with a narrow mass range.

5.4 GPC of the Vacuum Residue Sample to Produce Fractions with Narrow Mass Distribution

MALDI-TOF mass spectra revealed the complexity of the residue samples and determined the contained components mass range of 300 to 1000 m/z. Therefore the aim was a simplification of the sample into well defined sub classes by chromatographic methods. Size exclusion chromatography was tested in terms of its ability to further fractionate the vacuum residues aromatic fractions into subclasses with narrow mass distribution to enable consecutive chromatographic steps and to simplify subsequent mass spectrometric analysis.

First the elution time range of the residue samples was tested. The corresponding gel permeation chromatograms are shown in Figure V-10. Elution times vary with solvent strength. Elution with 85 % (v/v) tetrahydrofuran occurs between 7 and 20 min, shown in b), which corresponds to the expected elution window of partially permeating molecules between excluded moieties and totally permeating solvent molecules.

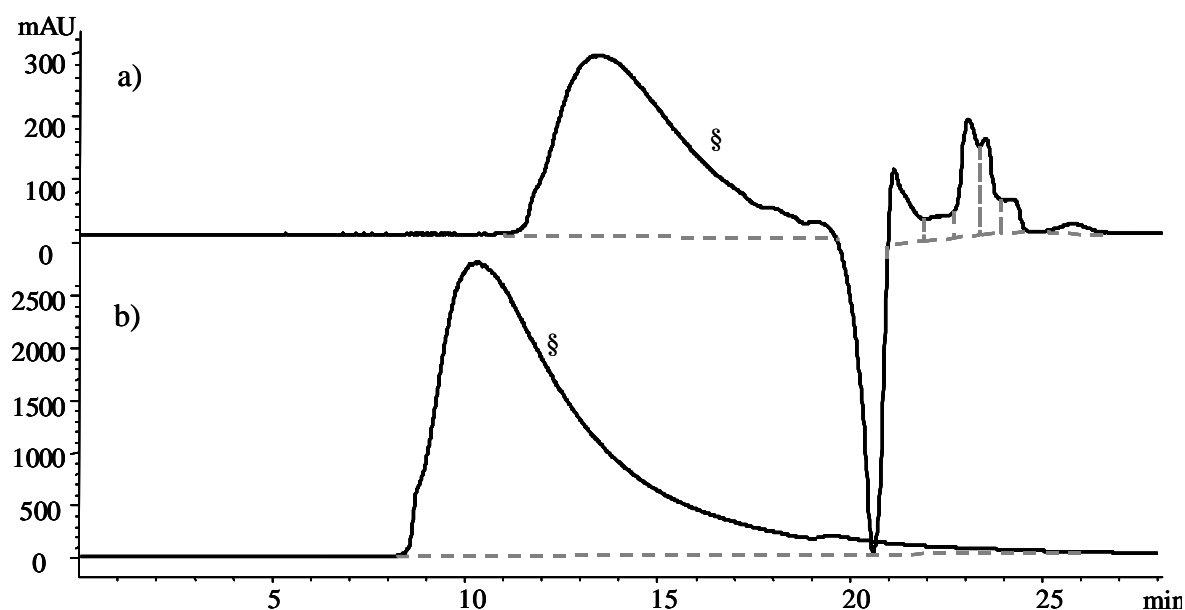


Figure V-10. Comparison between gel permeation chromatograms of the total aromatic fraction of the effluent a) with weakly solvating solvent: CH/THF 17:3 (v/v) and b) with strongly solvating solvent: CH/THF 1:10 (v/v). (§) indicates the retention time of CHNT. GPC 600x4.6 mm ID, PSDVB, 5 μ m 100 Å, flow rate: 1.0 mL/min, detection: 236 nm.

Using a weaker solvent with 15 % (v/v) tetrahydrofuran, shown in a), elution was observed after 20 min up to 26 min. This means that elution occurs after the solvent molecules and indicates an adsorption phenomenon similar to the one of aromatic compounds in lighter fractions [108].

In this thesis both modes of operation were investigated to obtain fractions with narrow mass range. The following procedures were employed for vacuum residue analysis by GPC and preparation for MS analysis:

Fractions were cut manually every 20 seconds in the case of stronger solvent as mobile phase and every 60 seconds when a weaker solvent was used. Following the fractionation the solvent was removed with dry nitrogen. Preparation of the samples for MALDI MS analysis was dissolution in cyclohexane, mixing with matrix compounds (e.g. dihydrobenzoic acid (DHB)) and co-crystallization by evaporation on a MALDI target plate.

The mass spectra of the collected matter in a single fraction were found to show weak intensities after only one GPC separation. Signals at high masses at the end of the molecular weight distribution fade into the background noise. Therefore the estimation of the highest molecular weights present in the residue samples is difficult, especially for mass spectra obtained from later eluting fractions with low sample mass. For that reason GPC fractions were collected by several repeated separations to accumulate sample matter in amounts that were detectable by the subsequent mass spectrometric analysis.

5.4.1 GPC with Strongly Solvating Solvent

The vacuum residue of the effluent was fractionated repeatedly on GPC using the strong solvent. A chromatogram with fractions indicated is depicted in Figure V-11. The MALDI-TOF mass spectrum of a representative sub-fraction (no. 11) is indicated in the inset in. It contains the eluate collected from 11.83 to 12.17 min.

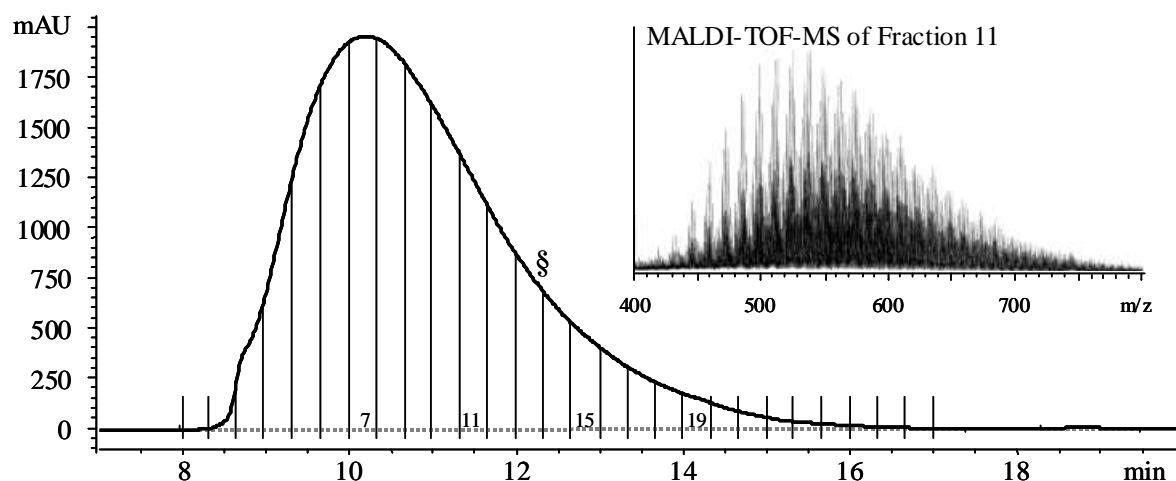


Figure V-11. Gel permeation chromatogram of the effluent fraction 1E (PASH) with strongly solvating solvent with sub-fractions specified. The inset shows the MALDI-TOF mass spectra of sub-fraction 11. (§) indicates the retention time of CHNT. GPC 600x4.6 mm ID, PSDVB, 5 μ m 100 Å, CH/THF 3:17 (v/v) at flow rate: 1 mL/min, detection: 236 nm.

Even in this narrow cut mass signals over a wide mass range from 400 to 800 m/z were observed. This range distribution of about 400 Da is representative for all analyzed fractions. Table V-E lists the signal mass ranges for the numbered fraction in the Figure V-11.

Table V-E. Range of masses of LEC fraction 1E (PASH) of the “effluent” after gel permeation chromatographic fractionation (with strongly solvating solvent).

Fraction No.	7	11	15	17	19
lowest mass [m/z]	550	400	350	290	260
highest mass [m/z]	1100	790	650	560	550

The tendency of earlier fractions to cover higher masses, as expected for GPC, can be seen in fraction no. 7, eluting from 10.17 to 10.50 min and covering the mass range 550 to 1100 m/z, and the later fraction no. 15, which corresponds to elution from 13.17 to 13.83 min, produced mass signals from 350 to 650 m/z. The interpretation of the corresponding mass spectra in detail is found in Chapter VI3, p. 61.

5.4.2 GPC with a Weakly Solvating Solvent

The fractions cut from GPC with the use of a weak solvent (15 % (v/v) THF in CH) are shown in Figure V-12. The fractions have been analyzed in the same way as the ones obtained with the strong solvent and show similar wide mass distributions.

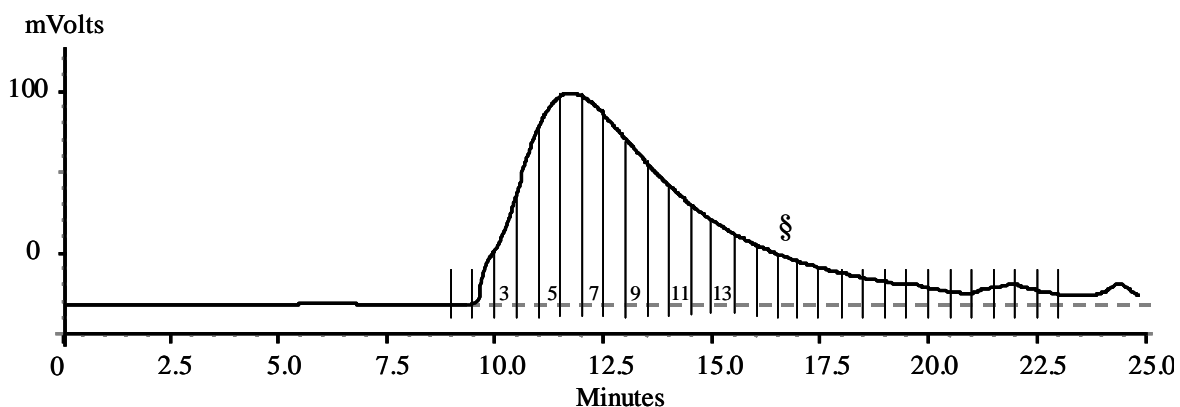


Figure V-12. Gel permeation chromatogram of the effluent LEC fraction 1E (PASH) with weakly solvating solvent with sub-fractions specified. (§) indicates the retention time of CHNT. The fractions were analyzed with GPC and strong solvent conditions as shown in Figure V-13. GPC 600x4.6 mm ID, PSDVB, 5 μ m 100 Å, CH/THF 17:3 (v/v) at flow rate: 1 mL/min, detection: 236 nm.

The aromatics contained in the vacuum residue feed were analyzed alike. Mass ranges from compounds in the listed fractions are shown in Table V-F.

Table V-F. Range of masses in MALDI-TOF-MS obtained from LEC fraction 1F and 2F of the vacuum residue feed after gel permeation chromatographic fractionation (weakly solvating solvent). The components eluted in the retention time range from 9 to 30 min.

Fraction 1F (non-PASH)	9-10 min	11-12 min	13-14 min	16-17 min
lowest mass [m/z]	750	650	500	420
highest mass [m/z]	1500	1500	1000	750
Fraction 2F (PASH)	10-11 min	11-12 min	13-14 min	16-17 min
lowest mass [m/z]	650	650	450	370
highest mass [m/z]	1400	1300	800	650

On the whole, earlier eluting GPC fractions show a higher average molecular weight than later fractions in agreement with the separation mechanism associated with GPC. The range of mass signals in a single fraction is surprisingly large, being $\Delta m/z$ = approximately

300 between the lowest and highest occurring masses for later fractions and up to $\Delta m/z = 750$ for earlier fractions.

5.4.3 Combination of GPC with “Weakly” and “Strongly” Solvating Solvent

In the previous sections it was described that each GPC “mode”, either elution with strongly solvating solvent by the use of high amounts of THF in the mobile phase or elution with weak solvent containing high amounts of CH, alone could not achieve the desired fractionation. Since at least two mechanisms were assumed to be responsible for the retention of aromatic compounds the effect of a combination of both GPC modes was tested. First, fractionation was performed with weakly solvating mobile phase and then those fractions, which had been obtained in the first step, were analyzed using strong solvent for elution. In principle, a combination of separations according to “aromaticity” and to molecular size should yield “sub-sub”-fractions with narrow mass distributions visible in MALDI-TOF mass spectra.

The first fractionation on GPC by a weakly solvating solvent is shown in Figure V-12 in the previous Chapter with four fractions (3, 5, 7, and 9) that were used for further analysis with strong solvent. The result of that second dimension chromatography step is illustrated in Figure V-13.

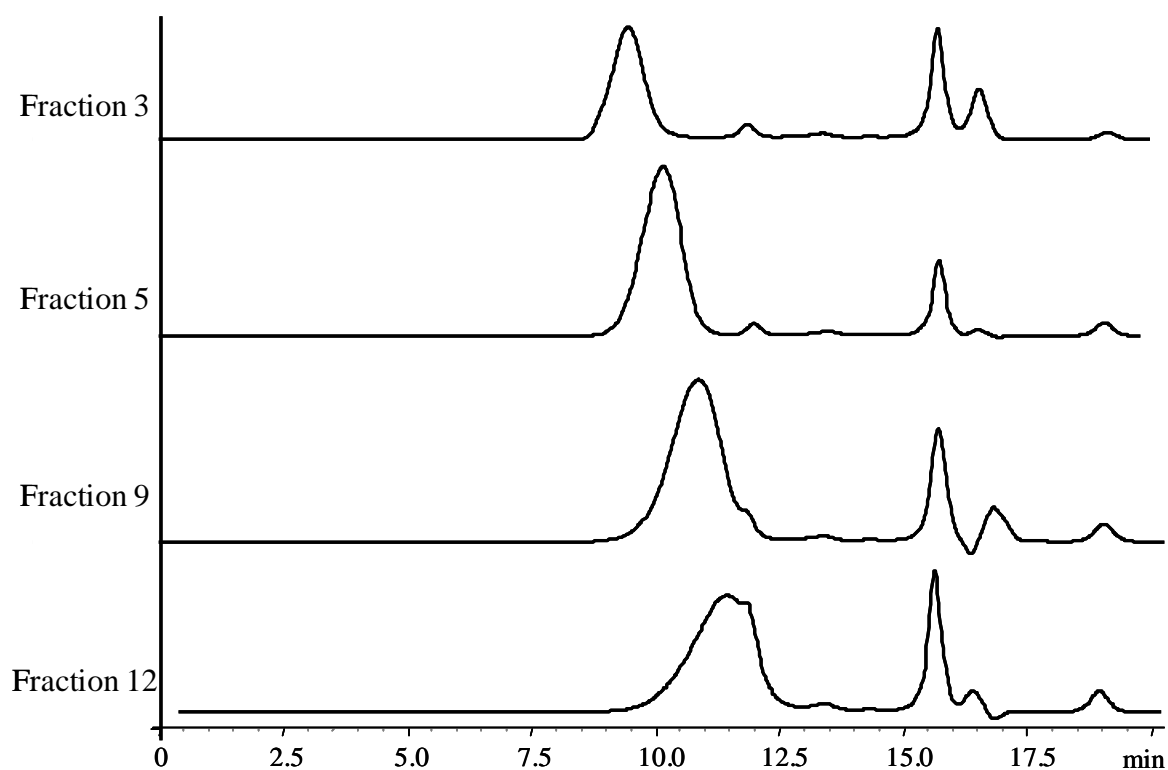


Figure V-13. UV chromatograms of the second chromatographic dimension with strongly solvating mobile phase of sub-fractions obtained by GPC with a weak mobile phase. Signals at 16.0, 16.5, and 18.3 min have been observed with injections of CH as well and should therefore not be attributed to the residue sample.

The chromatograms of the second dimension show narrow peaks of about 2 minutes width eluting in the range from 7.5 to 12.5 min. This can be interpreted as a comparable selectivity in both separation steps. The first step should retain molecules according to their aromaticity and the second one according to analyte size (and shape). Additionally, the mass spectrum of the fractions after the second GPC separation step confirms again wide mass range from over several hundred m/z .

6 Summary of Liquid Chromatography Applied on High Molecular Weight Aromatics

Due to the enormous number of molecules in vacuum residue samples a chromatographic isolation of single compounds is regarded as impossible. Therefore, at least a chromatographic fractionation of these samples into chemically well-defined groups

is desired on which subsequent mass spectrometric analysis can be based. Existing distinct features in the aromatic fraction include the number of sulfur atoms and the number and structure of fused aromatic rings. Several different chromatographic stationary phases have been tested and evaluated for their applicability to this task. Charge transfer chromatography is regarded as a valuable tool for the analysis of petroleum samples [48, 105]. Four stationary phases established in the literature for ring size analysis in petroleum fractions have been tested in this thesis for the ring size separation of vacuum residue aromatics. GPC, a method that has been widely used for heaviest fraction analysis, e.g. for the molecular weight distribution of asphaltenes, has also been successfully employed in preliminary studies [108] for the isolation of PASH with up to eight carbon atoms in side chains. GPC has been intensively investigated with respect to two different solvent mixtures providing complementary retention mechanisms. Furthermore, LEC on a stationary phase containing complexed Pd(II) has been routinely applied in our group for the isolation of PASHs in crude oils and transportation fuels. The vast majority of sulfur compounds in the latter are PASHs, therefore a quantitative isolation of OSC has been reported for such lighter petroleum fractions [112]. The same stationary phase was applied in this thesis on the much heavier vacuum residue samples than the fractions analyzed in the literature.

One can conclude that all chromatographic approaches based on separations according to molecular size or to carbon skeleton structure fail due to the sheer number of isomers in the sample and result in unresolved bulk elution. The only clear-cut fractionation was obtained by the chromatographic approach based on the Pd(II) column.

In contrast to experiments performed on lighter fractions not all sulfur species are isolated from hydrocarbons in this work. Some sulfur structures elute together with hydrocarbons in the first (non-PASH) fraction. Highly alkylated PASHs (CHNT, OctylDBT) were shown to be retained and elute in the second (PASH) fraction, indicating that even PASHs containing huge alkyl substituents can be separated from non-PASHs. This facilitates the distinction between different sulfur species in this thesis. Structures that contain thiophene rings (non-PASH) can be isolated from such OSC containing higher condensed thiophenes (PASH). This differentiation is a valuable tool in the interpretation of mass spectrometric results, which will be described in the next two chapters.

VI MASS SPECTROMETRY OF VACUUM RESIDUES

Mass spectrometry (MS) is based on physical techniques by which ions are separated and measured. Therefore the analytes have to be charged before the separation occurs, usually according to ion mass to charge ratio. After separation in the mass analyzer the ions are collected by a detector that converts this event into an electronic signal. From its early beginnings in 1889¹³ mass spectrometry was applied for many years only by few specialists using self-constructed instruments. Since the first commercial spectrometers were available in the 1950s the application of this technique has become widely spread and is nowadays a frequently used instrument for numerous analytical tasks. Various forms of MS and combinations with separation techniques like chromatography or electrophoresis exist and make mass spectrometry an analytical tool of equal significance to nuclear magnetic resonance spectroscopy and chromatography.

1 Matrix Assisted Laser Desorption and Ionization (MALDI)

For MALDI, like for other laser ionization (LIMS) techniques, a laser pulse is used to ionize the sample constituents. Herein, the analyte is imbedded in a matrix fixed on a target. The matrix consists of organic aromatic molecules with a chromophore, e.g. hydroxy or carboxylic groups that readily absorb light at the laser wavelength. Frequently used matrix materials are e.g. cinnamic acid, trans-2-[3-(4-*t*-butylphenyl)-2-methyl-2-propenylidene]malononitrile (DNHB) or 2,4-dihydroxybenzoic acid (DHB). To enable crystallization it is necessary that the matrix is used in excess (1000 fold). A laser pulse (usually a nitrogen laser, e.g. at wavelength = 337 nm) ablates the matrix and vaporizes even large analyte molecules into the gas phase. Excess thermal energy of the matrix ionizes the analytes so that they can be extracted into a mass spectrometer. The exact details of the desorption and ionization of analytes by the matrix is not yet fully understood. A number of chemical and physical pathways have been suggested for MALDI ion formation, e.g. gas-phase photoionization, ion-molecule reactions,

¹³ In 1889 E. Golstein discovered cathode rays as beam of positively charged ions.

disproportionation, excited-state proton transfer energy pooling, thermal ionization, and desorption of preformed ions [116, 117]. Nevertheless the resulting ionization is very soft. This allows the determination of the molecular weight of huge, fragile molecules with more than 1,000 kDa (polymers, biomolecules, complexes, enzymes), routinely 5 to 100 kDa, depending on the mass analyzer. Especially large and also nonpolar molecules are easily ionized by MALDI.

1.1 Time of Flight (TOF) Mass Analyzer

Time of flight (TOF) mass spectrometers are widely used for mass separations. These instruments make use of the fact that ions of different mass to charge ratio, but of the same initial translational energy, require different times to traverse a fixed distance in a field free region. A well-defined starting point in time, space, and velocity for the ions entering the analyzer is therefore desired. Generally, TOF analyzers are combined with pulsed ion sources (like MALDI) or the ions need to be gated into “packages” if continuous ion sources are combined with a TOF mass analyzer. In any case are the previously charged analytes accelerated by application of a short, strong electric field of 4 to 35 kV. Separation occurs in an evacuated drift tube of 0.1 to 4 m length. Measurand is the time of flight (between 1 and 100 μ s).

$$t = A\sqrt{\frac{m}{z}} \quad (\text{eq. 3.})$$

with:

t : time

m : ion mass

z : ion charge

A : instrument parameters incorporating length of the drift tube, acceleration voltage

Usually the ions are reflected at the end of the drift tube to compensate for slightly varying initial translational energy and starting time. The reflectron consists of a set of rings or grids on which high voltage forms an electric field where ions are accelerated in opposite direction back through the drift tube towards the detector. Ions are focused because faster ions enter the reflectron a little deeper than slower ones, so that the longer distance travelled compensates for their higher velocity. Further benefits of the reflectron

are the loss of neutral particles (improved signal to noise ratio) and the increase in separation length (higher resolution). This setup allows for the parallel analysis of ions of a mass range within 6-7 orders of magnitude from 10 Da to 10 MDa. Figure VI-1 illustrates the common combination of a MALDI-TOF instrument.

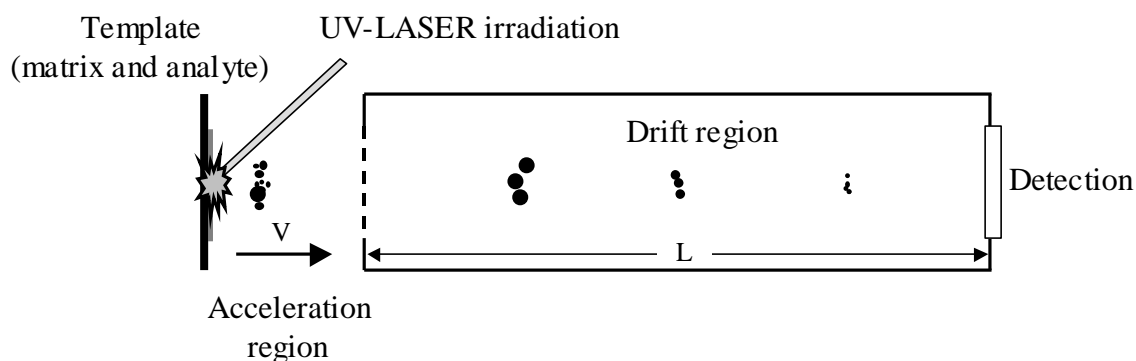


Figure VI-1. Combination of MALDI source with a time of flight (TOF) mass analyzer.

For complex mixtures it is highly desirable to only generate signals of unfragmented ions. As discussed above, MALDI is a suitable ionization procedure and widely used. Accordingly, several measurements of standard compounds and residue fractions presented in this thesis have been done using this instrument.

2 MALDI-TOF-MS of the Complete Vacuum Residues Aromatic Fraction

The MALDI-TOF-MS of the total aromatic fractions (without group separation into fraction 1 (non-PASH) and 2 (PASH) displays signals for masses from approximately 270 to above 1000 m/z as demonstrated in Figure VI-2. Using 2-octyldibenzothiophene and cholestano[2,3-*b*]-5,6,7,8-tetrahydronaphtho[2,1-*d*]thiophene (CHNT; $C_{37}H_{54}S$), it has been confirmed that no fragmentation of alkylated benzo- and dibenzothiophenes occurs under MALDI conditions, so one can conclude that all masses in the mass range mentioned represent the molar mass of compounds present in the sample.

The five signals between 200 and 250 m/z originate from matrix compounds. Signals originating from the effluent of the residue sample are observable at every mass between

300 up to ~1000 m/z, with signals at odd masses having a slightly higher intensity than those at even masses. Similar mass ranges have been observed by use of MALDI-TOF-MS for the vacuum residue feed and effluent of the HDS process, both spectra of feed (not shown) and effluent lack distinct features except the mass range.

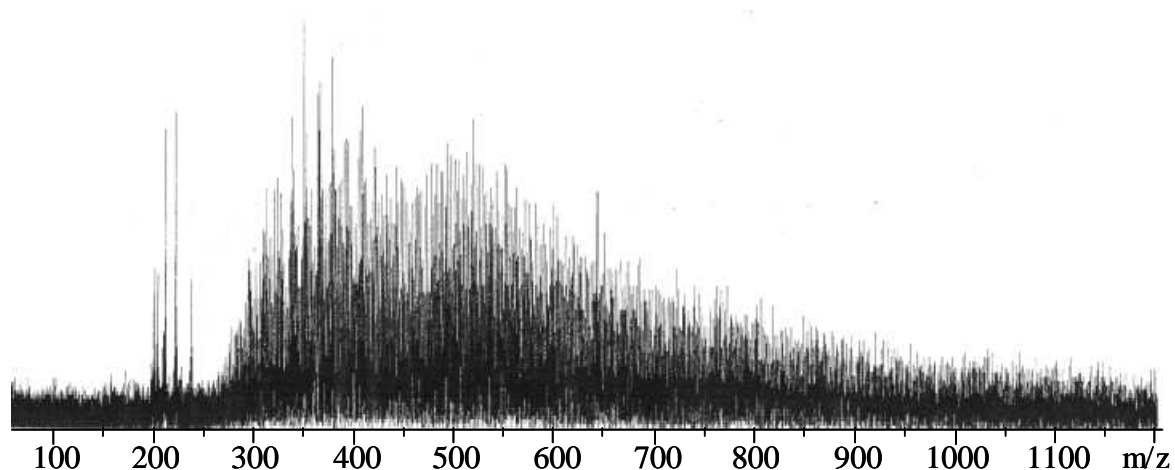


Figure VI-2. MALID TOF-MS of the total aromatic fraction of the effluent. Matrix was DCTB.

A detail of this mass spectrum is shown in Figure VI-3 a) for the mass segment from 650 to 660 m/z. It is striking that the odd masses are abundantly present throughout the mass range, and their intensity increases with m/z.

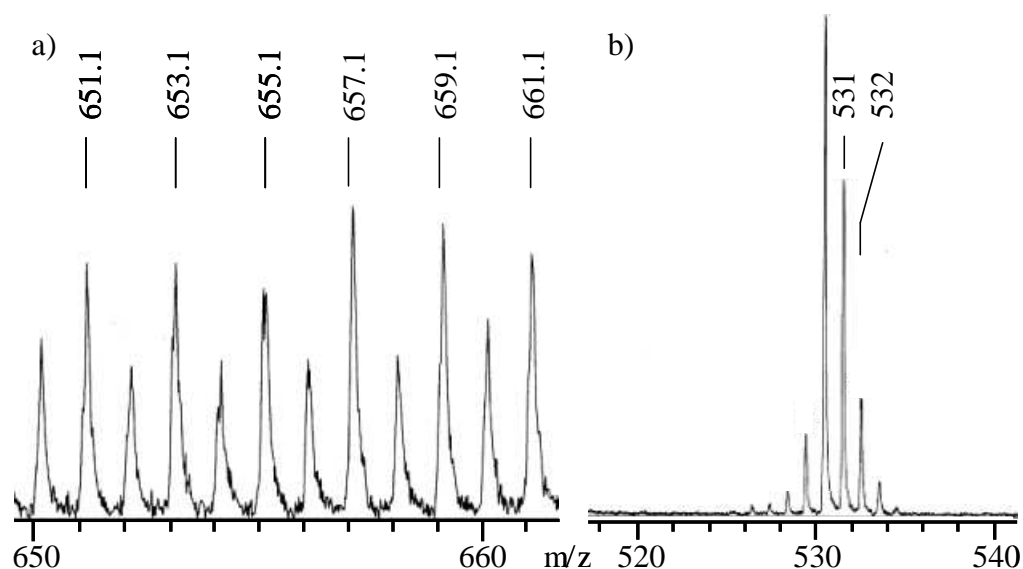


Figure VI-3. a) Detail of the mass range 650 to 660 Da of the MALDI-TOF spectrum shown above in Figure VI-2. On the right b) the MALDI-TOF spectrum of CHNT (C₃₇H₅₄S) as reference compound.

Since nitrogen compounds are removed in the work-up of the sample, resulting in a nitrogen content of <0.05 % (elemental analysis), signals at odd masses can be explained to a certain extent by the isotopic abundance of ¹³C. However, the odd masses are still somewhat more abundant than calculated from the presence of this isotope. The calculated intensity for the [M+1]-signal of a molecule containing 35 carbon atoms is 38 %, but the observed intensity is higher than 50 %. This is in agreement with the results for CHNT shown in the mass spectrum in b).

3 MALDI-TOF-MS of Chromatographically Cut Fractions

Chromatographic workup steps using LEC and GPC have been exploited in detail. This has been described in Chapter V: “Liquid Chromatography of Vacuum Residues”, and now the achieved improvements in the mass spectra obtained from chromatographic sub-fractions shall be discussed.

3.1 MALDI-TOF-MS of GPC Fractions Obtained with Weak Solvent

One major goal was a distinctive reduction of the mass range distribution in the sub-fractions through gel permeation chromatography. As described in Chapter V5 (p. 46), this could not be achieved. The mass ranges in individual sub-fractions of the LEC fraction of

the vacuum residue feed, cut with GPC using weakly solvating solvent, are also broad as can be seen from the data in Table V-F. A corresponding MALDI-TOF mass spectrum of the fraction cut from 14.5 to 15 min. is shown below in Figure VI-4

Although signals still cover masses over a wide range in the spectrum depicted in Figure VI-4, one can see that a certain structuring has been achieved by GPC fractionation. A distinctive pattern can be observed as signals with high intensity appearing at 12 or 14 mass unit intervals up to ~ 700 m/z. A mass difference of 14 units can be explained by the presence of homologous series, involving the addition of a methylene group to the molecule. A mass difference of 12 can occur through addition of a methylene group and at the same time formation of a ring in the molecule, resulting in a net addition of only one carbon atom.

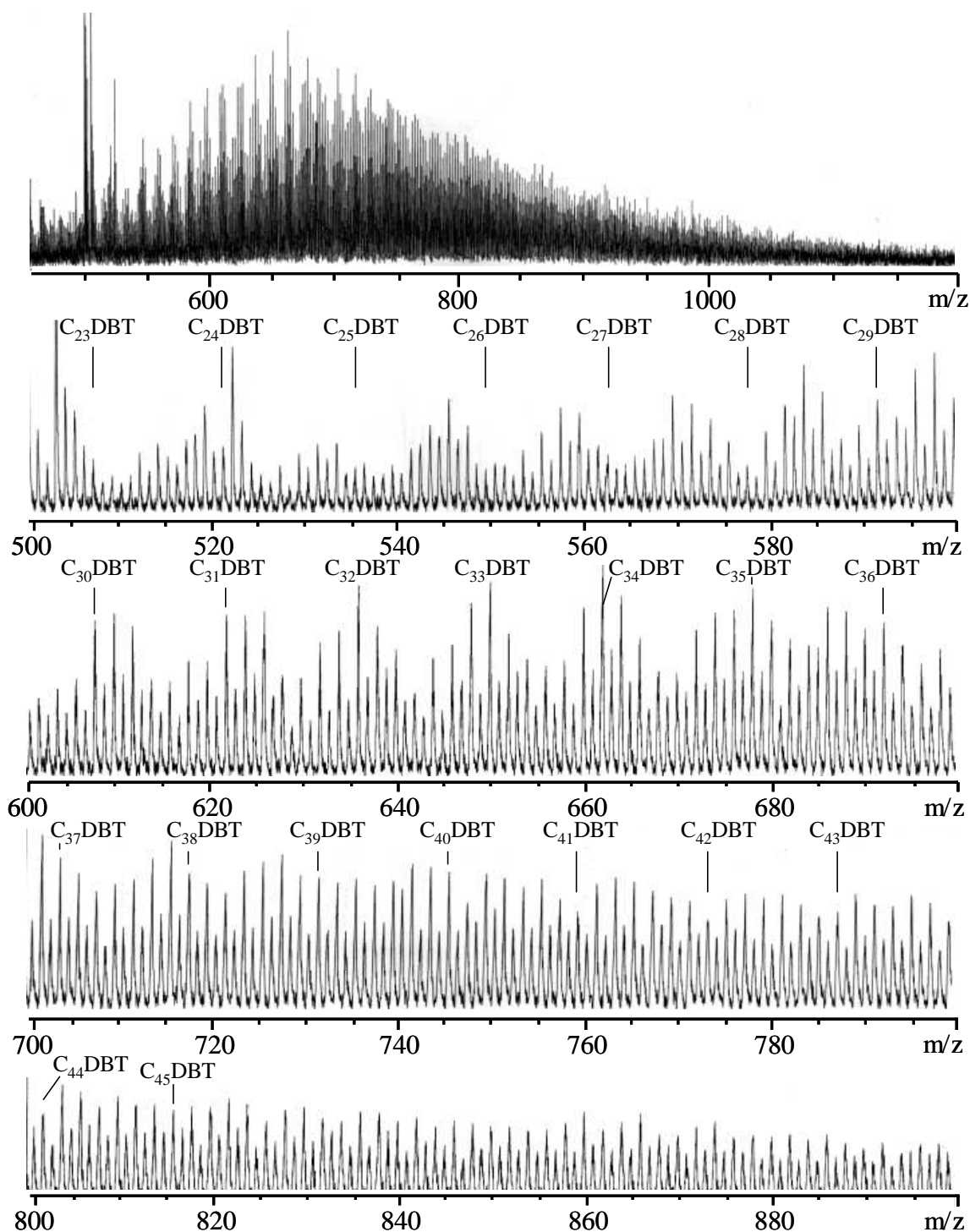
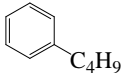
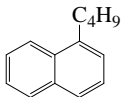
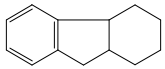
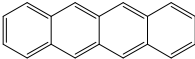
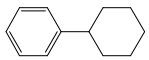


Figure VI-4. MALDI-TOF-MS of a GPC sub fraction cut from 14.5 to 15 min (with strongly solvating solvent) of the PASHs of the effluent. Signals that share masses with the series of alkylated DBTs are indicated with the corresponding number of alkyl carbon atoms. Matrix was DCTB.

In the mass spectrum depicted in Figure VI-4, mass signals that share masses with protonated alkylated DBTs are labeled with the number of carbon atoms in alkyl groups.

The identification of various homologous series in MALDI-TOF-MS spectra is based on nominal mass (NM) of the signals. The NM is the exact mass rounded to the nearest integer. A distinction between PASHs and PAHs is not clear-cut. The occurrence of other hetero atomic species is unlikely but cannot be completely excluded from the elemental analysis. The differentiation between series is impossible from the data given if species of two series share nominal masses or their masses are spaced apart by multiples of 14 mass units. Indenylthiophene (172 NM) and indanylthiophene (200 NM) differ by 28 mass units, therefore homologues from both series with molecular weight of 200 NM or higher cannot be distinguished based on MS data. The same problem arises between PASH and PAH series as well, as PAHs with identical NMs to PASHs cannot be excluded. Table VI-A lists some examples for PASHs and PAHs that share the same NM.

Table VI-A. Parent structures for homologue series of PASHs and PAHs, which are indistinguishable by nominal mass resolution mass spectrometry.

PASH	NM (PASH)	NM (PAH)	PAH	Structure
Benzothiophene	134	134	butylbenzene	
Dibenzothiophene	184	184	butylnaphthalin	
Indenothiophene	172	172	hexahydrofluorenone	
Indanylthiophene	200	228	benzo[b]anthracene	
Phenylthiophene	160	160	hexahydrobiphenyl/ phenylcyclohexane	

Although the hydrocarbon structures listed in the last column in Table VI-A might be present in the aromatic fraction obtained from petroleum samples, they are not expected to elute in fraction two of the Pd(II) column, which was investigated in this experiment.

3.2 MALDI-TOF-MS of GPC Fractions Obtained with Strong Solvent

The LEC fraction 2 (PASH) of the vacuum residue effluent has been fractionated in another experiment by the use of a more strongly solvating solvent, meaning a lower influence of the aromaticity of the analytes on the retention. A similar fractionation than

the one previously discussed was obtained. The mass distributions of the obtained sub-fractions are listed in Table V-E, p. 52. The corresponding GPC chromatogram is shown in Figure V-11 on p. 52.

Although a large range of masses is present in the mass spectrum of each investigated GPC sub-fraction, those spectra obtained from fractions by using GPC with strong solvent appear much more structured than the previous ones obtained with a weaker solvent. The mass spectra of the sub-fraction collected between $11\frac{1}{3}$ and $11\frac{2}{3}$ min. is depicted in Figure VI-5.

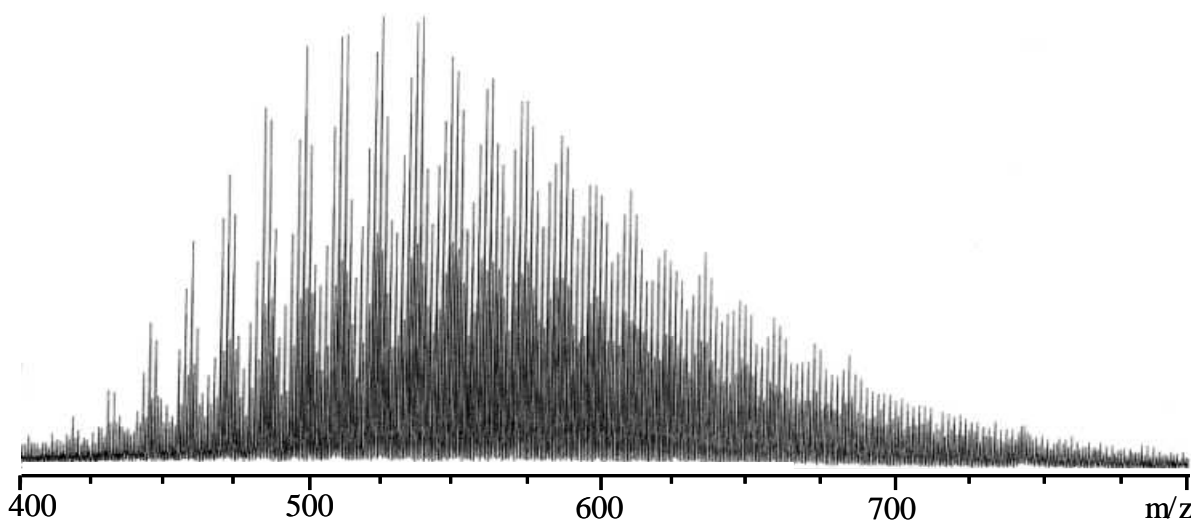


Figure VI-5. MALDI-TOF-MS of fraction 11 of the GPC separation (Figure V-11, p. 52) of LEC fraction 2E (PASHs) of the effluent.

Signals at even and odd nominal masses are present in the spectrum, similarly to the previous experiment using a weak solvent, with those signals at odd numbers originating from protonated molecules containing purely ^{12}C and the less intense ones at even masses from species containing one ^{13}C . Despite the huge mass range covered by components in the sub-fraction these signal groups are much more pronounced than those observed in the GPC fractionation obtained using weak solvent as mobile phase. Figure VI-6a) – c) depicts segments of the mass spectra (Figure VI-5) in greater detail. Signals that share masses with alkylated BTs and DBTs are indicated and the number of carbon atoms in alkyl chains is given in the Figure.

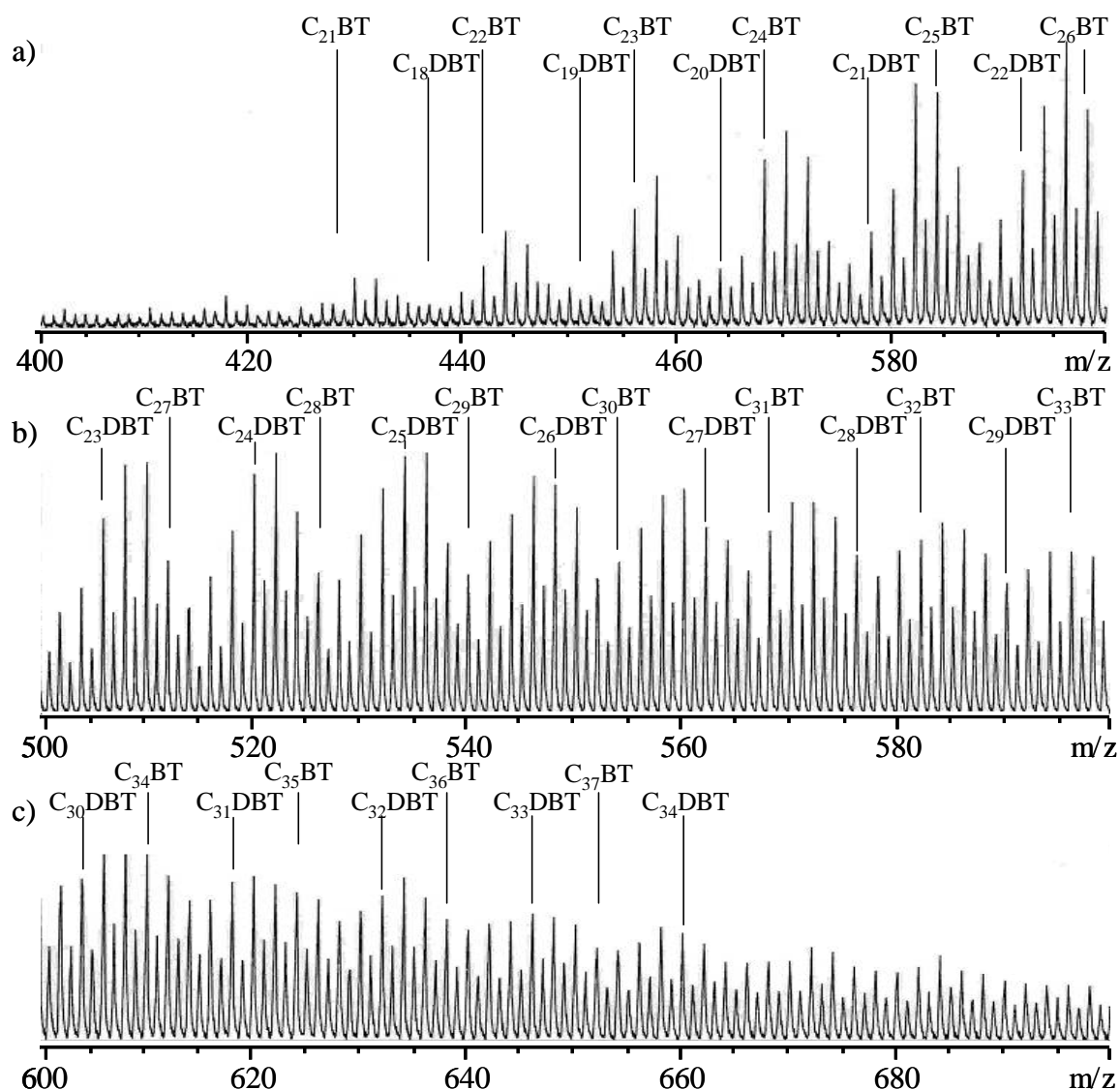


Figure VI-6. Detailed segments the spectra shown in Figure VI-5. Signals that share masses with the series of alkylated DBTs and BTs are indicated with the corresponding number of alkyl carbon atoms. Matrix was DCTB.

Figure VI-6a) and b) expand the mass ranges from 400 to 500 Da and 500 to 600 Da, respectively. Distinct signal groups spaced 12 Da apart are apparent. Higher masses from 600 to 700 Da are shown in c). These signal groups are less distinct due to the increasing probability for one ^{13}C in heavier molecules. Additionally, there is an increase in the number of possible isomers and the chance for naphthenic rings in the structures with the size of the molecules.

One can conclude from the regular spacing of the signal groups that homologous series, which feature a mass difference of 14 Da (CH_2), are present over a wide mass range in the

obtained sub-fractions. The distinct pattern of intense signals, spaced apart by an increment of 12 Da, is caused by different homologous series that share the same mass range. This observed increment of 12 Da suggests that the structures at increasing average molecular weight feature a decrease in saturation in addition to a higher number of methylene groups. The online UV data obtained during the GPC fractionation provide evidence against the occurrence of large condensed aromatic systems. The decrease in saturation can thus either be explained by an increasing number of naphthenic rings in the structures or by the presence of additional, uncondensed aromatic rings.

VII HIGH RESOLUTION MASS SPECTROMETRY

Mass spectrometers with a resolution higher than $\sim 10,000\ m/\Delta m$ are considered to be high-resolution instruments. This high resolution enables the determination of elemental compositions behind a mass signal. Although several instrument designs are capable of such resolution the Fourier transform spectrometers dominate this field. Since it is a relatively new technique with enormous resolution power and has a strong impact on this work, special focus in this chapter will be on Fourier transform ion cyclotron resonance mass spectrometry. This chapter first will give an overview about the instrument used in this work, starting with ionization techniques and secondly describing the mass analyzer. Then the data processing, especially of high resolution and high accuracy spectra of complex mixtures, and the sorting algorithm developed for data interpretation of vacuum residue samples will be discussed.

1 Ionization Techniques

After injection of a sample into the mass spectrometer the analytes must be charged prior to mass separation and detection. For ionization a great number of mechanisms and instrumental setups can be applied. Figure VII-1 shows the capability and limitation of common ionization methods. Generally, polar compounds with heteroatoms are more readily ionized than nonpolar ones. Aromatic molecules can be classified as nonpolar, but not to the same extent as aliphatic hydrocarbons.

In this work MALDI, atmospheric pressure chemical ionization (APCI), and electrospray ionization (ESI) were utilized for the ionization of aromatic molecules and residue fractions with strong aromatic character. The energies used for ionization in these techniques are weak in comparison to other ionization techniques ($\ll 30$ electron volt).

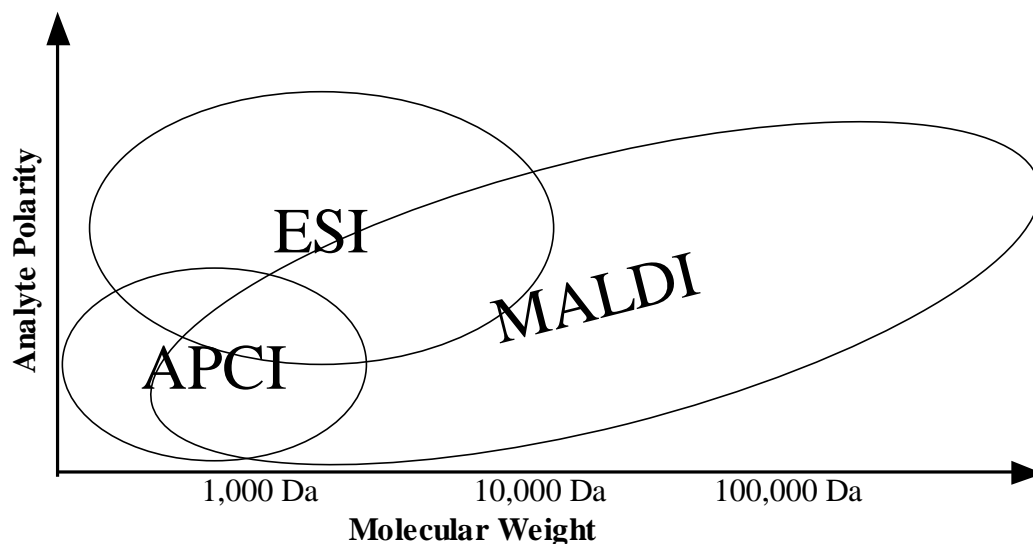


Figure VII-1. Comparison of the usability of atmospheric pressure chemical ionization (APCI), electrospray ionization (ESI) and matrix assisted laser desorption ionization (MALDI) in dependence on analyte polarity and accessible molecular weight.

Since ions produced under these conditions are quite stable, fragmentation usually does not occur. Therefore all of these techniques allow a “soft” ionization with low rate of fragmentation of analyte molecules. Thus the resulting mass spectra effectively feature only molecular ions.

1.1 Electrospray Ionization (ESI)

A solution of the analytes in a polar solvent like acetonitrile, methanol, dichloromethane or an aqueous solution with such an organic modifier is sprayed from a fine capillary into a high voltage field. The aerosol is dried in a heated capillary or heated nitrogen gas. Evaporation removes the solvent from the charged droplets in the aerosol. The solvent should have a low boiling point to support this process. The increase in Coulomb repulsion over surface tension results in Coulomb explosions. Several repetitions leave the analytes charged [78], they finally enter the mass spectrometer (and vacuum system) through a skimmer. The resulting spectra of polar analytes with a high molecular weight often show multiply charged $[M+nH]^{n+}$ ions. Both negative (deprotonated) and positive (protonated) ions are formed by reversion of polarity. Usually, electrospray ionization is the method of choice for proteins, oligonucleotides or metal complexes. However, the sample must be soluble in low boiling solvents. ESI of less polar analytes is

often improved by addition of metal ions that form charged complexes. PAHs and PASHs have been analyzed by addition of silver nitrate [79, 118] and palladium chloride [76, 81], respectively.

1.2 Atmospheric Pressure Chemical Ionization (APCI)

Atmospheric pressure chemical ionization (APCI) is comparable to ESI as the setup of both sources is similar. A solution of the sample in polar organic solvents or water is sprayed from a capillary with a heated sheath gas. The aerosol is further heated to form vapor. In addition to the electro-hydrodynamic spraying process used in ESI, a corona discharge needle is positioned in the vapor to create a plasma, in which proton and charge transfer occurs. Initially, the polar solvent molecules are charged, later they react with the less polar analytes by protonation or deprotonation. Depending on the solvent, only quasi-molecular ions like $[M+H]^+$, $[M+Na]^+$ and M^+ (in the case of aromatic compounds) are produced. To a small amount fragmentation can happen in the plasma, but unlike ESI multiply charged ions are usually not observed. Accessible analytes are less polar compounds and with lower molecular weight ($\sim 1,500$ Da) compared to ESI; aromatic compounds by and large are easily ionized.

2 Mass Analyzer

After a preferably reproducible, sensitive and matrix independent ionization the separation of the ions occurs according to their mass to charge ratio. All mass analyzers use electric and/or magnetic fields to apply force on ions. From

$$F = ma \quad (\text{eq. 4.})$$

(Newton's second law)

and

$$F = q(\vec{v} \times \overline{B_0}) \quad (\text{eq. 5.})$$

(Lorentz' force law)

with:

F	force applied to the ion
m	mass
a	acceleration
q	charge
E	electric field
$\mathbf{v} \times \mathbf{B}$	vector cross product of ion velocity and applied magnetic field

follows that ions are always separated according to their mass-to-charge ratio (m/z) rather than their mass alone. Six basic principles can be applied for mass separation in spectrometers¹⁴:

- 1) magnetic and sector field separation,
- 2) quadrupole mass filter
- 3) ion trap
- 4) resonance in a ion cyclotron resonance cell
- 5) time of flight or drift
- 6) mass accelerator

The separators are evacuated to high (10^{-1} Pa to 10^{-4} Pa) or ultra high vacuum ($< 10^{-5}$ Pa). Depending on field strength and/or geometry and number of electrical charges on an analyte diverse mass ranges can be accessed. Accuracy, resolution, limit of detection, accessible mass range and spectra acquisition time vary with the used principle and setup.

Mass resolution and resolving power for an ion of mass to charge ratio m/z may be defined as:

$$R = \frac{(m/z)}{\Delta(m/z)} \quad (\text{eq. 6.})$$

(mass resolution)

Usually $\Delta(m/z)$ is defined as spectral peak width at half peak height for an isolated signal, but $\Delta(m/z)$ can be defined as peak separation $(m_2/z_2) - (m_1/z_1)$, corresponding to a 10 % valley between two signals of equal magnitude:

¹⁴ K. Cammann, Hrsg. "Instrumentelle Analytische Chemie", Spektrum Akademischer Verlag GmbH, Heidelberg, Germany.

$$R = \frac{(m_1 / z_1)}{\Delta(m / z)} = \frac{(m_1 / z_1)}{(m_2 / z_2) - (m_1 / z_1)} \quad (\text{eq. 7.})$$

(mass resolution, 10 % valley, equal peak heights)

The valley definition depends not only on peak shape, width and separation but also on the relative heights of both peaks. Obviously the resolving power required by equation 7 is greater than that for equation 6 for a similar mass separation.

2.1 Ion Cyclotron Resonance (ICR) Mass Spectrometer

There are two principal trapped-ion mass analyzers: three-dimensional quadrupole ion traps ("dynamic" traps) and ion cyclotron resonance mass spectrometers ("static" traps). Both operate by storing ions in the trap and manipulating the ions by using direct current and radio frequency electric fields in a series of carefully timed events. The static trap has some unique properties which presently lead to the highest reachable mass resolution. It is a high-frequency mass spectrometer in which ions with a selected mass/charge ratio absorb energy through a high-frequency field perpendicular to a constant magnetic field. Maximum energy and excitation is gained by ions that satisfy the cyclotron resonance condition. The general principle is now described.

2.1.1 Principal of Operation: ICR

The Lorentz force F (p. 70) forces ions on a circular path in a magnetic field. The cyclotron frequency of an ion's circular motion depends on mass to charge ratio. By measuring the cyclotron frequency the ion's mass can be determined. The centripetal force ($F = \frac{mv^2}{r}$) balances the Lorentz force experienced by any ion in a magnetic field:

$$\frac{mv^2}{r} = qvB_0 \quad (\text{eq. 8.})$$

Solving for the angular frequency (ω) leads to the fundamental ICR equation:

$$\omega = \frac{qB_0}{m} \quad (\text{eq. 9.})$$

with

ω angular frequency

m : ion mass
 q : electric charge
 B_0 : external magnetic field
 r : radius of circular ion path
 v : ion velocity

A group of ions of the same mass to charge ratio will have the same cyclotron frequency, but they will move independently out of phase (at roughly thermal energies). If an excitation pulse (a radio-frequency electric field perpendicular to the magnetic field) is applied at the cyclotron frequency ions will absorb energy and their orbit increases. This set of ions moves close to the receiver plates in the ICR cell and induces detectable image currents that can be amplified and digitized. The signal induced in the receiver plates depends on the number of ions and their distance from the receiver plates. A schematic representation of a cubic FT-ICR cell is shown below in Figure VII-2.

2.1.2 Fourier Transform Ion Cyclotron Resonance (FT-ICR) Mass Spectrometer

If ions of several different masses are present in the cell an excitation pulse that contains components at the entire cyclotron frequencies must be applied. The cyclotron motion of all ions is essentially excited simultaneously and coherently by using a rapid frequency sweep ("chirp"), an "impulse" excitation or a tailored waveform. The image currents induced in the receiver plates contain frequency components originating from all different mass to charge ratios. The various frequencies and their relative abundances can be calculated by using a Fourier transformation, which converts the time-domain data (the image currents) to a frequency-domain spectrum that then results in the mass spectrum (eq. 9, p. 72).

The excited cyclotron motion of the ions is subsequently detected on receiver plates as a time domain signal that contains all the excited cyclotron frequencies. Fourier transformation of the time domain signal results in the frequency domain FT-ICR signal which, on the basis of the inverse proportionality between frequency and mass to charge ratio, can be converted to a mass spectrum.

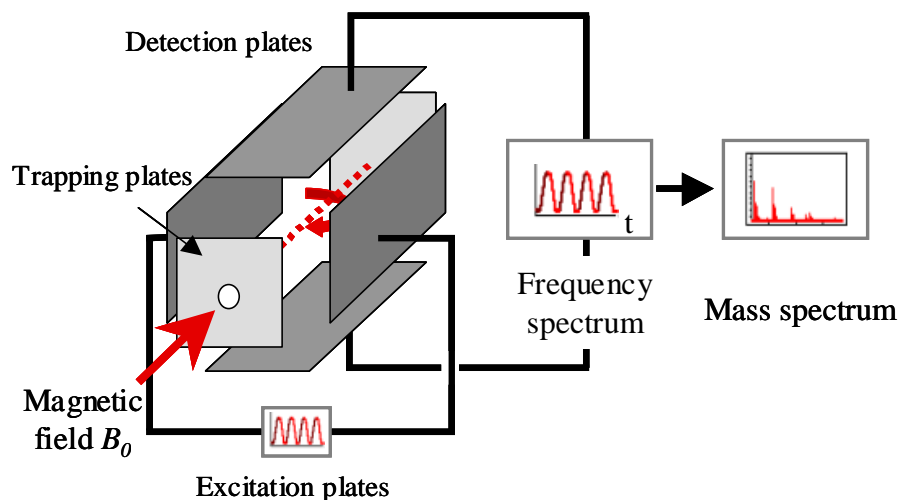


Figure VII-2. Scheme of a cubic FT-ICR cell.

As can be seen in Figure VII-2 the cubic ICR cell consists of three pairs of parallel plates. The functions of the excitation and detector plates are evident from the above discussion. As the magnetic field does not constrain ion motion along the direction of the applied magnetic field, a small potential is applied to the trapping plates to keep the ions contained within the ICR cell. Since the measuring is not destructive, ions can be re-measured repeatedly and the spectra accumulated to increase the limit of detection. On the other hand excitation events can be employed to increase the kinetic energy of ions to eject them. Ions of a given mass to charge ratio are expelled from the cell by increasing the orbital radius until they are lost by collisions with the cell walls.

The pressure in an ICR cell should be very low to minimize ion-molecule reactions, space charge effects and collisions that damp the coherent ion motion. Space charge effects describe the interaction of ions with each other. Even though this interaction is small, it can be a source of systematical errors and it is crucial to control mass accuracy with internal standards. Although super conducting magnets providing a fairly time stable mass calibration are used, best mass accuracy is obtained when additionally internal calibrants are used.

3 High Accuracy Data Interpretation

Due to the tremendous resolution power of FT-ICR instruments of below 1 ppm, the accuracy of measured signals is sufficiently precise to calculate the underlying elemental compositions [87]. Ions lighter than 300 Da measured with a precision of 1 ppm allow determination of the molecular weight with a resolution lower than ± 0.3 mDa (= mamu for comparison: The weight of an electron is 0.549 mamu). This very high resolution is sufficient to distinguish almost any given combination of relevant isotopes (^{12}C , ^{13}C , ^1H , ^{14}N , ^{16}O , ^{32}S , and ^{34}S) [87]. Marshall et al. [86, 87] and others [93] used high accuracy data for such assignments. Samples that cover higher mass ranges, however, need special considerations as the number of possible elemental composition increases dramatically and the resolution of the mass spectrometer decreases towards higher masses. This is discussed in detail below (see p. 77).

Compounds in fossil fuel samples can contain both atoms of typical organic molecules (C, H, N, O, and S) as well as metals like V, Ni or Fe, but in aromatic fractions the occurrence of elements is limited to the first mentioned group. High-resolution mass data analysis uses the masses of the most abundant isotopic pattern of molecular ions to identify series of homologues in the spectra. As the molecular weight of the sample increases, the contribution of less abundant isotopes goes up, too. A hydrocarbon with molecular weight of approximately 300 Da has about 21 carbon atoms¹⁵. Since ^{13}C isotopes have a ~1.1 % natural abundance, approximately $\frac{1}{4}$ of the hydrocarbon molecules will contain one ^{13}C atom and therefore feature an odd nominal mass. For a hydrocarbon with 46 carbon atoms (~650 Da) about half of the molecules feature one ^{13}C atom, thus even and odd masses are of equal intensities in the mass spectra. Signals from molecules including other isotopes, e.g. ^{34}S with ~4 % natural abundance are also present. However, they contribute only to signals of comparably weak intensity (about 1/25 to 1/9 of the corresponding pure ^{32}S compound, if one to three sulfur atoms per molecule are assumed), because unlike hydrogen and carbon those elements appear in much smaller numbers in a given molecule.

¹⁵ 21 carbons or more, depending on degree of saturation Z.

Table VII-A. Data for elements expected in the aromatic fraction of a vacuum residue.

Element	Expected number in sample	Most abundant isotope	Less abundant	Least abundant
Carbon	20 - 90	^{12}C 98.93 %	^{13}C 1.07 %	
Hydrogen	20 - 180	^1H 99.985 %	^2D 0.015 %	
Sulfur	0 - 5	^{32}S 94.93 %	^{34}S 4.29 %	^{33}S 0.76 %
Oxygen	0 - 5	^{16}O 99.757 %	^{18}O 0.205 %	^{17}O 0.038 %
Nitrogen	0 - 5	^{14}N 99.63 %	^{15}N 0.37 %	

Although carbon has a lesser natural abundance for the ^{13}C isotope of only 1.1 %, the chance for finding one ^{13}C nucleus in a molecule is about 50 % for a molecule with 45 carbon atoms. Since the investigated sample contains molecules with an average number of carbon atoms of 40 one can expect that for at least 43 % of a molecule's population ^{13}C can be detected. Table VII-A lists data on all isotopes of the elements expected for vacuum residues. For the discussed reasons a generally observable formula contains:

$$^{12}\text{C}_{(c-x)}\ ^{13}\text{C}_x\text{H}_{(2c-Z)}\text{N}_n\text{O}_o\text{S}_s \quad (\text{eq. 10.})$$

with:

c : total number of carbon atoms

x : number of ^{13}C carbon isotopes

Z : hydrogen deficiency (type) of the elemental composition

n : number of ^{14}N nitrogen atoms

o : number of ^{16}O oxygen atoms

s : number of ^{32}S sulfur atoms.

In petroleum analysis, a compound is typically characterized by its class and type. A compound's type is commonly designated by the hydrogen deficiency (Z) value, followed by elemental symbols of heteroatoms and coefficients that are greater than zero (class). The class „PAH“ or simply „H“ designates pure hydrocarbons. In this way, compounds are specified by Z and n, o and s. Homologues of a compound type are given by the carbon distribution number n, which stands for the number of methylene groups ($-\text{CH}_2-$) in the formula. The presence of ^{13}C isotopes is denoted by an asterisk preceding the carbon symbol (*C), but isotopes do not change the class or type a given formula. E.g., benzothiophene contain the following most abundant isotopically substituted species

$^{12}\text{C}_8\text{H}_6^{32}\text{S}$, $^{13}\text{C}^{12}\text{C}_7\text{H}_6^{32}\text{S}$, $^{12}\text{C}_8\text{DH}_5^{32}\text{S}$, and $^{12}\text{C}_8\text{H}_6^{34}\text{S}$, all being the first member of the 10S1 series. Homologues also will consist of more than one isomer. For example, 10S1 n designates benzothiophenes($\text{C}_8\text{H}_6\text{S}$ with $n(\text{CH}_2)$) as well as thiophenes with three rings or double bonds in aliphatic side chains($\text{C}_4\text{H}_4\text{S}$ with $n+4(\text{CH}_2) -6\text{H}$) or even thioethers with hydrogen deficiency only in hydrocarbon side chains($-\text{S}-$ with $n+8(\text{CH}_2) -12\text{H}$).

However, Z being negative and attaining the value -2 for a compound with no rings or double bonds, this definition is inconvenient in the present discussions and therefore the sum of rings and double bonds is defined as double bond equivalent (DE):

$$\text{DE} = \text{R} + \text{DB} \quad (\text{eq. 11.})$$

R: number of rings

DB: number of double bonds

For PAHs and PASHs, the relationship between DE and Z is simple: $\text{DE} = \text{Z}/2 + 1$.

As mentioned before, ICR resolving power alone is not sufficient to assign elemental compositions at higher molecular masses [87]. At lower masses established series of homologues can be applied [2] to extend the upper mass limit for unique assignment of elemental compositions to more than 900 Da. Members of such series are spaced at fixed intervals (14.01565 Da), the mass of a methylene group, in the mass spectra. Series of surely detected types can be “filled” with homologues. For a series designated by 10S1, for example that extends up to 900 Da, members with up to 55 methylene groups can be assigned using this procedure, which means an elemental composition of $\text{C}_{63}\text{H}_{116}\text{S}$ is assignable.

3.1 Kendrick Mass Scale

A visually display showing all resolved data from one broadband spectrum with about 800 Da mass range would have a length of about 200 m. Therefore a more compact display containing all data is useful. Since there are natural gaps in a typical mass spectrum at values where no commonly encountered ions have masses, it is possible to “slice” the spectra into 1 Da segments [119]. These segments then are scaled according to their mass defect (difference between exact and nominal mass) and rotated 90°. Stacking of the spectra segments leads to a compact pseudo two-dimensional display where mass defect is plotted against nominal mass. This is shown in Figure VII-3. The discussed series of

homologues appear as straight lines in such a plot, spaced at 14 units of nominal mass axis (x) and 0.01565 on the mass defect axis (y). The 0.01565 Da steps of the mass defect for each homologue result from the two hydrogen atoms added with a methylene group. These regular intervals allow the determination of molecular class and type simultaneously over a wide mass range within a single display.

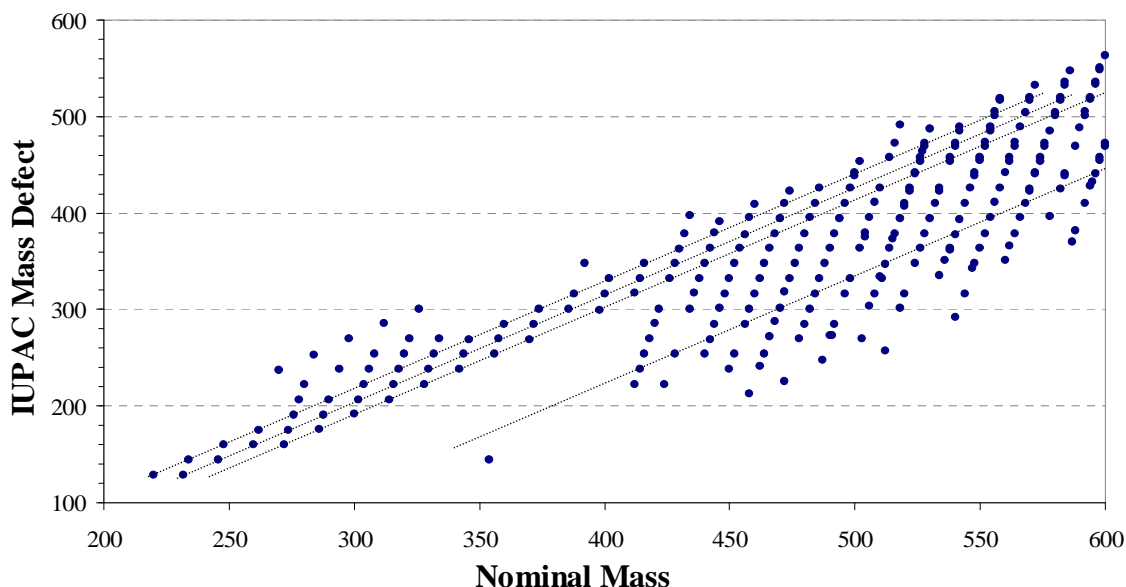


Figure VII-3. Plot of nominal mass (IUPAC scale) against mass (IUPAC scale) defect. Notice the straight lines, which denote members of same chemical class and type.

Kendrick suggested 1963 the use of a methylene unit as base of a mass scale, with mass (CH_2) = 14.000000 [120]. The mass defect of a compound is thus directly linked to class and type. As methylene groups do no longer contribute to it, all homologues share the same Kendrick mass defect (KMD). If KMD is plotted against Kendrick nominal mass (KNM) the skewed display of Figure VII-3 is converted into a rectilinear display. Now signals of compounds of different class and type are separated in horizontal lines. Those displays are further referred to as Kendrick mass plots. Kendrick mass plots of the investigated vacuum residue aromatics are extensively discussed in chapter VII6.3.1, p.98.

3.2 Software Aided Data Analysis

Vacuum residues are very complex mixtures with thousands or even millions of components. Even after several chromatographic pre-separations the fraction of aromatic

compounds includes thousands of hydrocarbons, PASHs and other heterocycles in minor quantities. Single MALDI ICR spectra of such a fraction of the investigated residue fractions revealed about one thousand distinct signals each. With APCI more than 1,500 signals could be found. Obviously, for data sets of this size manual interpretation is cumbersome and time consuming. Present personal computers have sufficient calculation power to perform elemental composition assignment if mass resolution is sufficient. Molecular weight calculator¹⁶ is a suitable program for this task. It has customizable settings (like isotopes and number of possible atoms, required precision) and allows batch computation of multiple mass signals. Conversion of mass data to Kendrick mass in combination with plotting of KMD against KNM then reveals series of homologue compounds. Methods for data interpretation by taking advantage of homologue series and related compound classes of such complex spectra are described in the literature [87, 119, 121, 122], but scanty in crucial details. Thus, a major effort in this thesis was the invention of a computer-supported procedure that reliably assigns class, type, carbon number and elemental composition to mass signals in high-resolution MS data.

A three-step procedure was established for computer supported data analysis. A scheme of the procedure developed is given in Figure VII-4. The raw data were recorded on a 7.0 Tesla APEX III ICR cell MS using the instrument developers' software¹⁷. After spectra acquisition and calibration followed the selection of mass signals exceeding a threshold value that excluded background noise. This list of masses was exported via word processing software¹⁸ and imported into an Excel¹⁹ spreadsheet. In the first step heteroatoms present in the sample were identified.

¹⁶ LIT6 Molecular weight calculator version 6.25 beta 9 (May 20, 2003) by Matthew Monroe is freeware and accessible at <http://alchemistmatt.com>

¹⁷ MIDAS software. Bruker APEX III Fourier transform ion cyclotron resonance mass spectrometer (Bruker Daltonics, Bremen, Germany), equipped with 7 T magnet.

¹⁸ Notepad, provided as part of Windows XP, professional release, Microsoft.

¹⁹ Excel 2000, (9.0.2812), part of Office2000, Microsoft.

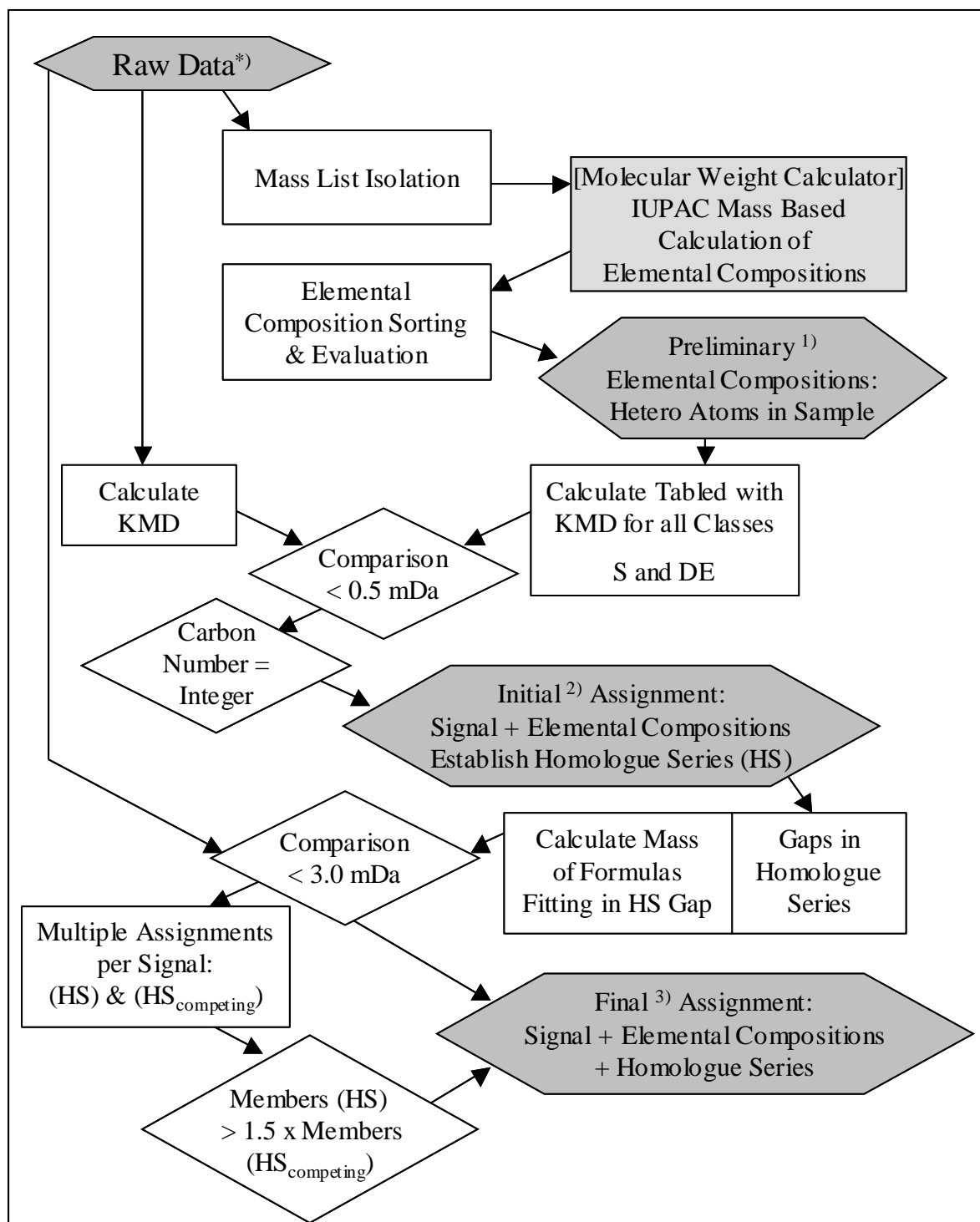


Figure VII-4. Flow diagram of the data analysis procedure developed for this work. Data are illustrated in gray hexagons, rhombs show decision criteria and squares contain calculation and sorting routines. *) Data from the MIDAS software for FT-MS control. ¹⁾, ²⁾, and ³⁾ are described in the paragraphs 3.2.1 to 3.2.3.

In the second step elemental compositions were assigned with strictest criteria based on tabled KMD. Thus, series of homologues have been established. In the last step gaps in the established series have been filled based on accurate mass and identifications of the previous step.

Of greatest importance for data interpretation, especially for assignment of elemental compositions based on accurate mass, is the number of charges on an observed ion. Only the mass to charge ratio is detectable, thus doubly or higher charged ions would appear at half or smaller m/z and thus be wrongly assigned. It must be stressed here that no evidence for ions with a charge z different from unity have been observed as discussed in chapter VII6.2, p. 96. For this reason a mass signal can be addressed by its mass in Dalton (Da).

3.2.1 First Step: Establishing Preliminary Elemental Compositions

The software molecular weight calculator (MWC) was applied for batch assignment of elemental compositions (for detailed procedure, IX1.2). For this purpose lists of the high accuracy masses without further information (e.g. signal numbers or intensities) were batch converted by MWC via Notepad documents. The resulting thousands of elemental compositions were evaluated in an Excel spreadsheet. Elemental compositions were sorted according to differences between measured and calculated accurate mass and evaluated based on them making chemical sense. Details of the spreadsheet application are given in IX1.3, p. 114. The best fitting composition was assigned, regardless of any homologue series. Results of this first assignment step for all four residue fractions, namely LEC fraction 1 and 2 obtained from each of the vacuum residue aromatic compounds, before and after hydrotreatment, are presented in Figure VII-5 for the classes containing sulfur and/or oxygen. In this step the presence of sulfur and the absence of nitrogen- and oxygen-containing molecules could be shown in agreement with elemental analysis of the whole aromatic fraction. The amount of clusters after derivatization could be estimated as well and is given in Table VII-F on p. 97.

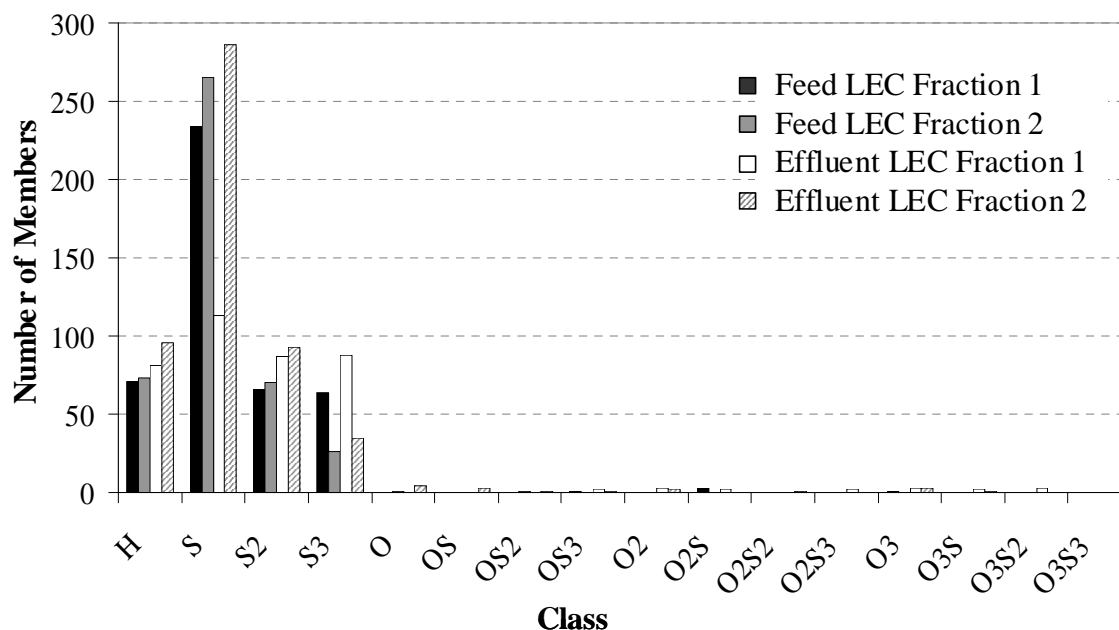


Figure VII-5. Number of members that have been preliminarily assigned by use of “Molecular Weight Calculator” and analyzed with the Excel® spreadsheet “MWCsort.xls” as described in appendix IX1.

The samples shown in Figure VII-5 were derivatized and mass analyzed as described below. The distribution of heteroatoms can be clearly estimated at this point, however, the decisions scheme of that algorithm is based solely on each single mass and results in the elemental composition with the smallest deviation of calculated to measured mass without regard to homologue series present in the sample. This simple computation of probabilities needs to be supported by further processing. Therefore further steps of assignment involving the discussed patterns of homologue series visible in Kendrick mass plots were employed.

3.2.2 Second Step: Tabled KMD to Assign Elemental Compositions

Following the test proving the absence of non-sulfur heteroatoms the raw data were further examined in a self-written Excel spreadsheet application. Details of the procedure and listings of the macros used are discussed in Appendix IX2.1, p. 117. The IUPAC masses were transformed into the Kendrick mass scale. Kendrick nominal mass and mass defect were calculated and compared with tabled KMDs. If a mass measured by FT-ICR-MS differed by less than 0.5 mDa (Kendrick mass scale) from a tabled value a match was considered to be possible. Then, as further evidence for this assignment, the mass of the

parent compound of that KMDs series was subtracted from the measured mass in question. The remaining molecular weight of that mass, representing solely methylene groups, must be divisible by 14 (in Kendrick mass scale) and result an integer number (n). This carbon distribution number n represents the number of methylene groups and ranks the compound in the homologue series. If more than one allocation was possible for a signal, no elemental composition was assigned. The maximal difference in mass of 0.5 mDa required for an assignment equals a resolution of 600,000 for a molecule of ~300 Da weight. A compound of ~800 Da requires a resolution of at least 1.6 Mio. which is not reproducibly achievable even with an FT-ICR instrument.

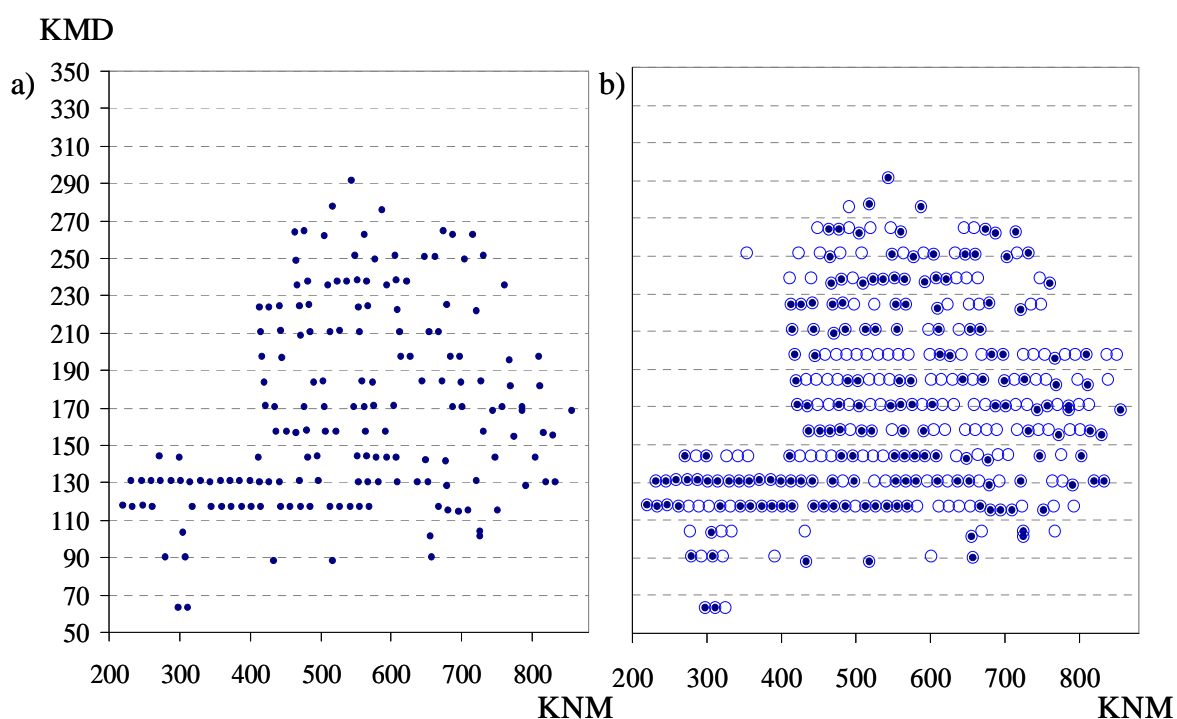


Figure VII-6. Kendrick plot of signals originating from the residue effluent PASH fraction identified as compounds with one sulfur atom after a) initial class and type assignment after the second step and b) final assignments after third step. (•) Refers to S1 initial assignments and (○) to S1 final assignments.

For this reason gaps within the homologue series are evident, if series are established with this procedure. Figure VII-6 a) shows the Kendrick plot after this second step of assignment. Only signals of identified compounds with one sulfur atom in the PASH fraction after ligand exchange chromatograph of the residue effluent are shown.

Not all signals in the spectra could be assigned in this step, especially at higher mass regions gaps of unassigned signals appear. In Figure VII-6 b) white dots mark final assignments while filled dots represent signals identified in the 2nd step for comparison. Most of the gaps in the homologue series could be filled, even in the higher mass range. The third step assignment procedure is now described.

3.2.3 Third Step: Use of Homologue Series for Extended Assignments

In a third step mass signals that were still unassigned were matched up to “gaps” in the established series of homologues. Herein, assignment was based on differences between measured and calculated mass for the missing compound smaller than 3.0 mDa and unrivaled assignment (see also IX2.3). Assignment was considered unrivaled when no other competing series with more than half the number of initially assigned members in the competing homologue series was lying within a 3.0 mDa range. This ensures that the series established in earlier steps with stricter criteria were preferred over stochastically series with few members. The resolution required for a compound of approximately 900 Da molecular weight that is to be assigned within 3.0 mDa is about 600,000 m/ Δ m, which is achieved with the instrument and internal calibration.

4 MALDI FT-ICR-MS Analysis of the Vacuum Residue Aromatics

The FT-ICR-MS measurements with a MALDI ionization interface were inadequately calibrated, so data interpretation as described above was not possible. Nonetheless, data could be used to demonstrate the enormous difference in resolution to the TOF instrument. In Figure VII-7a) the mass spectrum obtained by using the second LEC fraction of the effluent sample is shown, with b) - d) three consecutively expanded sections of this spectrum showing the signal group at one nominal mass.

The signals in this spectrum cover a slightly smaller mass range than those in the corresponding TOF spectra, which might be explained by the smooth decrease of signal intensities as they blend with background noise at higher masses. The signals observed in the TOF spectra at all odd and even nominal masses are resolved in the high-resolution spectra into groups of several distinct signals as can be seen in Figure VII-7c) and d). It must be kept in mind that MALDI generates protonated ions, so that the isotopic pattern is incremented by approximately one Da.

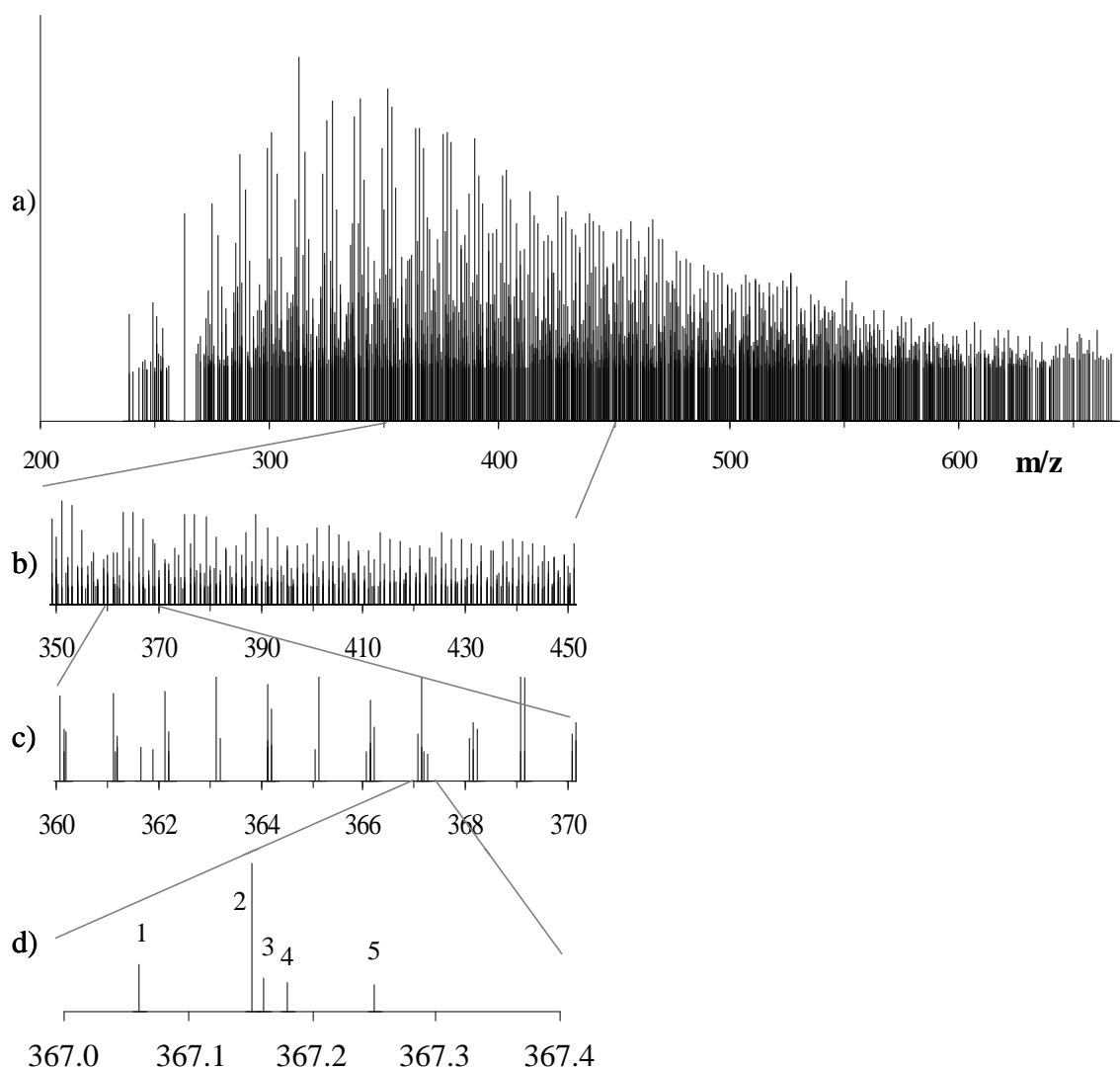


Figure VII-7. a) Mass spectra generated from the raw data of the effluent LEC fraction 2 by a FT-ICR-MS experiment using MALDI as ionization interface. The matrix was DCTB. b) - d) show consecutively expanded sections of the mass spectrum. The numbers in d) are for identification purposes only; those signals could not be assigned to molecules from these data.

Due to insufficient calibration the identification of elemental compositions is not possible from these data, but the signal group shown in d) might be explained by structures belonging to several series, e.g. 1: $C_{24}H_{14}S_2$, 2: $C_{29}H_{18}$, 3: $C_{26}H_{22}S$, 4: not identified, and 5: C_{13} -DBT, based on the nominal mass and the first two digits of each signal. The data presented here agree with that obtained by the use of a TOF-MS. Furthermore, signals that indicate alkylated DBTs not only by NM, but as well by KMD, have been measured. The

presence of hydrocarbons at equal NM masses as PASHs is indicated by KMD values, complicating the interpretation of the spectra measured using MALDI as ion source.

5 APCI FT-ICR-MS Analysis of the Vacuum Residue Aromatics

The APCI experiment has been performed with the use of external calibration. A method has been developed to test the achieved mass accuracy on its value for the assignment of elemental compositions described in Chapter VII3.2, p. 78. The Kendrick mass plot of the whole effluent (not derivatized) is given in Figure VII-8. Distinct horizontal lines at Kendrick mass defects (KMD) are apparent, but the horizontal lines typical for Kendrick plots are somewhat inclined in the Figure. The data have been recalibrated based on the slope of the Kendrick series, but one cannot finally decide between PASH or PAH series without use of an internal calibrant.

5.1 Recalibration

Parallel to and below each of the horizontal lines formed by thick dots at KMDs ranging from 100 to 250 in the center of Figure VII-8 is a second set of smaller signals. Those have been identified by the difference in KMD

between small and thick dots (~ 2.2 KMD) and their ratio of intensities as isotopic pairs caused by ^{13}C in the less intense series. Three series identified in experiments using an ESI interface and derivatized compounds, namely BTs **1**, DBTs **2**, and benzonaphthothiophenes **3** (BNTs), have been assigned in the plot obtained by APCI MS (Figure VII-8). Identification of these series in the skewed plot is based on their average KMDs and isotopic ^{13}C pattern. The three pairs of series are shown in Figure VII-9a. (•)

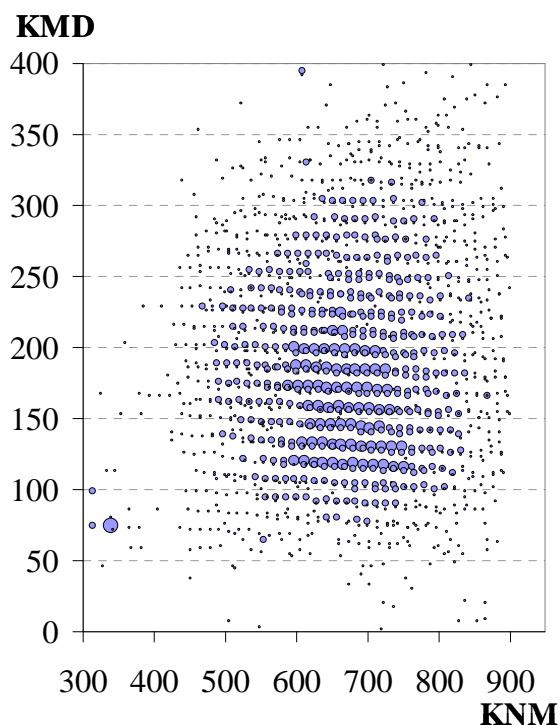


Figure VII-8. Kendrick mass plot of the effluent aromatics. The relative intensity is marked by the size of the dots. APCI with external calibration was used.

indicates elemental compositions with only ^{12}C , (\circ) indicates those containing one ^{13}C isotope. The average slope of the series and the axis intercept of the fitted lines in the figure have been determined and the complete set of data recalibrated. Figure VII-9b shows pairs of series in the recalibrated data with KMDs very close to some PASHs, namely naphthophenanthrothiophenes **4** (NPT, KMD = 278.0, DE = 18) and benzonaphthothiophenes **5** (BPT, KMD = 251.2, DE = 15) or the previously mentioned BNT (KMD = 211.0, DE = 12), DBT (KMD = 170.8, DE = 9), or BT (KMD = 130.6, DE = 6). Of course also other isomers could be present in the residue sample, but the suggested parent structures are benzologues of PASHs identified in another experiment using ESI and they cover the main range of KMDs (130 to 280) observed in the mass spectrum.

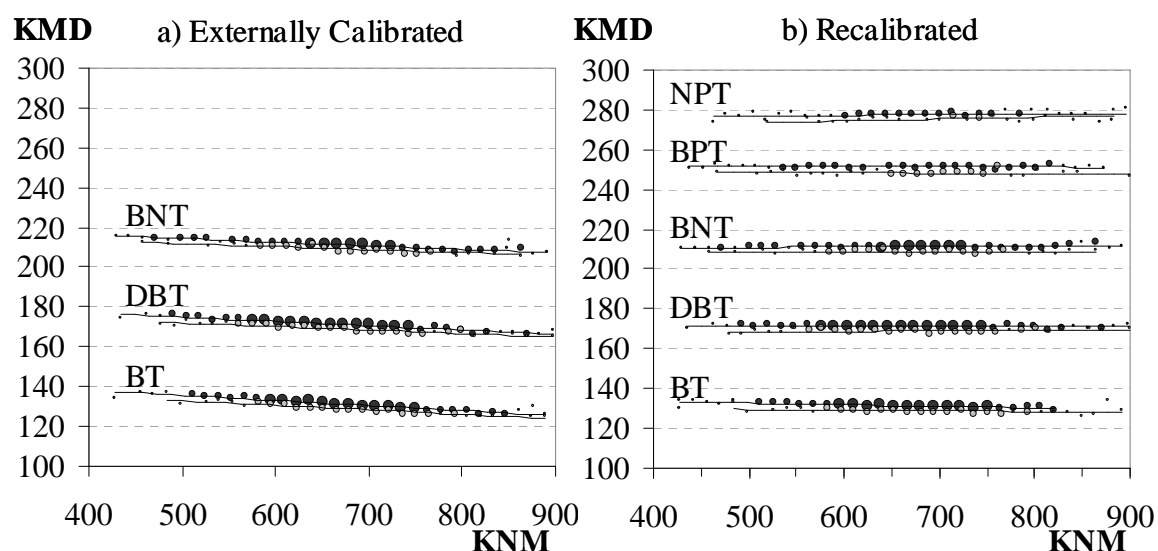


Figure VII-9. Series **1** to **5** in Kendrick plots of a) raw data acquired with external mass calibration and b) same data after recalibration.

The slope of these series depends on the digits of the mass data that determine the KMD (definition of KMD, p. 77) and can be regarded as the contribution of a methylene group being different from zero. The average slope of the three pairs of series in Figure VII-9a) is $(-2.0 \pm 0.4)^{-2}$ [KMD/KNM] which is consistent with a Kendrick mass for CH_2 of 13.99917 Da and not 14.00000 Da. For recalibration all masses have been recalculated by the following equation:

$$M_{\text{recalibrated}} = M_{\text{rawdata}} * (1 - 2.0^{-2}) + b \quad (\text{eq. 12.})$$

This correction slightly “stretches” the mass spectrum so that the KMD of a methylene group is exactly zero. All members in each of the five series in Figure VII-9b) feature the same KMD, so the series appear as horizontal lines. Parent structure (for PASHs assumed), carbon number and molecular weight have been calculated from KMD and nominal mass of each signal. Theoretical and measured masses differ by a constant 1.0015 Da, which is interpreted as b in the equation 12. It has to be mentioned here that if b is increased by an additional 0.00337 Da, the series for a PASH exactly fits a PAH series with a DE more than five. For example, $C_{22}H_{12}$ as parent compound with DE = 17 only differs from BNT with DE = 12 by $\Delta KMD = 3.37$.

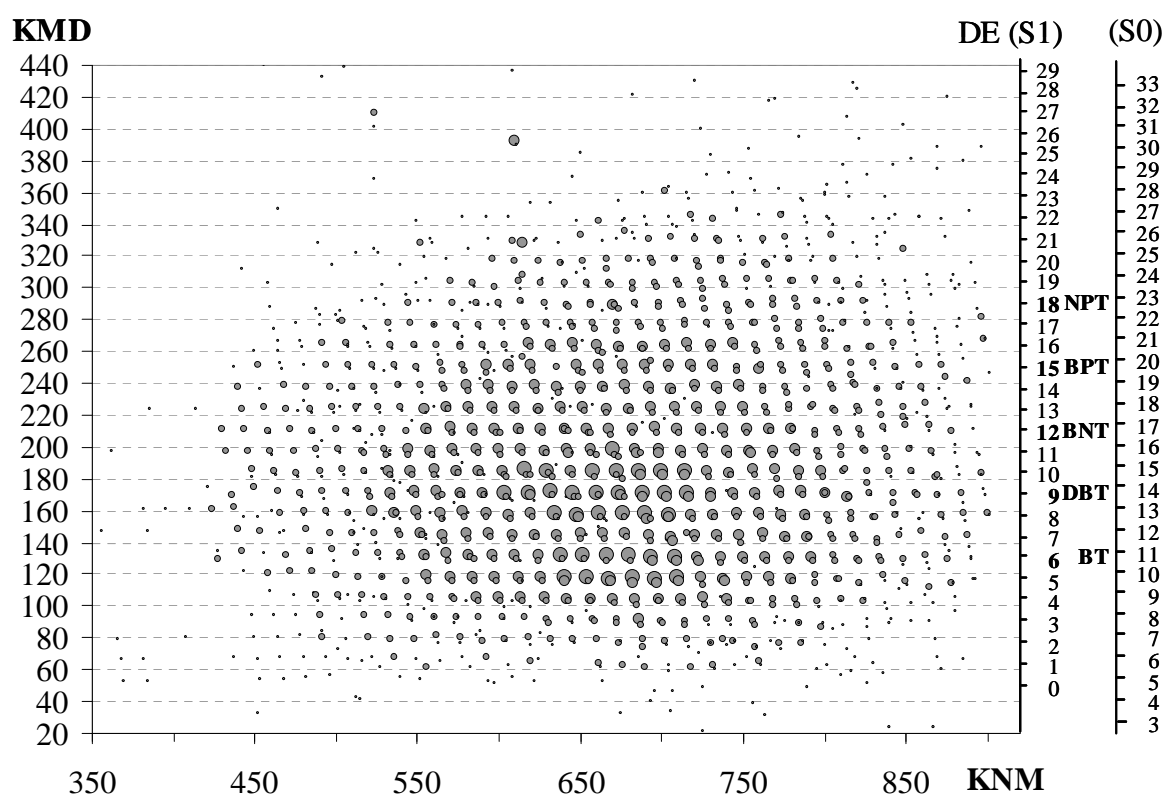


Figure VII-10. Kendrick plot of the effluent aromatics from recalibrated data recorded with APCI ion source. The right axis provides DE values for structures with no (S0) and one sulfur atom (S1).

Therefore it cannot be confidently distinguished between PASHs and PAHs in the spectrum, but regardless which one gives rise to the signal, only one species, S0 or S1, is present in the MS. The complete recalibrated set of data is depicted in Figure VII-10 with DEs for series containing no or one sulfur atom given on the left axis.

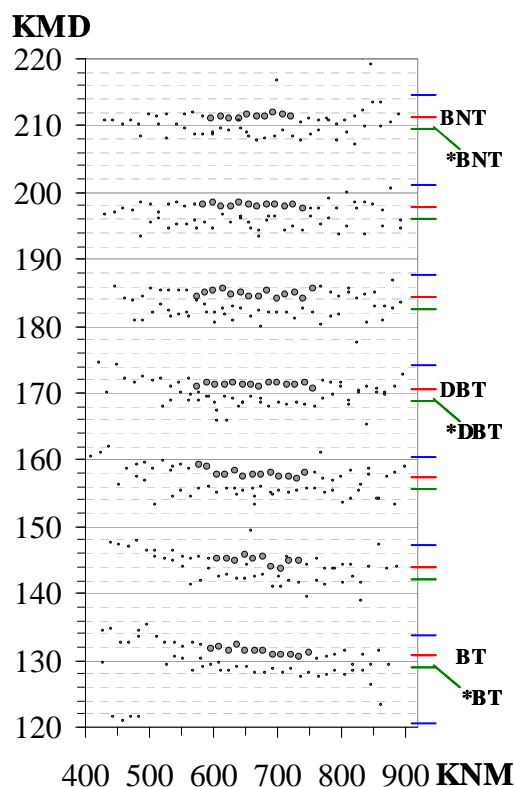


Figure VII-11. Detail of Figure VII-10, with BT, DBT, BNT and *corresponding ^{13}C series indicated by red and green lines. Blue lines indicate KMDs of PAH series.

Figure VII-11 shows an expanded region of Figure VII-10 to stress the fact that the gaps of $\text{KMD} = 13.4$ between series are only explainable by either PASHs (red marks and green marks for ^{13}C species) or by PAHs (blue marks).

6 ESI FT-ICR-MS Analysis of the Vacuum Residue Aromatics

Since the ionization of aromatic compounds with electrospray techniques is not very efficient [76, 78, 81] derivatized compounds are desirable. ESI is a good choice for the ionization of very polar compounds and dissolved salts, which can be produced, e.g. by selective derivatization targeting the sulfur atoms in the complex sample mixture. For selective ionization of PASHs, palladium(II) has been used as a sensitivity enhancing reagent in standard resolution experiments using an ESI ion trap MS [76]. This technique, however, may show problems if samples of unknown sulfur content are investigated, as concentration ratios of palladium(II) and sulfur seems to be crucial. In addition, with the

use of palladium(II) salts, instrumental parameters like flow rate for sample injection and spray voltages must be finely tuned to suppress the ionization of hydrocarbons.

6.1 Methylation Reaction of Sulfur Compounds

The derivatization of organic sulfur to methylsulfonium salts to achieve selectivity for sulfur aromatics in the presence of PAHs was investigated.

One 1 mmol of the standard and 1 mmol of iodomethane were dissolved in 3 mL of dry 1,2-dichloroethane (DCE). A solution of 1 mmol silver tetrafluoroborate in 2 mL DCE was added and yellow silver iodide precipitated immediately. The mixture was allowed to react for 48 h followed by the removal of the precipitate using centrifugation/filtration. The precipitate was washed with DCE. DCE from the combined reaction and washing solution and excess iodomethane were distilled off under reduced pressure. The resulting sulfonium salts were dried under vacuum before mass spectrometric analysis. This derivatization reaction is shown in Figure VII-12.

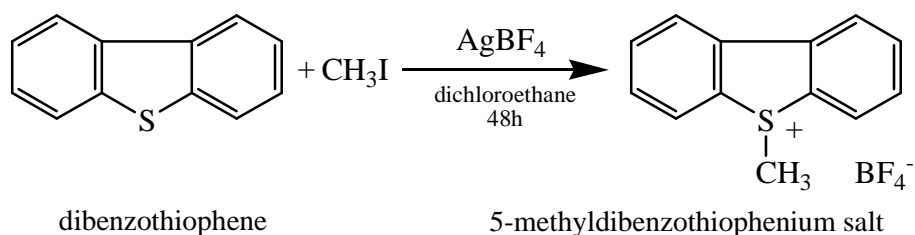


Figure VII-12. Derivatization reaction of dibenzothiophene.

Of particularly interest are sulfur species that show high recalcitrance to HDS, such as PASHs. Such compounds often possess alkyl groups in positions adjacent to the sulfur atom [22, 123] and it is possible that such substituents can act as a steric hindrance to this reaction. To test the influence of different alkyl substituents on the yield of the derivatization reaction, six reference compounds were methylated using the procedure described in the literature [124]. Phenanthrene was taken as a control to study the behavior of a non-sulfur species but it was inert under the applied conditions. The sulfur selective methylation described in the literature for thiophene, benzothiophene and several di- and trimethylated benzothiophenes, dibenzothiophenes, and other non-alkylated sulfur compounds [62] was found to give a quantitative yield even for 2,4,6,8-tetramethyldibenzothiophene after 16 h.

6.1.1 Standard Molecules

The influence of alkyl substitution near the sulfur atom on the methylation reaction was tested with seven reference compounds: dibenzothiophene, 4-methyldibenzothiophene, 2,4,6,8-tetramethyldibenzothiophene, 2,7-dimethylbenzothiophene, cholestano[2,3-*b*]-5,6,7,8-tetrahydronaphtho[2,1-*d*]thiophene (CHNT, Chapter IV, p. 25). Phenanthrene was used as control. The reaction products and side products obtained from standards are provided in Table VII-B.

Table VII-B. Mass spectral data of standards and side products

Compound	$[M+CH_3]^+$	Main m/z	m/z [Side products]
DBT	199	199	484 $[2M+BF_4]^+$
4MeDBT	213	213	-
4EtDBT	227	227	199 $[DBT^a+H]^+$
2468TetraMeBDT	255	255	-
127TriMeBT	177	177	299 $[2Ag+BF_4^b]^+$
$C_{34}H_{54}S$ (CHNT)	543	543	-

a) DBT was an impurity in the 4EtDBT standard. b) Signal may be $2Ag+BF_4$, although the isotopic pattern does not match.

The last column in Table VII-B lists mass signals found in the spectra of methylated standard compounds, revealing the presence of clusters formed by silver, tetrafluoroborate and standard compounds. To minimize cluster formation, an additional washing step following the filtration and centrifugation of the precipitated silver iodide was performed.

6.1.2 Vacuum Residue Samples

Sulfur compounds in all fractions were methylated at the sulfur atom [124]. All four residue fractions, containing between 10^{-2} and $4 \cdot 10^{-3}$ mmol sulfur, and 1 mmol of iodomethane were dissolved in 3 mL of dry 1,2-dichloroethane (DCE). A solution of 1 mmol silver tetrafluoroborate in 2 mL DCE was added and yellow silver iodide precipitated immediately. To adjust for the possibly stronger steric hindrance that may be present in the large compounds in a vacuum residue, the reaction time was extended to

48 h. Workup was performed as described above for standard compounds. The resulting oils were dried under vacuum before mass analysis

The resulting mass spectra of LEC fraction 1F and 1E, before and after partial HDS, are shown in Figure VII-13 and Figure VII-14, respectively.

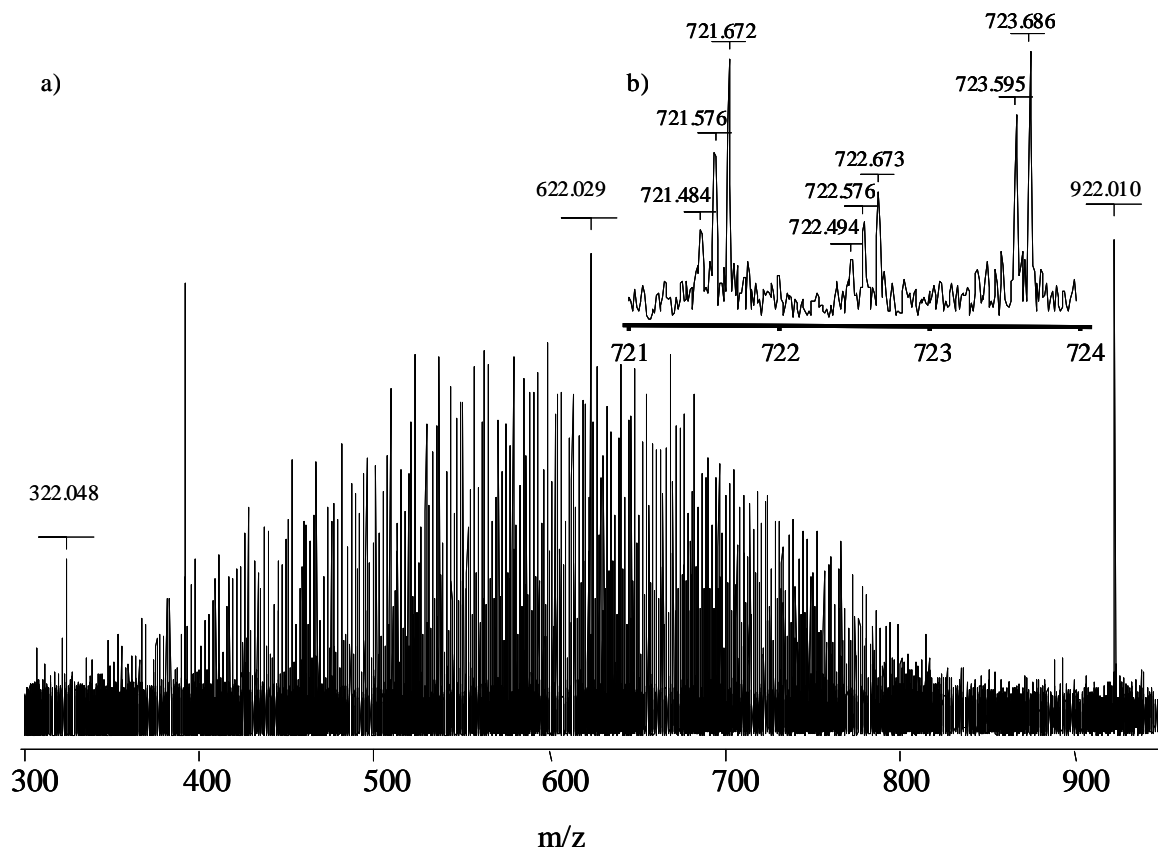


Figure VII-13. a) High resolution mass spectra of the fractions 1F obtained by LEC before partial HDS process. The three internal standards used for mass calibration are indicated by their exact masses. b) The inset shows a mass scale expanded section from m/z 721 to 724 of spectrum a) in more detail.

In previously described experiments using other ionization techniques (APCI and MALDI) from non-derivatized samples signals in similar mass ranges as those shown in Figure VII-13 were observed. However, without the methylation, APCI as well as MALDI ionization of underivatized sample showed poor signal to noise ratios in some cases. Table VII-C provides the deviation between theoretical and observed masses of the internal mass standards in ppm.

Table VII-C. Deviation between theoretical and observed masses of the internal mass calibrants in ppm in the ESI mass spectra of the four vacuum residue fractions.

Standard [MW in Da]	Feed fraction 1F [ppm]	Feed fraction 2F [ppm]	Effluent fraction 1E [ppm]	Effluent fraction 2E [ppm]
322.04812	±0.06	±0.14	-	±0.01
622.02896	±0.04	±0.11	±0.12	±0.04
922.00980	±0.00	±1.13	±0.30	±0.05

All standards in all samples are found to differ by up to 0.3 ppm from the theoretical value, with the exception of the heaviest standard compound in feed fraction 2 (1.13 ppm) and the lightest one in fraction 1E of the effluent, which could not be found in the corresponding spectrum. For the samples feed fraction 1F and effluent fraction 2E all standards are within a 0.06 ppm margin. From this result one can conclude that the required precision of 2.0 ppm is achieved with the ESI measurements of methylated samples and computed data analysis has a solid base.

Table VII-D. Signals shown in Figure VII-13b with elemental compositions assigned.

Measured	Theoretical	Elemental composition ^a	Difference	Alternative composition	
721.484	721.487	C ₄₅ H ₇₀ S ₃	4.7 ppm	C ₅₁ H ₆₂ S ₁	721.481 -4.6 ppm
721.576	721.575	C ₅₀ H ₇₄ S ₁	-2.1 ppm		
721.672	721.668	C ₄₉ H ₈₆ S ₁	-4.8 ppm		
722.494	722.491	*C ₄₅ H ₇₀ S ₃	-4.5 ppm	*C ₅₁ H ₆₂ S ₁	722.484 not found
722.576	722.578	*C ₅₀ H ₇₄ S ₁	2.7 ppm		
722.673	722.672	*C ₄₉ H ₈₆ S ₁	-2.1 ppm		
723.595	723.594	C ₄₇ H ₈₀ S ₂	-1.8 ppm		
723.686	723.684	C ₄₉ H ₈₈ S ₁	-2.4 ppm		

^{a)} The elemental compositions given in the table are corrected for the methyl group added by derivatization. (*) The asterisk indicates elemental compositions that include one ¹³C. (Gray) text in the table refers to a calculated elemental composition not found in the spectra.

The inset in Figure VII-13b shows the region from 721 to 724 Da in more detail. Groups of signals that fall together in the TOF mass spectra are resolved into signal groups separated by about one Da from each other. Data processing using the algorithm presented in Chapter VII.3.2 identified those signals to be the PASHs listed in Table VII-D.

The first signal group in the Figure VII-13b at ~721.5 consists of three signals. The first signal within this group with the mass 721.484 Da can originate from two elemental compositions, $C_{45}H_{70}S_3$ or $C_{51}H_{62}S$. The next signal group at ~722.5 Da should reflect the elemental compositions of the previous signal group with one ^{12}C replaced by the ^{13}C isotope. In the latter group a signal at 722.494 Da only permits the composition $^{13}C^{12}C_{44}H_{70}S_3$ (for a given maximum mass deviation of 5 ppm), thus invalidating the S1 class and supporting the S3 class for the corresponding signal in the previous signal group. In this 3 Da segment of the mass spectrum already members of several overlapping homologue series can be identified, but identification must take advantage of whole series to ensure reliable identification.

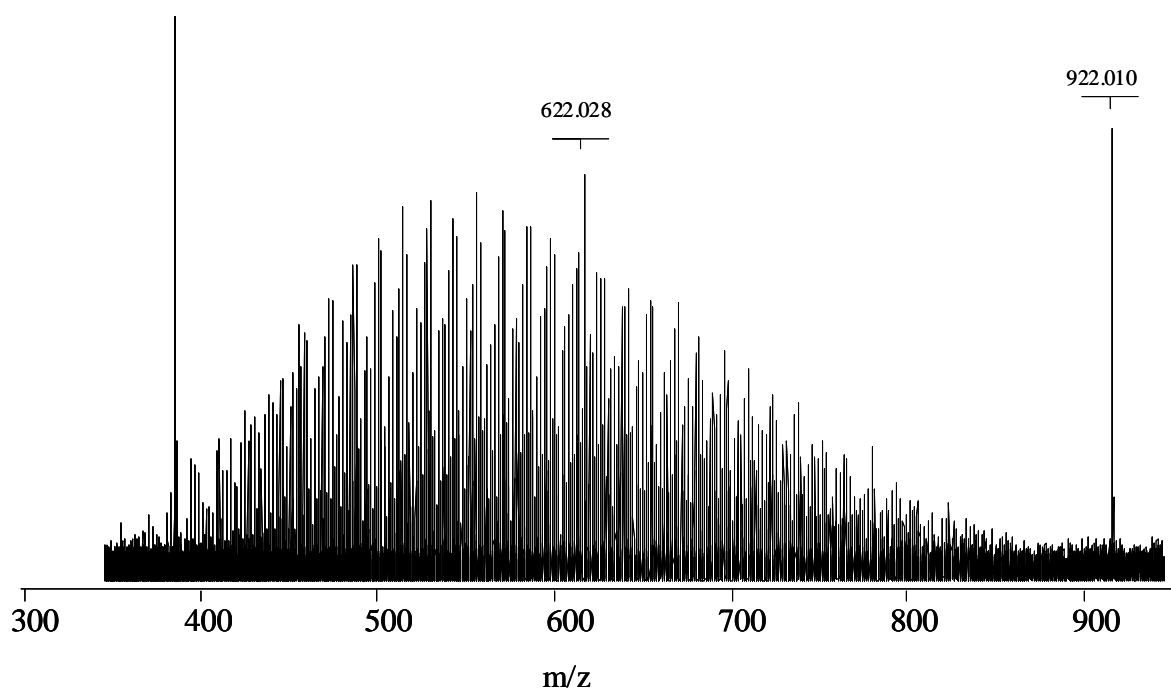


Figure VII-14. High-resolution mass spectra of LEC fraction 1E of the residue after HDS. Two internal calibrants are identified by their exact masses.

A comparison of the mass spectra of the LEC fractions 1F of the residue samples before (Figure VII-13) and 1E after (Figure VII-14) HDS shows signals in similar mass ranges from ~400 to ~850 Da which differs slightly from those observed with APCI and

MALDI presented above. The maximum of the signal intensity envelope is reduced from ~600 to 550 Da for the HDS processed fraction, possibly reflecting the conversion of some structures by the hydrotreating.

The more readily desulfurized OSC are expected in the first LEC fraction as PASH elute in the second fraction. The second fractions 2F and 2E of the Pd(II) column, which in the case of lighter petroleum fractions contain all PASHs, were analyzed in the same way as the first ones. The mass spectrum of this fraction of the residue sample after partial hydrodesulfurization is shown in Figure VII-15a with the inset b) of a detailed region of one mass calibration standard.

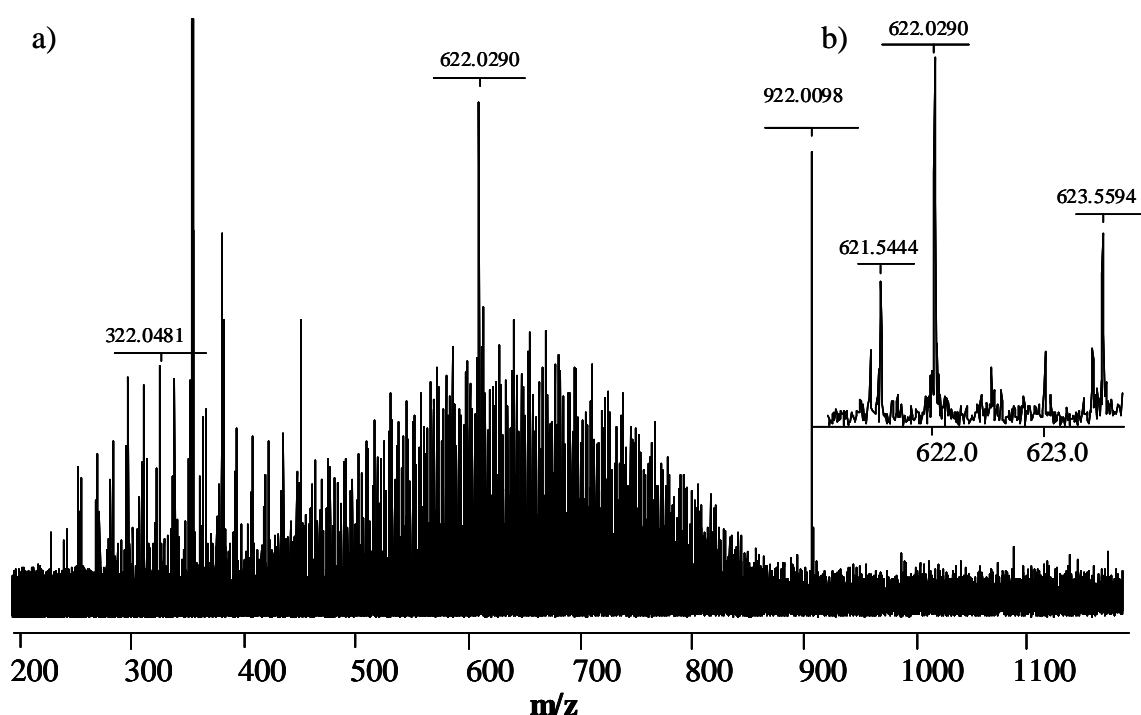


Figure VII-15. a) High resolution mass spectra of LEC fraction 2E of the effluent of HDS process. Internal calibrants are indicated by their exact masses. The inset b) shows the mass region from 621 to 624 in detail.

The signals shown in the inset b) were assigned to the series shown in Table VII-E:

Table VII-E. List of the signals shown in Figure VII-15b) with elemental compositions assigned.

Measured	Theoretical	Elemental composition ^{a)}	Difference	DE	Relative intensity
621.4496	621.44937	C ₄₃ H ₅₈ S	0.4 ppm	15	0.204
621.5444	621.54327	C ₄₂ H ₇₀ S	1.8 ppm	8	0.388
622.0290	-	Calibration standard	-	-	0.979
622.5468	622.54327	*C ₄₂ H ₇₀ S	0.3 ppm	8	0.157
623.4647	623.46502	C ₄₃ H ₆₀ S	0.5 ppm	14	0.207
623.5594	623.55892	C ₄₂ H ₇₂ S	0.8 ppm	7	0.514

^{a)} The elemental compositions given in the table are corrected for the methyl group added by derivatization. (*) The asterisk indicates elemental compositions that include one ¹³C.

The fourth row in Table VII-E contains values fitting a ¹³C compound, which confirms the elemental composition assigned to the mass 621.5444 Da in the second row. The relative intensities for this signal pair ¹²C:¹³C 100:41 agree quite well with the theoretical 100:47 ratio.

6.2 Mass Range, Multiply Charged Ions and Clusters in the Mass Spectra

Clusters of several molecules of the reference compounds containing silver or tetrafluoroborate ions could be identified to some extent based on their accurate mass. Data analysis has shown that the number of signals caused by clusters can be estimated to lie below 10 %. Even a larger abundance of clusters would not jeopardize the elemental composition assignment procedure since clusters can be identified easily using the high accuracy mass data and treated separately. The absolute numbers of signals, clusters, non-assigned mass signals, and assigned classes for the four investigated fractions are given in detail in Table VII-F. The relative intensities of all types sharing a class are given in brackets. The signals of ¹³C isotopes have been subtracted from the numbers of identified elemental compositions in the Table VII-F, although those signals were used to support the assignment of elemental composition.

Table VII-F. Number of the mass spectrometric signals for compound classes in the vacuum residue fractions^a. The values in brackets refer to the relative intensity over all signals identified in the given class.

	Class				Unassigned	Cluster
	PAH	S1	S2	S3		
Feed fraction 1F	92 (15.9%)	289 (71.7%)	44 (7.8%)	27 (4.9%)	42	18
Feed fraction 2F	102 (22.8%)	256 (65.7%)	30 (7.9%)	12 (3.6%)	53	87
Effluent fraction 1E	95 (16.1%)	267 (68.5%)	64 (11.4%)	13 (3.9%)	38	52
Effluent fraction 2E	144 (24.1%)	325 (63.7%)	44 (8.4%)	16 (3.7%)	58	48

^a The number of signals and the signal intensity of a class are corrected for signals resulting from elemental compositions containing ¹³C isotopes.

The dominance of compounds with one sulfur atom is evident, whereas structures that were identified to contain three sulfur atoms were negligible. The slight increase in hydrocarbon intensity may arise from the HDS process. The slight increase of S2 compounds in fraction 1E is also remarkable and might be explained by partial removal of sulfur from molecules of higher sulfur content.

6.3 Vacuum Residue Analysis by Combination of FT-ICR-MS with LEC

The interpretation of mass spectrometry data (without fragmentation) does not permit an identification of analyte structures since by this technique one cannot distinguish between isomers. LEC on Pd(II) showed the best group separation abilities for vacuum residue derived aromatics in comparison to all tested chromatographic systems. The separation of sulfur species into a PASH and a non-PASH fraction is a valuable tool for determination of compound structures and will be taken as starting point for further discussion of structures in the residue fractions.

6.3.1 Vacuum Residue before HDS: Feed

The advantages of a plot of Kendrick nominal mass (KNM) against Kendrick mass defect (KMD) has been described in chapter VII.3.1, p. 77. The Kendrick mass defect plots of the sulfur-containing aromatics in LEC Fraction 1F in Figure VII-16a show a different pattern from the one observed for the sulfur-containing aromatics in Fraction 2F (Figure VII-16b). The KMDs on the y-axis are related to the hydrogen deficiency as explained above (p. 75). They are related to the sum of rings and double bonds defined as double bond equivalent (DE): $DE = R + DB$ (R = number of rings, DB = number of double bonds).

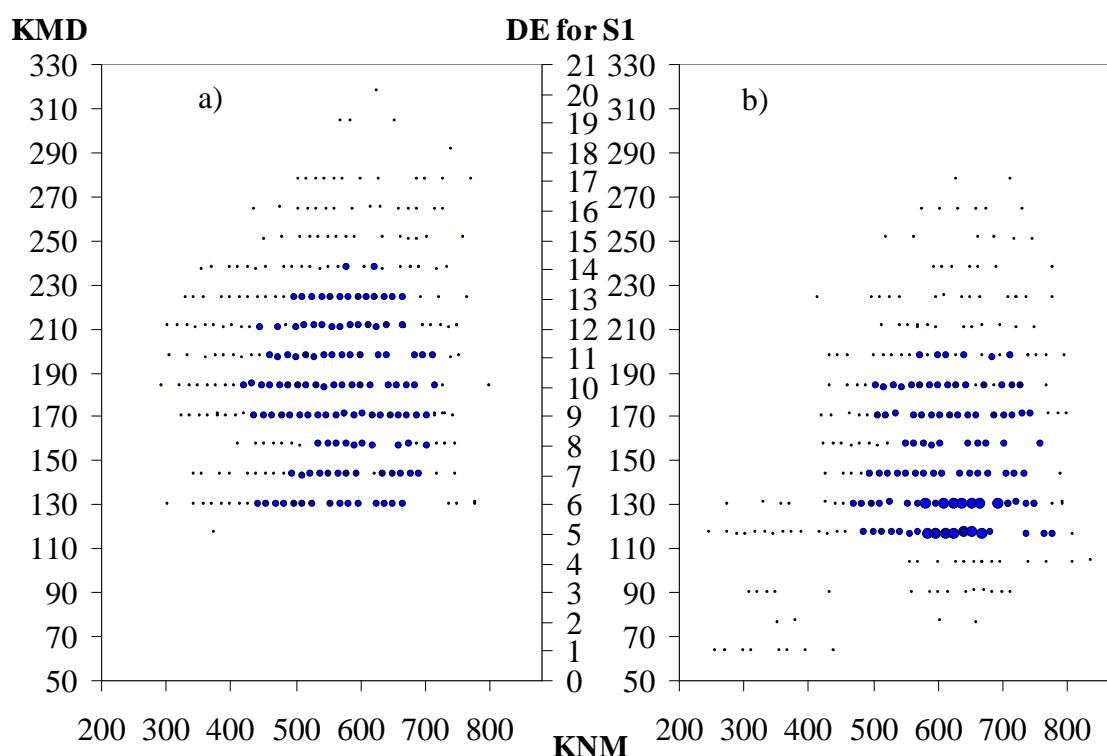


Figure VII-16. Kendrick mass defect (KMD) plots of the S1 compounds of a) LEC fraction 1F before HDS and b) LEC fraction 2F before HDS. The KMD corresponds in case of S1-class compounds to the given double bond equivalent (DE) and the size of the dots in the Figure reflect the relative signal intensity.

The vast majority of compounds show a DE value between 4, which corresponds to one aromatic ring and 21, which permits the existence of up to eight condensed aromatic rings. For DE numbers exceeding 9, the number of possible parent systems becomes very large and a lack of data on such high-boiling materials impedes reliable comparisons. UV

data on the whole PASH fraction show absorption bands up to 340 nm so that at least three (DE = 10) to four condensed aromatic rings (DE = 13) are expected to be present in detectable concentrations. Naphthenic rings do not exhibit UV absorption, but they are likely to contribute to the high DE-values observed. A large number of PASHs with several condensed naphthenic rings have been tabulated for crude oils [125].

The results presented here allow one to draw some conclusions about the parent structures present in the vacuum residue samples. A Kendrick mass defect of approximately 130.6 translates into DE = 6 (or Z = -10) for compounds containing one sulfur atom, and thus the lowest row of points in Figure VII-16a) and b) could represent benzothiophenes with an increasing number of carbon atoms in the side chains toward higher Kendrick nominal masses. Benzothiophenes are retained by Pd(II) so they should appear in fraction 2. The first thick point in that row in Figure VII-16b appears at a nominal mass of 456 and thus represents the elemental composition $C_{31}H_{52}S$. If it is a benzothiophene all side chains must be $C_{23}H_{47}$. However, the mass spectrum cannot tell whether it is one C_{23} side chain or several shorter ones or whether the side chains are linear or branched. The largest molecular weight for a compound in this row in Figure VII-16b is 792 Da, implying 47 carbon atoms in side chains if the parent structure is benzothiophene.

Compounds with a KMD of 144.0 have DE = 7, i.e. they contain one more ring or one more double bond than benzothiophene, and compounds with a KMD of 157.4 have DE = 8. These groups of compounds are represented on the second and third row of points in Figure VII-16a). Previous investigations of ring systems in fossil materials identified several parent structures. A thorough examination of fairly low-boiling PASHs in a shale oil from Austria showed the presence of a large number of different parent systems [63, 126, 127]. Several alkylated phenylthiophenes (DE = 7) were found with up to 9 carbon atoms in the side chains in material boiling at 168 - 175 °C/3.5 torr. Further experiments have shown that both 2- and 3-phenylthiophene elute in fraction 1 from the Pd(II)-column, so one can assign the second lowest row (KMD of 144.0) of compounds in Figure VII-16a) to alkylated phenylthiophenes. Other conceivable structures for DE = 7 are tetrahydrodibenzothiophenes and cyclopentabenzothiophenes, the latter have also been found in the Austrian shale oil. However, substituted representatives of both of these parent structures should elute in LEC fraction 2 and appear in Figure VII-16b) since

unsubstituted 1,2,3,4-tetrahydrodibenzothiophene is retained by the Pd(II) column and elutes in fraction 2.

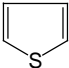
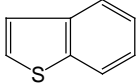
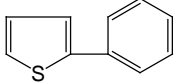
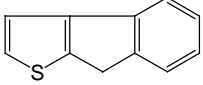
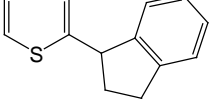
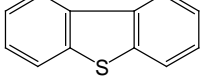
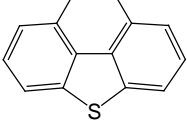
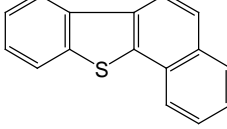
Compound classes with $DE = 8$ include indenothiophenes and indanylthiophenes which were reported to occur in the Austrian shale oil [126, 127]. Indenothiophenes can be regarded as bridged phenylthiophenes and therefore presumably behave like them on the Pd(II) column (see above) and appear in fraction 1 (Figure V-10). Indanylthiophenes are substituted thiophenes and are also expected to elute in fraction 1.

A major group of compounds appearing at $DE = 9$ (KMD of 170.8) could be indenothiophenes or indanylthiophenes with an additional naphthenic ring. $DE = 9$ is also expected for dibenzothiophenes or naphthothiophenes, which are among the most common sulfur species in petroleum samples. Both groups are separated on the Pd(II)-column, with the condensed thiophenes being strongly retained, and eluting with the PASHs in fraction 2 (Figure VII-16b) while structures with isolated thiophenes elute in fraction 1 (Figure VII-16a).

In Figure VII-16b), the heaviest signal in the DBT series has a molar mass of 828.7564 Da, which means that there are 46 carbon atoms in the side chains. The next higher benzologues are the benzonaphthothiophenes with a DE of 12 (KMD 211.0). They are often identified in crude oils but there are only relatively few points in Figure VII-16b corresponding to such ring systems. $DE = 11$ fits with phenanthro[4,5-*bcd*]thiophenes, a class of compounds frequently found in heavy oil fractions [128].

The series with higher DE s than the above discussed could be explained by additional naphthenic rings. For DE increments of three, e.g. for $DE = 12, 15$ and 18 , additional aromatic rings are also possible. Those could be fused to the benzene ring in the indanyl rest or form higher benzologues of the PASHs. The existence of such structures would be consistent with the number of aromatic rings indicated by the UV spectra.

Table VII-G. Parent structures for homologue series [63, 125, 127-129]. The last column shows fractions from LEC where such series are expected.

Parent Structure	Name	DE / Z	KMD ^a	LEC fraction
	Thiophene	3 / -4	90.4	1
	Benzothiophene	6 / -10	130.6	2
	2-Phenylthiophene	7 / -12	144.0	1
	8H-Indeno[2,1- <i>b</i>]-thiophene	8 / -14	157.4	1
	2-(1'-Indanyl)-thiophene	8 / -14	157.4	1
	Dibenzothiophene	9 / -16	170.8	2
	Phenanthro-[4,5- <i>bcd</i>]thiophene	11 / -20	197.6	2
	Benzo[<i>b</i>]naphtho-[2,1- <i>d</i>]thiophene	12 / -22	211.0	2

^a The Kendrick mass defect relates to non-protonated molecules without ¹³C.

In a vacuum gas oil BTs with up to 16 carbon atoms in side chains, up to 6 carbon atoms for DBTs, phenanthrothiophenes with 7 and benzonaphthothiophenes with up to 5 carbon atoms in alkyl chains have been found [128]. In a Middle East crude oil (from the Iraqi Kirkuk field) DBTs with up to 8 alkyl carbon atoms have been found [108]. Other investigations revealed as many as 31 carbon atoms in alkyl chains substituting BT and DBT [130].

6.3.2 Vacuum Residue after HDS: “Effluent”

The Kendrick plots of LEC fractions 1E and 2E of the residue aromatics after HDS processing are given in Figure VII-17. In a) apparent gaps in the series of homologues after standard data processing could be “filled” by taking masses into account with a maximum deviation of 3.0 ppm in the described assignment procedure. These signals appear as green dots in Figure VII-17a.

Manual inspection of these newly assigned signals proved that no interference with other homologue series occurred during the procedure. It is an open question if this phenomenon of “missing” structures is caused by an absence of those structures in the homologue series as the mass calibration achieved for this sample was consistent with that for the other samples.

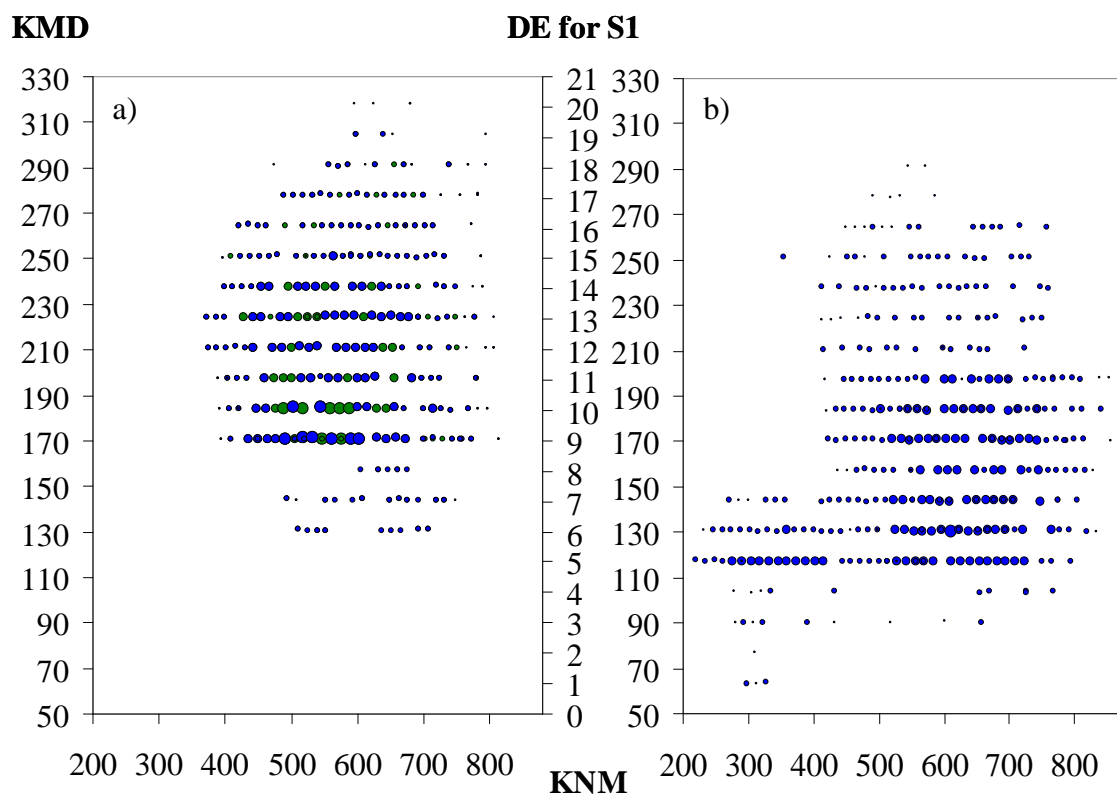


Figure VII-17. KMP plots of the S1-class compounds of the vacuum residue after HDS (effluent) a) LEC fraction 1E and b) fraction 2E. The size of the dots represents the relative intensity.

The distribution of signals of the effluent in Figure VII-17 can be compared to the one in Figure VII-16 showing the feed fractions. Structures with DE lower than 6 have not

been identified in fraction 1E of the effluent. The first significant series in Figure VII-17a) has a KMD of 170 according to a $DE = 9$. Signals for molecules with lower condensation are visible, but are of relatively low intensity. A DE of 9 fits with indanylthiophenes or indenothiophenes with one additional naphthenic ring, BTs with three naphthenic rings or DBTs, except that the latter two are well retained on the Pd(II)-column and therefore appear in LEC fraction 2.

Thiophenes with 4 or 5 naphthenic ring substituents could also account for signals at DE s of 7 and 8. These structures have been reported to be present in petroleum samples [125]. However, noncondensed thiophenes are readily desulfurized during HDS. This contradicts the fact that these series seem to survive the partial HDS process and therefore might not be present in hydrotreated samples.

A DE of 9 in fraction 2E Figure VII-17b) fits with dibenzothiophene, but does not explain the DE 9 series in fraction 1E as DBTs are the PASHs that are retained most strongly by the Pd(II) column. Again, a combination of the structures described above seems to be unlikely because they are easily removed while this unidentified higher condensed series shows a certain recalcitrance. From the mass spectrometric data further conclusions cannot be drawn. However, with the structures being pronounced in LEC fraction 2E after HDS some sterical shielding of the sulfur atom in the molecule must be assumed.

Homologue series in LEC fraction 2E as shown in Figure VII-17b) start with DE s of 5 and 6 with members over a wide mass range. The first dot in the BT series ($DE = 6$) has a mass of 232 Da, corresponding to a BT with C_7H_{15} as substituent(s). This series extends to 834 Da allowing for 50 carbon atoms in side chains. The series of DBTs starts at a mass of 422 Da and reaches up to 856 Da equal to 17 to 48 methylene groups, respectively.

6.4 Changes in the Vacuum Residue during HDS

During HDS the more reactive sulfur structures are removed at higher rates. A comparison between both residue samples before and after HDS allows one to draw conclusions about the structure of sulfur molecules that readily react and those which are recalcitrant.

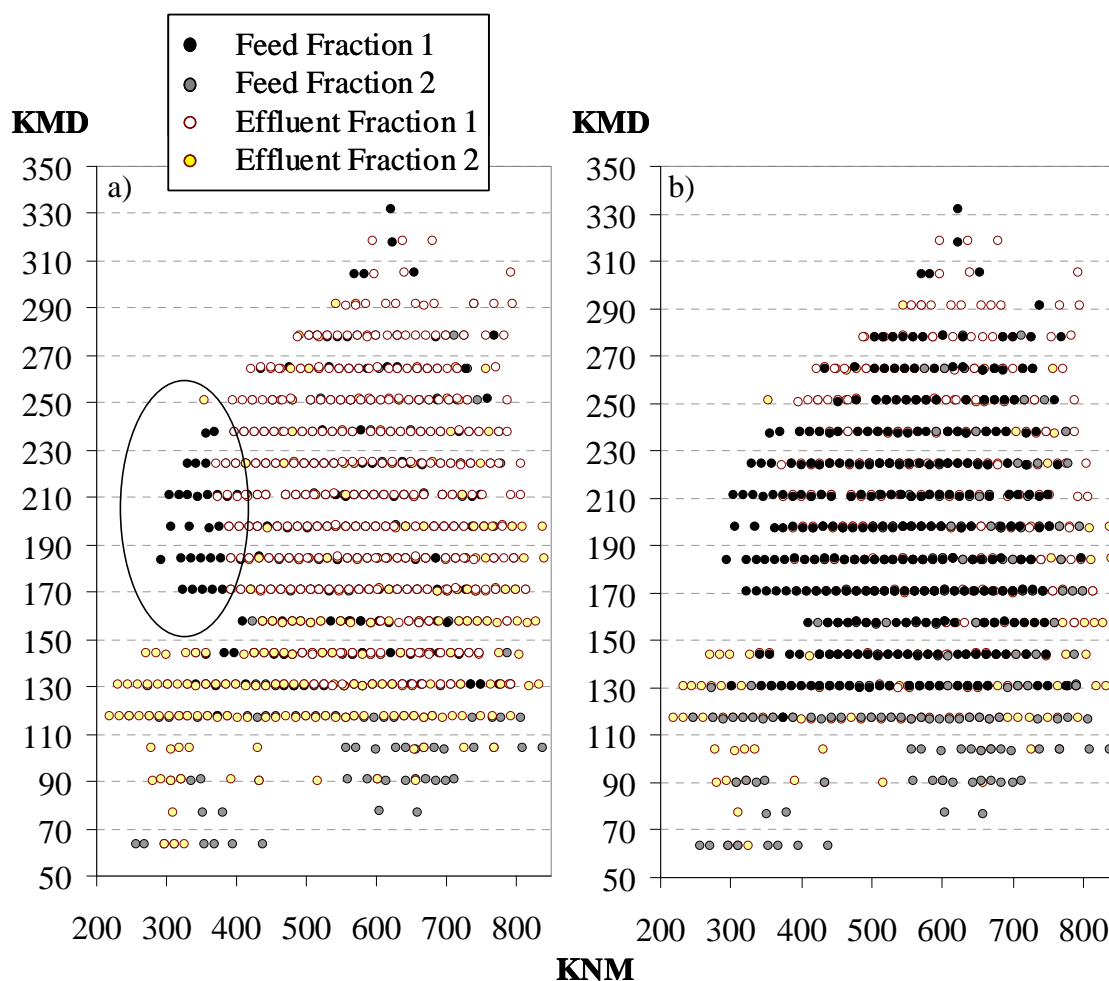


Figure VII-18. Two Kendrick mass plots of all S1 series before and after HDS. Signals of the effluent fraction 1E are indicated by (○) white dots and the corresponding fraction 2E by (●) yellow dots and layered above them signals obtained from the feed fraction 1F and 2F, being (●) black and (●) gray. In the plot a) on the left the effluent dots cover the feed dots so that if a signal is present in both feed and effluent, only the effluent signal is visible. In b) on the right the feed dots cover the effluent.

In Figure VII-18a) (left) the white/yellow effluent signals are layered onto the gray/black signals from the fractions before HDS so that if a S1 compound is present in the sample before and after HDS it will appear as a white/yellow dot. However, the effluent derived signals (white/yellow) do not cover all S1 signals in the feed. These gray and black dots therefore reflect compounds that were removed during HDS process. Figure VII-18b) (right) shows the reverse case, where those of the feed cover the effluent dots. Only few white/yellow dots and, more important, no regular pattern of them is visible, reflecting the

fact that during HDS no compounds have been “formed”. In Figure VII-18a) (left) black dots below 370 Da and KMD values higher than 150 (indicated in the Figure by the ellipse) relate to compounds that seem to be converted. This group of signals is found in LEC fraction 1 (black dots in the Figure), therefore these compounds are noncondensed thiophenes, containing the sulfur in isolated thiophenic rings. Their KMD values correlate with a DE = 9 to 14 which means indenothiophenes or indanylthiophenes with one to 5 naphthenic rings or up to one additional benzene and two naphthenic ring, respectively.

Sterically hindered sulfides are another recalcitrant non PASH sulfur structure reported by Albrecht et al. [131] who recently identified 1,1,4a,6-tetramethyl-9-alkyl-1,2,3,4,4a,9b-hexahydrodibenzothiophene in highly desulfurized diesel oils, but this and other related sulfides can be excluded for this discussion due to their strong affinity to the Pd(II) stationary phase. They do not elute from the column if present.

6.4.1 Selected S1 Series Obtained from Processed Data Before and After HDS

Plots of selected homologue series that have been calculated from the processed data and corrected or signals from compounds with ^{13}C are very similar in appearance to mass spectra, and therefore convenient to interpret. The most heavily populated S1 series of all four residue fractions are shown in appendix IX8, p. 127. Figure VII-19 shows such “mass spectra” of series with one sulfur atom a) feed and b) effluent fraction 1. Two groups can be visually distinguished, the series with DE 9 and 10 (black symbols) retain their members during HDS. The series with DE 6 to 8 (white symbols in the Figure) lose a lot of “signals” by HDS and the remaining signals have a much lower intensity in comparison to series with DE 9 and 10.

Both mass spectra were obtained from LEC fraction 1 and thus should not contain thiophenes condensed to further aromatic rings. The complete overview over S1 class series obtained from all investigated residue fractions is presented in Appendix IX8, p. 127. Table VII-G on p. 101 gives an overview on aromatic sulfur structures reported to be present in other petroleum related samples.

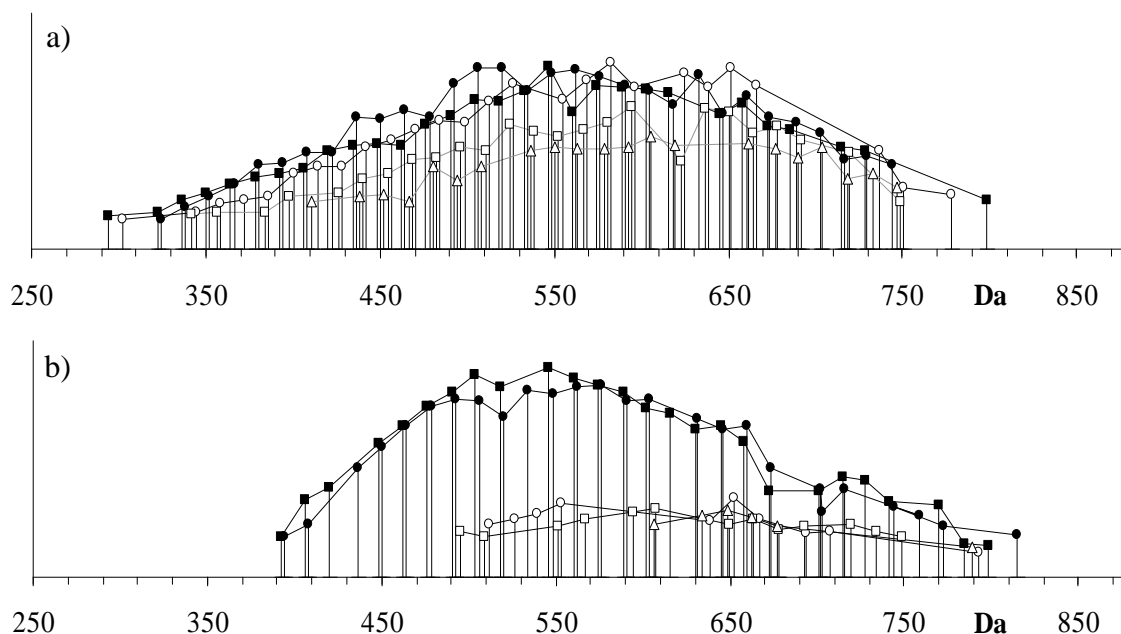


Figure VII-19. (○) S1-DE6, (□) S1-DE7, (Δ) S1-DE8, (●) S1-DE9, and (■) S1-DE10 series of LEC fraction 1F of a) feed and b) 1E of effluent. The Figure shows ^{13}C -corrected relative signal intensities.

Parent structures, which are likely to account for DE 7 and 8 are phenylthiophenes and indeno- or indanylthiophenes, respectively. A DE of 6 would match with benzothiophene, but those are retained on the Pd(II)-column, even with sterically demanding substituents like the reference compound CHNT with $\text{C}_{29}\text{H}_{48}$ in alkyl chains. S1 class structures with a DE of 6 in this fraction should be ascribed to a combination of thiophenic and three naphthenic rings. The lowest mass after HDS for DE 6 is 512 Da, which refers to $\text{C}_{31}\text{H}_{56}$ in methylene groups. The smallest member with DE 7 weighs 496 Da corresponding to 24 methylene groups on a phenylthiophene. The DE 8 series starts with 606 Da according to 31 methylene groups for an indenothiophene or 29 for an indanylthiophene. The series with DE = 9 in the LEC fractions 1 remains unsolved as DBTs elute in fraction 2 of the Pd(II)-column and structures with isolated thiophene rings should be readily desulfurized.

The following homologue series have been identified in the vacuum residue fractions:

Table VII-H. Carbon numbers in alkyl chains of homologue series identified in the vacuum residue fractions using ESI FT-ICR-MS of sulfur selectively derivatized samples.

Homologue series	Feed fraction 1F	Feed fraction 2F	Effluent fraction 1E	Effluent fraction 2E
BT (DE = 6)	-	C ₁₄ -C ₄₇	-	C ₇ -C ₅₀
BT with one add. naphthenic ring (DE = 7)	-	C ₁₄ -C ₄₇	-	C ₁₀ -C ₄₈
BT with two add. naphthenic rings (DE = 8)	-	C ₂₁ -C ₄₆	-	C ₂₂ -C ₄₉
DBT (DE = 9)	-	C ₁₇ -C ₄₄	-	C ₁₇ -C ₄₆
DBT with one add. naphthenic ring (DE = 10)	-	C ₁₈ -C ₄₃	-	C ₁₇ -C ₄₇
Phenanthro-[4,5- <i>b</i>]thiophene (DE = 11)	-	C ₁₆ -C ₄₂	-	C ₁₅ -C ₄₃
Benzo[<i>b</i>]naphtha[2,1- <i>d</i>]thiophene (DE = 12)	-	C ₁₈ -C ₄₀	-	C ₁₃ -C ₃₈
Phenylthiophenes (DE = 7)	C ₁₃ -C ₄₄	-	C ₂₇ -C ₃₈	-
Indenothiophenes or Indanylthiophenes ^a (DE = 8)	C ₁₅ -C ₄₁	-	C ₁₆ -C ₄₃	-
Indenothiophenes or Indanylthiophenes ^a with one add. naphthenic ring (DE = 9)	C ₁₁ -C ₄₂	-	C ₁₆ -C ₄₃	-

a) The number of carbon atoms is calculated for indenothiophenes. Indanylthiophenes have 2 carbon atoms less than the numbers listed in alkyl chains.

The presented combination of LEC with high-resolution FT-ICR-MS impressively extends the molecular weight for petroleum component class analysis.

7 High Abundance of the [M+1]⁺ Signals in Mass Spectra of PACs

All mass spectra acquired by a MALDI-TOF-MS and on a FT-ICR-MS showed highly abundant signals at even and odd nominal mass (p. 59 and p. 84). This has been previously observed for PAHs using standard resolution spectrometers with MALDI [99] and LDI [100] ion sources. Jackson et al. reported that [M+1]⁺ signals with an abundance of ~ 1/3 to 1/2 of the molecule peak are present in spectra of anthracene, benzo[*a*]pyrene, and

dibenzo[*a,h*]anthracene. This is approximately twice the abundance expected for molecules with one ^{13}C isotope (15 to 25 %). Though no obvious proton source could be found, protonation of $[\text{M}]^+$ was assumed. The high accuracy mass data from the FT-ICR spectrometer enables one to distinguish between signals from protonated species and those containing a ^{13}C isotope. Signal pairs that result from one ^{13}C isotope differ by 1.00335 Da from the corresponding molecular ions, the protonated ions by 1.00782 Da, respectively.

Although experiments with MALDI and APCI source have been performed without internal calibrant the interval between even and odd nominal mass of approximately one Da was precisely measurable. Table VII-I gives numbers of $[\text{M}]/[\text{M}+1]$ pairs identified and isotope ratios determined in high resolution mass spectra of three ion sources.

Table VII-I. Abundancy of $[\text{M}]$ and $[\text{M}+1]$ for HRMS experiments with three ion sources. Numbers and relative numbers of signals, protonated species, and pairs of signals deriving from pure ^{12}C elemental compositions and the corresponding ^{13}C isotope analogs are shown.

Ion Source	Sample	No of Signals	No of Pairs $[\text{M}]$ & $[\text{M}+1]$	measured	No of Pairs	measured $^{12}\text{C}/^{13}\text{C}$ ratio ^b	calculated $^{12}\text{C}/^{13}\text{C}$ ratio ^c
				$[\text{M}]^+ / [\text{M}+1]^+$ ratio ^a	$[\text{M}(^{12}\text{C})]^+ \& [\text{M}(^{13}\text{C})]^+$		
MALDI	AEPAC	1751	303 (17.3%)	1.04	192 (11.0%)	0.96	0.40
MALDI	AEPAH	1617	498 (30.8%)	1.17	150 (9.3%)	1.02	0.27
MALDI	AEPASH	1420	316 (22.3%)	1.12	100 (7.0%)	0.77	0.30
APCI	AEPAC	1589	70 (4.4%)	1.00	330 (20.8%)	0.60	0.49
ESI ^d	AEPAH	543	17 (3.1%)	0.77	105 (19.3%)	0.49	0.44
ESI ^d	AEPASH	677	34 (5.0%)	0.94	88 (13.0%)	0.51	0.47
ESI ^d	AFPAH	550	9 (1.6%)	0.84	108 (19.6%)	0.51	0.46
ESI ^d	AFPASH	562	9 (1.6%)	0.75	74 (3.2%)	0.52	0.47

a) The ratios of signal intensities for all pairs of $[\text{M}]^+ / [\text{M}+1]^+$ have been averaged. ^{13}C should be present in both species in equal amounts so that this ratio is 1. b) The ratio of signal intensities for all pairs of $[\text{M}(^{12}\text{C})]^+ / [\text{M}(^{13}\text{C})]^+$ have been averaged. The values should reflect the isotopic abundance for ^{13}C and thus be smaller than 1. c) The ratio of signal intensities for all pairs of $[\text{M}(^{12}\text{C})]^+ / [\text{M}(^{13}\text{C})]^+$ has been calculated. The values reflect the isotopic abundance for ^{13}C and depend on the number of carbon atoms in each structure. The intensity of the $[\text{M}(^{13}\text{C})]^+$ was calculated from the intensity of the corresponding $[\text{M}(^{12}\text{C})]^+$ signal based on an estimated carbon number $c = \text{Molecular weight} / 15$. The identified carbon numbers c have been used for the sets of data obtained using ESI. d) For ESI mass analysis sulfur selective methylated sample has been used.

The use of ESI circumvents the phenomenon reported for ionization of PAH via MALDI. Previous authors have suspected this high abundance of [M+1] signals to derive from [M+H] protonated species and only to some extent from ^{13}C containing species that agrees with the isotopic abundance.

The high-resolution data confirm that a large number of signals derive from protonated ions. However, the data acquired by FT-ICR-MS using a MALDI ion source still show an unexplainable intensity ratio of $^{12}\text{C}/^{13}\text{C}$. Mass spectra achieved by APCI and from derivatized compounds via ESI show intensity ratios of $^{12}\text{C}/^{13}\text{C}$ in agreement with theoretical considerations.

The data in Table VII-I additionally confirms that ESI of derivatized compounds prevents protonation of the analytes, only a tiny number of such pairs of signals is observed. The $\text{C}^{12}/\text{C}^{13}$ ratios have been calculated from the pure ^{12}C signals (based on KMD and signal intensity) and then compared with the ^{13}C isotopic twin. This comparison can be used to check:

- a) mass calibration
- b) assignment procedure (based on good mass calibration)

and has therefore been used as a quality control for the latter. The data in the last two columns in Table VII-I, which has been obtained with MALDI from non-derivatized samples show some discrepancy between observed and theoretical $\text{C}^{12}/\text{C}^{13}$ ratios, with observed ratios being 2.8 fold higher than theoretical values. For a large number of statistical pairs the ratio of signal intensities averages to 1. This ratio near 1 reflects the effect of insufficient calibration as signals are paired that are no $\text{C}^{12}/\text{C}^{13}$ pair. The data gained in the experiments using ESI of methylated compounds with three internal mass calibrants, however, show good agreement between measured and theoretical $^{12}\text{C}/^{13}\text{C}$ ratios.

8 Summary of High-Resolution Mass Spectrometry of Vacuum Residues

The aromatics of a vacuum residue before and after partial desulfurization by hydrotreatment on metal catalyst were fractionated using ligand exchange chromatography (LEC) on a stationary phase containing complexed Pd(II) into two fractions each. This

separation separated non-condensed thiophenes, which were collected with hydrocarbons in fraction 1, from polycyclic aromatic sulfur heterocycles (PASHs), which were eluted in fraction 2.

These fractions were investigated using Fourier transform ion cyclotron resonance mass spectrometer (FT-ICR-MS). Matrix assisted laser desorption ionization MALDI and atmospheric pressure chemical ionization (APCI) were tested for their potential to produce mass spectra of unfragmented ions with high signal intensities. A computer supported data interpretation algorithm was developed for the complex mass spectra with hundreds to thousands of signals. This procedure assigns elemental compositions to each mass signal based on the high accuracy data and by establishing series of homologues. Although mass spectra were obtained with MALDI and APCI, mass calibration and signal intensities presented some difficulty for the data interpretation. A differentiation between series containing PASH and hydrocarbons was partly possible.

Therefore the organic sulfur compounds (OSC) in the four LEC fractions, namely fraction 1F and 2F of the feed of the hydrodesulfurization (HDS) process and fraction 1E and 2E obtained from the effluent after HDS, were sulfur selectively derivatized via a simple methylation at the sulfur atom.

The derivatized samples were analyzed using FT-ICR-MS and electrospray ionization ESI. High precision and high mass accuracy in the mass data were obtained by the use of three internal calibrants per mass spectrum.

Using the data interpretation procedure developed in this thesis in combination with the fractionation on the Pd(II) LEC stationary phase, series of sulfur-containing structures over a wide mass range could be identified. Among others, benzothiophenes containing up to 50 carbon atoms in aliphatic side chains and DBT with 46 carbon atoms were identified.

VIII SUMMARY

The catalytic conversion of heavy fractions is often hampered by heteroatoms present in the feedstock, especially nitrogen and sulfur. Necessary desulfurization is difficult and not always possible due to recalcitrance of some organosulfur species. Analysis of lighter petroleum fractions revealed alkylated polycyclic aromatic sulfur heterocycles (PASHs) to be the major sulfur contributor, especially those with alkyl substitution that sterically shield the sulfur in the molecule. For the heaviest fractions hardly any structural knowledge of the recalcitrant species is available. Consequently, for rational development of efficient hydrodesulfurization (HDS) procedures and new catalysts, structural knowledge of the relevant sulfur species is needed.

A major obstacle for heavy fraction analysis is the complexity in composition as the number of possible isomers increases tremendously with rising average molecular weight. Due to their non-volatile nature heavier fractions additionally defy common powerful analytical techniques like gas chromatography or some ionization techniques for mass spectrometry.

A representative PASH was defined, based on preliminary bulk analysis, to mirror the average properties of the investigated aromatic fraction of a vacuum residue like molecular weight, degree of aromaticity and number of aromatic rings per molecule. This model compound, $C_{37}H_{54}S$ with a benzothiophene parent structure contains 29 aliphatic carbon atoms (CHNT) and was synthesized starting from cholestanone. Characterization by MS, UV and NMR showed two isomers to be present. These isomers had the same overall characteristics and thus were not purified. These compounds were used to investigate various chromatographic systems in respect to the retention behavior of highly alkylated PASHs.

Taking the complexity of the vacuum residue samples into account, a chromatographic separation that provides chemically clearly defined sub-fractions of the vacuum residue aromatics was sought. Several chromatographic methods have been tested for the separation of heavy vacuum residue aromatics into classes according to number of fused aromatic rings. Charge transfer chromatographic stationary phases, octadecylsilica in

reversed phase partition chromatography, gel permeation chromatography (GPC) in dependency of the mobile phase composition and ligand exchange chromatography (LEC) on a Pd(II) bound stationary phase were applied to serve the purpose. The presented investigations suggest that such a chromatographic separation of the fraction of aromatic compounds in vacuum residues according to ring size, as desired, is not possible. This is probably because of the chemical homogeneity among aromatic compounds of different ring size classes. Existing distinctive features like the presence or absence of sulfur, the number of fused aromatic rings that could be exploited for such group separation are counterbalanced by the enormous number of alkyl chains and the tremendous number of isomers. Even a clear-cut fractionation according to molecular size by the use of GPC failed in the end. The only clear-cut chromatographic fractionation was obtained by the use of a LEC approach based on a Pd(II) column.

In contrast to experiments performed on lighter fractions not all organic sulfur compounds (OSC) were isolated by LEC from hydrocarbons in this work. Some sulfur compounds eluted together with hydrocarbons in the first (non-PASH) fraction. Highly alkylated standard PASH standards (CHNT, OctDBT) were shown to be retained and eluted in the second (PASH) fraction, indicating that even PASHs containing huge alkyl substituents can be separated from non-PASHs. This separation facilitates distinguishing between different sulfur species in this thesis. Structures that contain non-condensed thiophene rings (non-PASH) can be isolated from such OSC containing condensed thiophenes (PASH). This differentiation was a valuable tool for the interpretation of mass spectrometric results.

The LEC fractions were investigated using Fourier transform ion cyclotron resonance mass spectrometer (FT-ICR-MS). Matrix assisted laser desorption ionization (MALDI) and atmospheric pressure chemical ionization (APCI) were tested for their potential to produce mass spectra of unfragmented ions with high signal intensities of the vacuum residue aromatic compounds. A computer-supported algorithm was developed for data interpretation of the complex mass spectra with hundreds to thousands of signals. This procedure assigns elemental compositions to each mass signal based on the high accuracy mass data and by using series of homologues. Although mass spectra were obtained with MALDI and APCI, mass calibration and signal intensities presented difficulties for data

interpretation. A differentiation between series containing PASH and hydrocarbons was partly possible.

Therefore the organic sulfur compounds (OSC) in the four LEC fractions, namely fraction 1F and 2F of the feed of the hydrodesulfurization (HDS) process and fraction 1E and 2E obtained from the effluent after HDS, were sulfur-selectively derivatized via a simple methylation reaction targeting the sulfur atom.

The derivatized samples were analyzed using FT-ICR-MS and electrospray ionization (ESI) for sample introduction. High precision and high mass accuracy in the mass data were obtained by the use of three internal calibrants per mass spectrum. Elemental compositions could be assigned to the vast majority of signals in all four investigated vacuum residues. For structural identification of such elemental compositions additional information, e.g. chromatographic properties, desulfurization behavior, or spectroscopic properties was used.

Series of sulfur containing structures over a wide mass range could be identified using the data interpretation procedure developed in this thesis in combination with the fractionation on the Pd(II) LEC stationary phase. Among others, benzothiophenes containing up to 50 carbon atoms in aliphatic side chains and dibenzothiophene with up to 46 carbon atoms were identified.

The combination of chromatography and high resolution mass spectrometry greatly extends the molecular weight of identified sulfur structures in complex and high or non-boiling petroleum derived mixtures like the investigated vacuum residues and can provide a very detailed view on the effect of hydrotreatment of these materials. The comparison between unprocessed and partially desulfurized vacuum residue aromatics showed that structures with uncondensed thiophenes with a high degree of saturation are easily desulfurized while PASHs and also thiophenes with a lower degree of saturation in the molecule survive the partial HDS process. In the future, this method can be applied on residues and vacuum residues obtained from different stages of the HDS process to identify the most recalcitrant species.

IX APPENDIX

1 Procedure & Parameters for Preliminary Elemental Composition Assignment by “Molecular Weight Calculator”

The operation parameters used in this thesis for batch elemental composition assignment, based on molecular weight, with the software Molecular weight calculator²⁰, are explained in detail in the paragraphs below. The program by Matthew Monroe is freeware and proved to be a valuable support for this work.

1.1 Raw Data

Raw data are in ASCII format (*.txt) directly from ICR-MS-software. Before batch assignment data are imported into Excel with separator: “blank” and “ignore consecutive separators” checked. Decimals set to “,” and 1000 separator to “.”. Only the column containing the exact masses is copied into an empty NotePad document and a first line containing “FF=” (to activate the formula finder module) must be attached. A filename (*.txt) referring to the sample and parameters for the next step should be chosen.

1.2 Molecular Weight Calculator

In the software the formula finder (menu “tools”) is activated to set the following (Table IX-A) parameters (using isotopic elemental weights).

The settings given in Table IX-A are optional, the absence of nitrogen was also controlled by including ¹⁴N in the assignment process. The maximum number of hits is set to 10, if reached, clear assignment is considered not possible.

²⁰ LIT6 Molecular weight calculator version 6.25 beta 9 (May 20, 2003) by Matthew Monroe is freeware and accessible at <http://alchemistmatt.com>

Table IX-A. Settings for the “formula finder” module. The symbols given in the output file appears in resulting elemental compositions as shown.

Isotope	Minimal number	Maximal number	Accurate mass	Symbol in output file
^{12}C	0	90	12,000000	C
^1H	0	180	1,0078246	H
^{16}O	0	5	15,994915	O
^{32}S	0	5	31,972072	S
^{13}C	0	1	13,00335	C2_
$^{11}\text{B}^{19}\text{F}_4^-$	0	1	87,00292	C3_
^{107}Ag	0	1	106,905095	Ag

Further settings (in the formula finder options) include:

Weight tolerance:	2
ppm mode	
Match molecular weight	
Sort results:	Sort by formula
Bounded search	
Smart H atoms	
Find charge:	unchecked
Find m/z:	unchecked
Limit charge range:	unchecked
Find Target m/z:	unchecked
Automatically adjust Min and Max	
in bounded search:	unchecked

After calculation all assignments are saved in a file (*.txt.out)²¹ and can be opened by Notepad. Import into Excel was done by select the data²² of "*.txt.out" in Notepad and copy paste it in one column in the Excel spreadsheet “import”.

1.3 Decision-Scheme of Spreadsheet “MWCsort.xls”

The Excel spreadsheet application MWCsort evaluates data files directly from MWC. The application consists of two relevant worksheets named “RawData” and “Sort1”. Raw

²¹ File name is best changed to “out*.txt” for simpler use.

²² Select all: “Strg” + “a”

data directly from ICR control software as well as output files of MWC are entered (or copied) here. In “Sort1” the elemental compositions are processed and assessed. In this section the crucial decision procedures developed for this work are described in detail. The numbers in brackets refer to lines of code in Appendix 0, p. 141.

Data from MWC are opened with the text-processor “Notepad” and copied into the designated columns (F to H) in the sheet “RawData”. Since multiple assignments are frequent and vary in number, values are brought in a more concise form (all assignments per signal into one row). Therefore signal number is chosen as a marker and the number of suggested assignments is grouped behind it (L335-341). The pre-sorted data are transferred (L342+343) to sheet “sort1” where the elemental compositions are verified according to chemical sense. For better calculability the elemental coefficients are extracted (L344-358) from the string (text format data type²³) that contains the elemental composition and converted into number format. Values for carbon and/or hydrogen numbers are subtracted by the amount eventually added due to ionization (L345-349). Clusters are identified through presence of BF_4^- or Ag^+ ions (L348-350) and the hydrogen deficiency Z is calculated (L361). Chemical sense of the EC in question is rated based on Z being greater than -2 and even. Clusters are nominated and odd Z values interpreted as protonation/methylation. Impossible formulas are rated as wrong (L362+363). Mass deviation of each assigned composition is multiplied according to its “rating” so that assignments with small mass deviation which show methylation/protonation are favored (L364-370). Elemental coefficients are extracted of the best rated elemental composition and class and type are assigned.

2 Elemental Composition Identification Based on Tabled Kendrick Mass Defects

Formula assignment was done by a self-written Excel spreadsheet application HP2000²⁴. This consists of several worksheets, which are described, now in suggested order of use.

²³ The data type string can contain up to 255 characters including letters and numbers. Mathematical operations, e.g. multiplication can not be performed with this data type.

²⁴ “HP2000.xls

2.1 Settings and Parameters

The sheet “Settings” contains crucial parameters for all calculations.

Mass added by ionization:	If sample is protonated, methylated or otherwise changed prior or during ionization the mass of that change must be entered here (added mass positive, e.g. methylation, subtracted mass negative, e.g. deprotonation).
Initial assignment:	Maximum difference between measured and calculated (Kendrick) mass for initial assignment. Value should be between 0.3 and 0.8 [mDa].
Secondary assignment:	Maximum difference between measured and calculated (Kendrick) mass. For compounds <900 Da it should not exceed 3.0 [mDa]. Minimum value should be higher than initial assignment
Member factor:	Takes the number of initially assigned members in a homologue series into account. If two or more series are possible, only the nearest one with “MemFac” members more than the other possible series will be assigned. Value should be between 0.5 (weight on mass accuracy) to 2 (weight on initially assignments).

2.2 Initial Identification and Assignment of Class and Type

(Lines 1-99, 372-409) The raw data from the ICR software are imported into the sheet “RawData”, from where it is automatically accessible. Initial assignments are done in “Sort1”. KNM and KMD are calculated and listed to the right of the signal number and IUPAC mass. Then, macro “DerFinder10” (see listing in Appendix IX9, p. 131) compares previously calculated and tabled KMD (L17) with those of the imported mass list (L29-55). If the difference is less than previously given in “Initial assignment” a match is considered to be possible. Changes in elemental composition caused prior to or during ionization due to methylation, protonation or deprotonation are also taken into account (L56-75). This way signals caused by successful derivatization in addition to those originating from underivatized analytes are correctly identified. Since multiple assignments are possible, results were sorted according to smallest discrepancy between measured and calculated KMD (L373-375). Data were extracted from integer to numerical format (L376-383) Integer format compresses class and type, e.g. M*S1Z10 for a methylated compound

with one sulfur atom, hydrogen deficiency of 10 and one ^{13}C isotope. The carbon number for each assignment was calculated as additional criteria for the assigned KMD series. The mass of the parent structure of the homologue series in question was subtracted from the measured (L386-389). The remaining rest, representing solely methylene groups, must be dividable by 14 (in Kendrick mass scale) and result an integer number (n). This carbon distribution number n represents the number of methylene groups and ranks the compound in the homologue series. If more than one allocation was possible for one signal, which for all investigated samples was observed only once, no elemental composition was assigned. The data (class, Z, n, x, and M = methylation) were used in sheet “Sort3” to construct elemental compositions $^{12}\text{C}_{(c-x)}^{13}\text{C}_x\text{H}_{(2c-z)}\text{N}_n\text{O}_o\text{S}_s$ (L395-409). Assignments after this step were counted for each class and type and stored for use in the next step (L390-393).

2.3 Secondary Assignments to Fill Gaps of Unassigned Signals in the Mass List

In the third step (L100-200) the previously established series are extended. The sheet “ArtMass” calculates in combination with the macro “Lückenfüller03” elemental compositions masses which are then compared with the Raw Data mass list. Therefore, the macro provides class and type of all series in the order of members per series, which are used in the sheet to calculate elemental compositions for all carbon numbers up to 100 and the corresponding masses (IUPAC mass scale). Those masses are compared with the ones measured of the spectra. To include derivatized molecules, the molecular weight was increased for the mass of the structure introduced for ionization, e.g. methyl group, proton. If measured and calculated mass differ less than 1.5 to 3.0 mDa the secondary assignment is accepted. Later, the multiple assignments are corrected automatically with the macro “DoItNow01” (L201-333). All data are grouped according to signal number (L). If a signal has multiple possible elemental compositions they are weighted according to members assigned in the first step (L) and according to the differences between measured and hypothetical mass (L). Series with initially (clearly identified) more members are considered first (L). The parameter “MemberFactor” is the factor in member number that one homologue series need in excess over a competing series to be assigned, e.g. factor = 2 means: Series A needs double as many members from step one as series B to be assigned to the vacant point of data under consideration. Settings for a mass difference in this step higher than 1.5 mDa result in increased multiple assignments which have to be consulted manually, but general assignment improved with values up to three.

3 Sulfur Quantification.

Total sulfur in two vacuum residue fractions after separation by LEC was quantified by combustion in oxygen atmosphere and following sulfate quantification by ICP-OES.

3.1 Oxidation to Sulfate by Combustion of the Sample

Sulfur in the LEC fractions of the “effluent”, 18.15 mg of fraction 1 and 7.38 mg of fraction 2, were combusted to sulfate in an oxygen atmosphere according to Schöninger [132]. The samples were dissolved aided by ultrasonification in 100 μ L cyclohexane and the solution was placed on an ash free paper filter. After careful drying for 5 min the paper was folded, ignited and rapidly enclosed in a Schöninger flask filled with 10 mL of 10 % (v/v) H_2O_2 in twice distilled water. 10 min after complete combustion the remaining H_2O_2 was removed by boiling followed by dilution with 0.1 molar nitric acid to 100 mL. These solutions were then analyzed by ICP-OES.

3.2 Sulfate Quantification by Inductively Coupled Plasma – Optical Emission Spectroscopy (ICP-OES)

External calibration with sodium sulfate (2, 4, 6, 8, and 40 ppm) was utilized. Sulfur was detected at atom lines S(I) 142.503, 143.328, 147.400, 166.669, 180.731, and 182.034 nm wavelength. Fraction 1E (PAH of the effluent) contained 2.0 ± 0.2 %wt sulfur and fraction 2E (PASH of the effluent) 2.8 ± 0.2 %wt.

4 Supporting Material: Initial Data (Provided by IFP, Vernaison, France)

The data presented (in IX4) were graciously provided by the Institute Français du Pétrole, Vernaison, France.

Table IX-B. Preliminary bulk analysis for complete aromatic fraction of the effluent before and after HDS.^a

Elemental analysis	Feed Aromatics	Effluent Aromatics
%C	84.33	86.66
%H	11.11	10.57
%N	<0.05	<0.05
%S	4.66	2.91
%O	0.25	0.22
¹³C NMR		
%C arom	22.9	23.5
%C quat	14.9	14.8
%C quat condensed	6.9	7.1
%C quat substituted	8.0	7.8
%CH	8.0	8.7
%C sat	77.1	76.5
%CH	10	13.8
%CH ₂	54	45.9
%CH ₃	13.1	16.8
Simulated Distillation		
Initial boiling point	466.8 °C	
Final AEBP	717.1 °C (90%)	

5 Materials and Devices

1,2,3,4-Tetrahydrodibenzothiophene	>98 %	astec
1,2-Dichloroethane	technical grade	Fisher Chemicals
1-Methylnaphthalene	>97 %	Fluka
1-Methylphenanthrene	98 %	Janssen
1-Mercapto-5,6,7,8-tetrahydronaphthalene	n.a.	in house
2,4,6,8-Tetramethyldibenzothiophene	>98 %	astec
2,7-Dimethylbenzothiophene	>98 %	astec
2-Methyldibenzothiophene	>98 %	astec
2-Methylnaphthalene	97 %	Fluka

2-Octyldibenzothiophene	n.a.	in house
3-Cholestanone	n.a.	Sigma
4,6-Dimethyldibenzothiophene	>98 %	astec
4-Ethyldibenzothiophene	90 %	in house
4-Methyldibenzothiophene	>98 %	astec
4-Octyldibenzothiophene	n.a.	in house
Acenaphthylene	99 %	Aldrich
Aceton	residue analysis	Fluka
Acetonitrile	GC	Fluka
Aluminiumoxid 90(neutral)	for chromatography	Fluka
Aminopropanosilica	for HPLC	in house
Aminopropene	>98 %	Fluka
Anthracene	pure	Riedel-de-Häen
Benzo[<i>b</i>]naphtho[2,3- <i>d</i>]thiophene	>98 %	astec
Benzothiophene	0,97	Fluka
Bromime	p.a.	Janssen
Chrysene	>98 %	Aldrich
Cyclohexan	residue analysis	Fluka
Deuteriochloroform + 0.01v/v TMS	99.5 %	Fluka
Dibenzothiophene	98 %	Fluka
Dibenzothiophene	98 %	Fluka
Diethylether	technical grade	Fluka
Dimethylchlorosilane	97 %	Fluka
Dinitroaminopropano silica	for HPLC	in house
Ethanol	technical grade	Fluka
Ethanol	residue analysis	Fluka
Fluoranthene	p.a.	Riedel-de-Häen
Fluorenone	99	Merck
Glacial acetic acid	technical grade	Merck
Hexachloroplatinic acid	>99 %	Alpha
Hydrogen bromide dissolved in acetic acid	47 %	Merck
Hydrogenperoxide	p.a.	Grüssing
Isopropanol	technical grade	Merck
Kieselgel 60	for chromatography	Fluka
Magnesium sulfate (dry)	p.a.	Grüssing
Methanol	residue analysis	Fluka
Methylene chloride	for HPLC	Fluka
Methylene chloride	residue analysis	Fluka
Methyliodide	99	Merck
Naphthalene	99 %	Merck
Nitric acid	p.a.	Grüssing
Nitrogen	Purity 4.6	institute supply
Perylene	99 %	Aldrich
Phenanthrene	98 %	Fluka
Polyphosphoric acid	83 %	Fluka
Potassium hydroxid	p.a.	Grüssing
Pyrene	97 %	Fluka

Pyridine	99 %	Aldrich
Quinoline	technical grade	in house
Silica 10 µm 100A	for HPLC	Merck
Silver(I) tetrafluoroborate	>95 %	Aldrich
Sodium sulfate	p.a.	Merck
Sulfuric acid	p.a.	Grüssing
Tetrachlorophthalic acid anhydrid	97 %	Fluka
Tetrahydrofuran	for HPLC	Acros Organics
Theobromine deposited on silica	p.a.	in house
Toluene	residue analysis	Fluka
Trichlorosilane	99 %	Aldrich
Trimethylchlorsilane	n.a.	in house
Water	twice distilled	institute supply

6 Instrumental Parameters

HP1050

Hewlett-Packard 1050 HPLC system with a quaternary pump, degasser, manual injection valve and a diode array detector set to record the UV spectra from 200 to 450 (or 600) nm. Instrument control and data recording were done with Chemstation version 9.03, (Agilent, 71034 Böblingen, Germany).

Knauer Wellchrom

Knauer system consisting of an interface box, 4 channel solvent degasser, two Ministar K 501 analytical pumps, mixing chamber, electrical injection valve or basic marathon plus autosampler, variable wavelenght UV detector set to 236 or 254 nm. Instrument control and data recording were done with Chromgate version 2.8 (Knauer, 14163 Berlin, Germany).

GPC

For GPC separations a Phenogel (Phenomenex, Torrance, California 90501, USA) 5 µm, 50 Å, 600 x 7.8 mm ID column with a fractionation range of 100 – 2000 Dalton was used. The mobile phase was tetrahydrofuran:cyclohexane 85:15(v/v) or pure tetrahydrofuran (for strongly solvating properties) or tetrahydrofuran:cyclohexane 15:85(v/v) as a weakly solvating mixture at a flow rate of 1.0 mL per minute, fractions were collected manually.

LEC

Ligand exchange chromatography was used for the group separation of PASHs from PAHs on a Pd(II)-bonded stationary phase with 10 μm 100 Å silica in a column of 125x4.6 mm ID. Solvent was CH/DCM 7:3 (v/v) for 15 min, then 0.5 % (v/v) isopropanol was added to the composition until elution of the second fraction (usually 15 min). Flow rate was 1.0 mL, fractions were collected manually.

Charge Transfere Chromatography

TCPP: Tetrachlorophthalimidopropano silica was synthesized according to Holstein [47] on nucleosil 100 Å 10 μm and was packed according to the slurry method using methanol and a pneumatic pump (Knauer, 14163 Berlin, Germany). Column dimensions were 120x4 mm ID. Three consecutively coupled columns were used for the analysis of the vacuum residue samples.

DNAP: 2,4-Dinitroanilin-N-propano silica, on nucleosil 100 Å 10 μm , 120x3mm ID, in house²⁵.

TB: Theobromine deposited on Nucleosil 100 Å 5 μm , 120x4mm, in house.

AP: Aminopropano silica (Polygosil ® (60-10) NH₂, 125x4 mm ID, Macherey-Nagel

MALDI-TOF-MS

MALDI-TOF analysis was done by co-crystallization with DCTB (trans-2-[3-(4-*t*-butylphenyl)-2-methyl-2-propenylidene]malononitrile) as matrix. The instrument was a Reflex IV (Bruker Daltonics, Bremen, Germany) with a nitrogen laser at 337 nm, pulse 3 ns, voltage 19 kV.

FT-ICR-MS

Mass spectra were recorded using an APEX III FT-ICR-MS (Bruker Daltonics, Bremen, Germany), equipped with a 7 T magnet and an Agilent electrospray (ESI) ion source.

The methylated samples were introduced as a solution in dichloromethane/methanol 1:1 (v/v) and injected in the infusion mode with a flow rate of 2 $\mu\text{L}/\text{min}$ at an electrospray voltage of 4.5 kV. The ions were collected for 0.5 s in a hexapole before release into the

²⁵ Synthesized by Thomas Schade, 02/2001, Department of Analytical Chemistry, 48149 Münster, Germany.

cyclotron cell. At least 64 scans were accumulated for each spectrum to improve the signal to noise ratio. Internal and external mass calibration was performed using the Agilent electrospray calibration solution, covering the mass range of the sample with the exact masses 322.04812, 622.02896, and 922.00980 Da.

7 Abbreviations

ABC	Asphaltene bottom cracking
ACDA	2-Aminocyclopentene-1-dithiocarboxylic acid
ACN	Acetonitrile
AEBP	Atmospheric equivalent boiling point
AP	Aminopropano
APCI	Athmospheric pressure chemical ionization
BBL	per Barrel
BNT	Benzonaphthothiophene
BPT	Benzophenanthrothiophene
BT	Benzothiophene
CH	Cyclohexane
CHNT thiophene; "Oskar"	Cholestano[2,3- <i>b</i>]-5,6,7,8-tetrahydronaphtho[2,1- <i>d</i>]-
Da	Dalton
DBT	Dibenzothiophene
DCE	1,2-Dichloroethane
DDS	Direct desulfurization
DHB	2,4-dihydroxybenzoic acid
DNAP	3-(2,4-dinitroanilino)propano
DNHB	
DNHB propenylidene]malononitrile	trans-2-[3-(4- <i>t</i> -butylphenyl)-2-methyl-2-
EI	Electron impact ionization
EPA	Environmental protection agency
EPA	Electron pair acceptors
EPD	Electron pair donors
ESI	Electrospray ionization
FCC	Fluid catalytic conversion
FD	Field desorption
FI	Field ionization
FT-ICR-MS spectrometry	Fourier transform ion cyclotron resonance mass
GPC	Gel permeation chromatography

h	Hour(s)
HDS	Hydrodesulfurization
HPLC	High performance liquid chromatography
HYD	Hydrogenation desulfurization route
ICP-OES spectroscopy	Inductively coupled plasma optical emission
ICR	Ion cyclotron resonance
IFP	Institut Français du Pétrole
kDa	kilo Dalton
KMD	Kendrick mass defect
KNM	Kendrick nominal mass
laser radiation	Light amplification by stimulated emission of
LC	Liquid chromatography
LEC	Ligand exchange chromatography
LIMS	Laser ionization mass spectrometry
MALDI	Matrix assisted laser desorption and ionization
mDa	milli Dalton
MDa	Mega Dalton
min	minute(s)
MS	Mass spectrometry
NM	Nominal mass
NMR	Nuclear magnetic resonance
NPT	Naphthophenanthrothiophene
NY	New York
OSC	Organic sulfur compounds
p.	Page
PAC	Polycyclic aromatic compounds
PAH	Polycyclic aromatic hydrocarbons
PANH	Polycyclic aromatic nitrogen heterocycles
PASH	Polycyclic aromatic sulfur heterocycles
PB	Particle beam ionization
PSDVB	Polystyrene-divinylbenzene
RFCC	Residue fluidized catalytic cracking
s	Second(s)
SARA	Saturates, aromatics, resins and asphaltenes
TB	Theobromine
TCP	Tetrachlorophthalimidopropane

THF	Tetrahydrofuran
TOF-MS	Time of flight mass spectrometry
TSP	Thermospray
UV	Ultraviolet
V	Voltage
v/v	Volume per volume
Vis	Visible light
VPO	Vapor pressure osmosis
wt	weight
XANES	X-ray absorption near edge structure
XPS	X-ray photoelectron spectroscopy

8 Calculated “Mass Spectra” of S1 Class Homologue Series

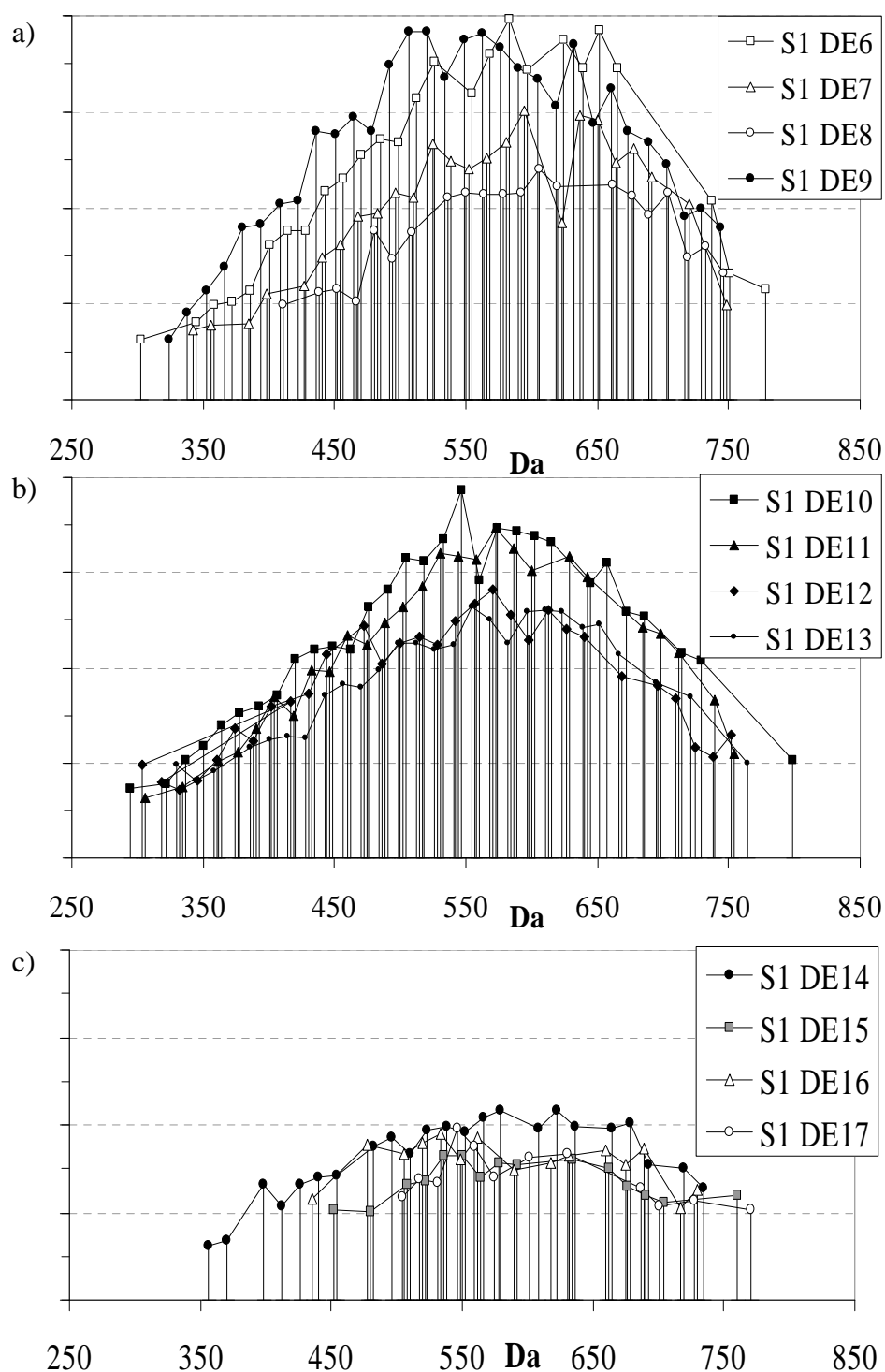


Figure IX-1. Plots of S1 class series of Feed fraction 1.

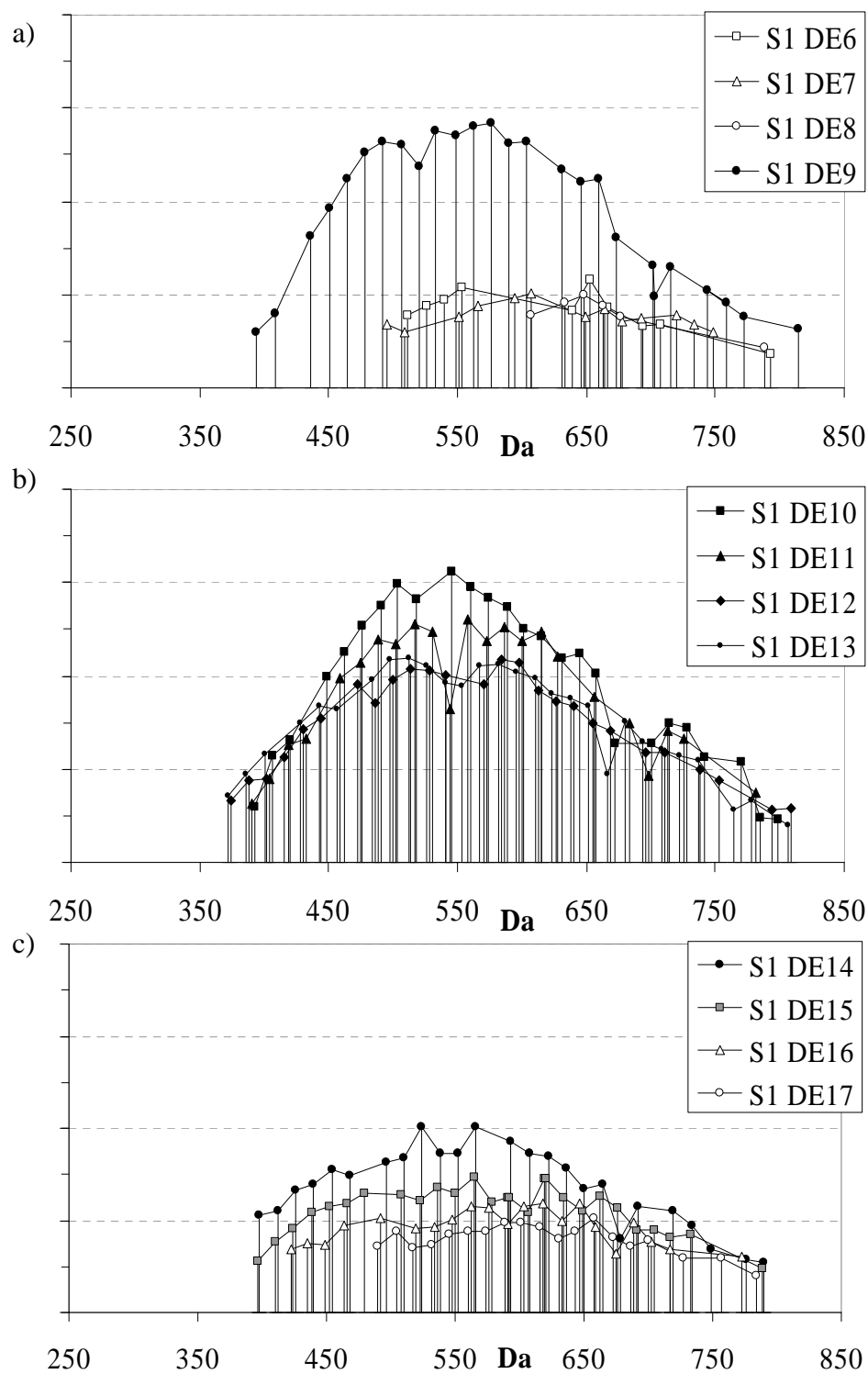


Figure IX-2. Plots of S1 class series of Effluent fraction 1.

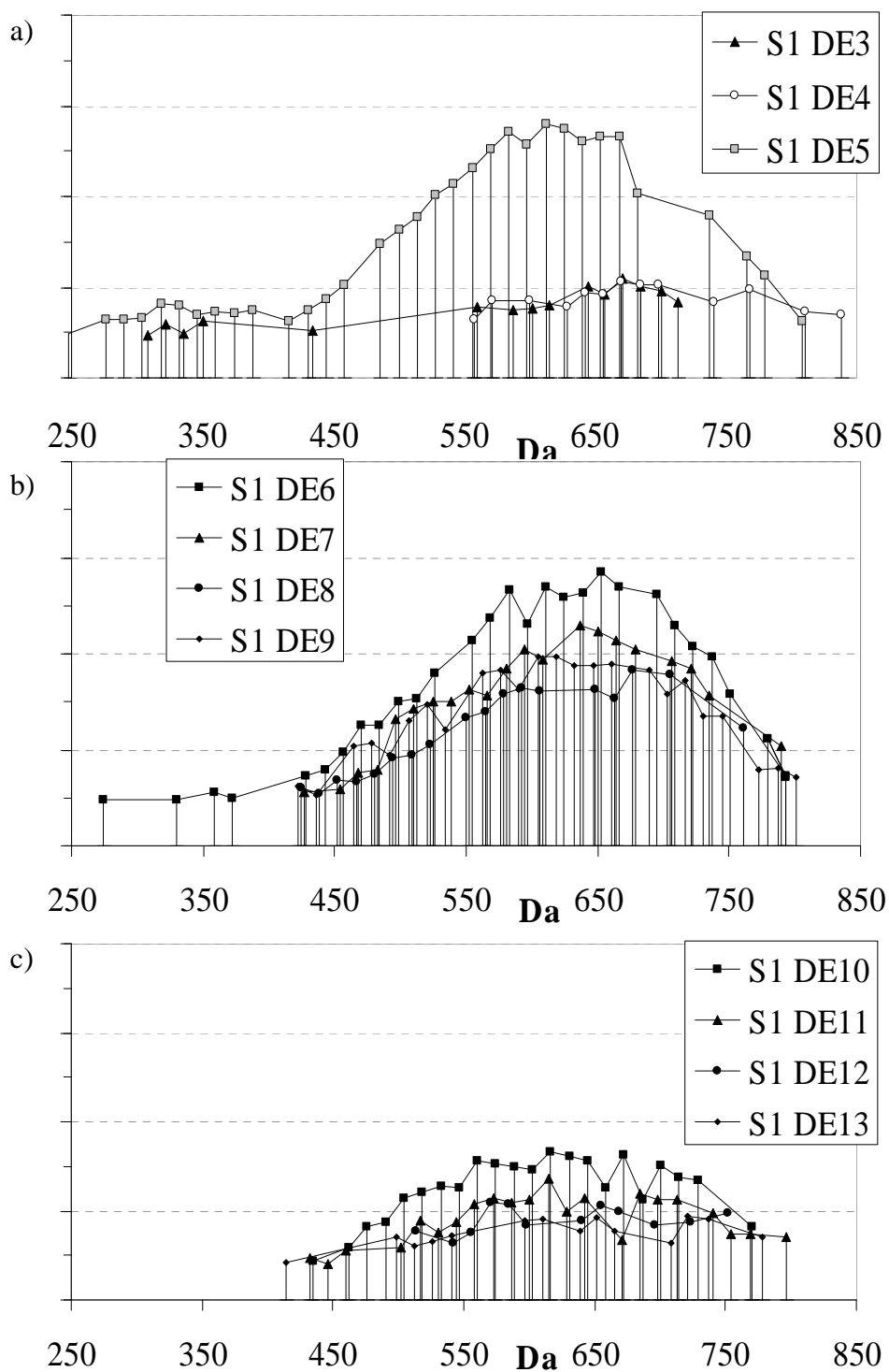


Figure IX-3. Plots of S1 class series of Feed fraction 2.

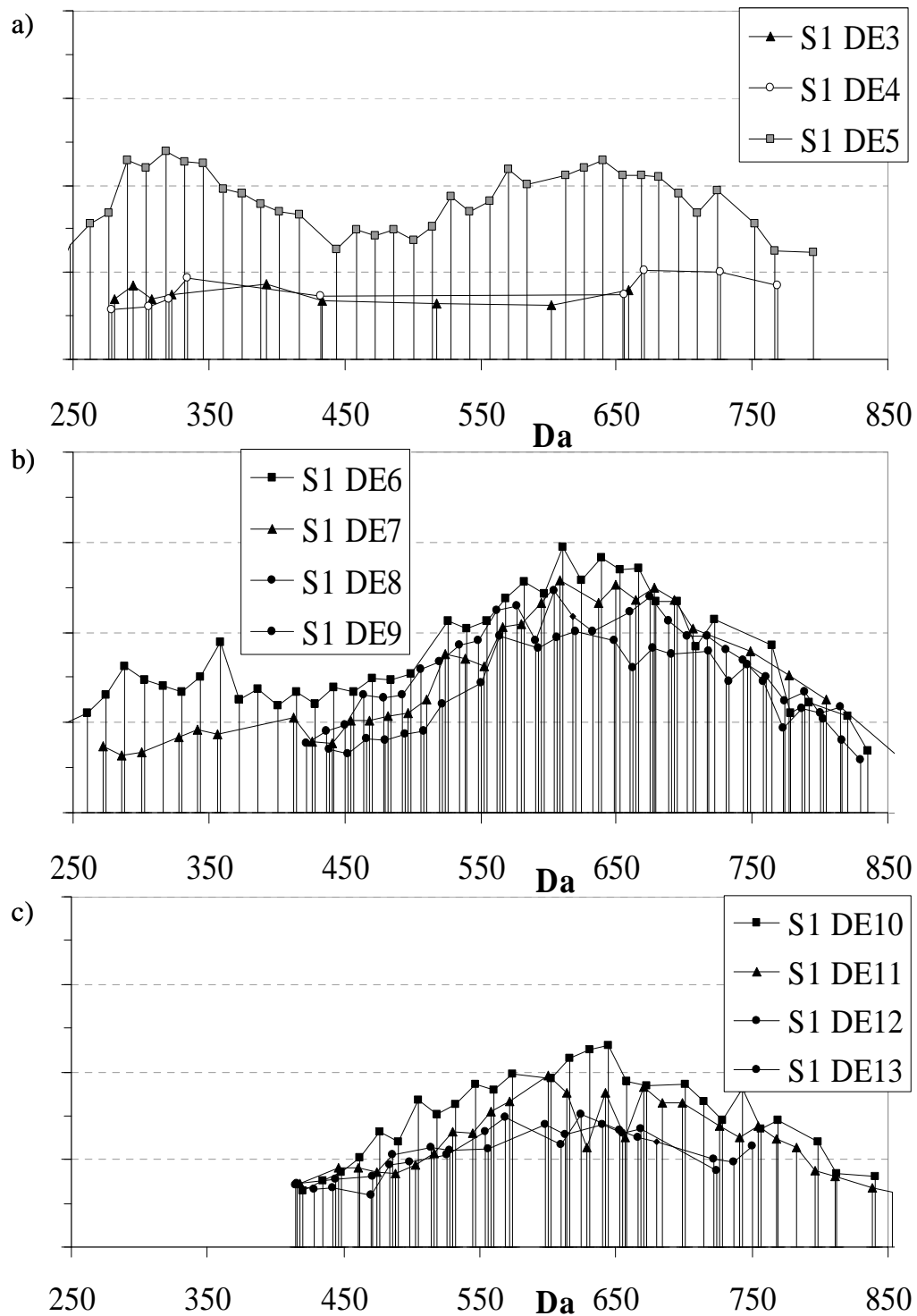


Figure IX-4. Plots of S1 class series of Effluent fraction 2.

9 Code for Data Processing Makros

Sub "DerFinder10()"

```
' Makro am 11.06.2165 von Hendrik aufgezeichnet
5 ' Tastenkombination: Strg+f

Dim Interval As Single
Dim Methylated As Double
Dim x, y, z As Integer
10 Methylated = 0
    x = 1
    y = 0
    z = 0

15 'Tabellierte KMD in Array KMDTable einlesen
Windows("HP2000.xls").Activate
Sheets("KMDTable").Select
KMDTable = Range("K83:M273")

20 Sheets("Sort1").Select
Interval = Range("L1").Value

Application.Goto Reference:="Sort3" 'delete old data
Selection.ClearContents

25 MsgBox "1. Step: Class & types will be initially assigned
difference (calculated - measured mass) of " & Interval & " m amu."

Range("H4").Select

30 Do Until ActiveCell.Value = ""
    y = 0
    x = 1
    Do While KMDTable(x, 1) - ActiveCell.Value <= Interval + 7
35 'Methylation included
```

```

Select Case KMDTable(x, 1)
Case Is <= ActiveCell.Value
    If Interval >= ActiveCell.Value - KMDTable(x, 1) Then
40         ActiveCell.Offset(0, 3 + y) = KMDTable(x, 2)
            ActiveCell.Offset(0, 15 + y) = ActiveCell.Value -
KMDTable(x, 1)
            y = y + 1
            'MsgBox "2 ActiveCell.Value = " & ActiveCell.Value
45 & "KMDTable(" & x & ", 1) = " & KMDTable(x, 1)
            End If
Case Is > ActiveCell.Value
    If Interval >= KMDTable(x, 1) - ActiveCell.Value Then
            ActiveCell.Offset(0, 3 + y) = KMDTable(x, 2)
50         ActiveCell.Offset(0, 15 + y) = KMDTable(x, 1) -
ActiveCell.Value
            y = y + 1
        End If
    End Select

55

Methylated = ActiveCell.Value + 6.8

Select Case KMDTable(x, 1)
Case Is <= Methylated
60     If Interval >= Methylated - KMDTable(x, 1) Then
            ActiveCell.Offset(0, 3 + y) = "M" & KMDTable(x, 2)
            ActiveCell.Offset(0, 15 + y) = Methylated -
KMDTable(x, 1)
            y = y + 1
65     End If
Case Is > Methylated
    If Interval >= KMDTable(x, 1) - Methylated Then
            ActiveCell.Offset(0, 3 + y) = "M" & KMDTable(x, 2)
            ActiveCell.Offset(0, 15 + y) = KMDTable(x, 1) -
70 Methylated
            y = y + 1
        End If
    End Select

```



```
75         x = x + 1
           If x = 191 Then Exit Do
           Loop
ActiveCell.Offset(1, 0).Select
Loop
80
MsgBox "Succesfully assigned class and type within " & Interval &
" m amu ! Press 'Enter' to copy data. Continue with CTRL + SHIFT +
L to start the makro: Lückenfüller03."

85 Range("K4:AF2003").Select
   Selection.Copy
   Range("AI4").Select
   Selection.PasteSpecial Paste:=xlValues, Operation:=xlNone,
SkipBlanks:= _
90       False, Transpose:=False

       Sheets("ArtMass").Select
       Range("Z2").Select

95 End Sub
```

Sub "Lückenfüller03()"

```

' Lückenfüller01 Makro
' Makro am 12.06.2004 von Hendrik aufgezeichnet
100 '
' Tastenkombination: Strg + L

Dim col, Typ, Class, Initial, IsoCarb, Interval, x As Integer
col = x = Typ = Class = Initial = IsoCarb = 0
105 Interval = Sheets("Settings").Range("D20").Value

'Prepare the Sheet Test
Sheets("TEST").Select
110 Cells.Select
Selection.ClearContents
Range("A1").Value = Sheets("RawData").Range("A2").Value
Range("A2").Value = "Interval : " & Interval

115 'Copy the actual KMTable and sort it according to initially
assigned homologue members
Sheets("KMTable").Select
Range("I82:M273").Select
Selection.Copy
120 Sheets("ArtMass").Select
Range("AD4").Select
Selection.PasteSpecial Paste:=xlValues, Operation:=xlNone,
SkipBlanks:= _
False, Transpose:=False
125 Application.CutCopyMode = False
Selection.Sort Key1:=Range("AH5"), Order1:=xlDescending,
Key2:=Range( _
"AE5"), Order2:=xlAscending, Header:=xlGuess,
OrderCustom:=1, MatchCase _
130 :=False, Orientation:=xlTopToBottom

Sheets("ArtMass").Select
Range("AH5").Select

```

```
135 MsgBox "Now trying to fill gaps in homologue series. Only signals
within +-" & Interval & " m amu will be considered"

Do Until ActiveCell.Offset(col, 0).Value = ""
    Typ = ActiveCell.Offset(col, -3).Value
140    Class = ActiveCell.Offset(col, 1).Value
    Initial = ActiveCell.Offset(col, 0).Value
    IsoCarb = ActiveCell.Offset(col, 2).Value

    'MsgBox "Considering Class S" & Class & " / Typ Z " & Typ & " /
145 13C = " & IsoCarb & ". Initial Assigned have been " & Initial &
    "Members. Press Enter!"

    Range("C2").Value = Typ
    Range("D2").Value = Class
150    Range("E2").Value = IsoCarb
    Range("I2").Value = Initial

    'MsgBox "Now calculating Class S" & Class & " and type Z = " &
    Typ & " ..."
155

    Range("AL5:AS50").Select
    Selection.Copy

    Sheets("TEST").Select 'Den Quatsch kopieren nach TEST
160    Range("A1").Select
    Selection.End(xlDown).Select
    ActiveCell.Offset(1, 0).Select
    Selection.PasteSpecial Paste:=xlValues, Operation:=xlNone,
    SkipBlanks:= _
165    True, Transpose:=False
    Sheets("ArtMass").Select

    x = x + 1
    Range("AH5").Select
170    col = col + 1
    Loop
```

```
MsgBox "Finished: " & x & " loops done. Sorting results.."
```

```
175     Sheets("Sort3").Select 'Attach initial assigned data
        Range("B3:I3").Select
        Range(Selection, Selection.End(xlDown)).Select
        Selection.Copy
        Sheets("TEST").Select
180     Range("A1").Select
        Selection.End(xlDown).Select
        ActiveCell.Offset(1, 0).Select
        Selection.PasteSpecial    Paste:=xlValues,    Operation:=xlNone,
SkipBlanks:= _
185         False, Transpose:=False

        Sheets("TEST").Range("A3:H6").Select
        Range(Selection, Selection.End(xlDown)).Select
        Selection.Sort    Key1:=Range("A3"),    Order1:=xlAscending,
190     Key2:=Range("D3") _
        ,    Order2:=xlAscending,    Header:=xlGuess,    OrderCustom:=1,
MatchCase:= _
        False, Orientation:=xlTopToBottom

195     MsgBox "Please continue with the next Makro: CTRL + d for:
        DoItNow01"

End Sub
```

Sub "DoItNow01()"

```
200 ' Makro am 13.06.2004 von Hendrik aufgezeichnet
    ' Tastenkombination: Strg + D

    Sheets("TEST").Select ' Kopieren der Daten nach SORT4
    Range("A3:H3").Select
205 Range(Selection, Selection.End(xlDown)).Select
    Selection.Copy
    Sheets("Sort4").Select
    Range("B6").Select
    Selection.PasteSpecial Paste:=xlValues, Operation:=xlNone,
210 SkipBlanks:= _
        False, Transpose:=False

    Range("K6:R2030").Select 'Erster Schritt automatische
215 Sortierung
    Application.CutCopyMode = False
    Selection.Copy
    Range("S6").Select
    Selection.PasteSpecial Paste:=xlValues, Operation:=xlNone,
220 SkipBlanks:= _
        False, Transpose:=False
    Application.CutCopyMode = False
    Selection.Sort Key1:=Range("S6"), Order1:=xlAscending,
    Key2:=Range("W6") _
225 , Order2:=xlDescending, Header:=xlGuess, OrderCustom:=1,
    MatchCase:= _
        False, Orientation:=xlTopToBottom

    MsgBox " Comparing formulas for multiple assigned signals. First
230 Step " & _
    Range("J5").Value & " multiple assignments. Continue with next
    step.."

    Range("AB6:AI2030").Select 'Zweiter Schritt automatische
235 Sortierung
    Selection.Copy
    Range("AJ6").Select
```

```

        Selection.PasteSpecial    Paste:=xlValues,    Operation:=xlNone,
SkipBlanks:= _
240        False, Transpose:=False
        Application.CutCopyMode = False
        Selection.Sort    Key1:=Range("AJ6"),    Order1:=xlAscending,
Key2:=Range("AN6" _
        ), Order2:=xlDescending, Header:=xlGuess, OrderCustom:=1,
245 MatchCase:= _
        False, Orientation:=xlTopToBottom

MsgBox " Comparing formulas for multiple assigned signals. Second
Step " & _
250 Range("AA5").Value & " multiple assignments. Continue with next
step.."

        Range("AS6:AZ2030").Select    'Dritter    Schritt    automatische
Sortierung
255        Selection.Copy
        Range("BA6").Select
        Selection.PasteSpecial    Paste:=xlValues,    Operation:=xlNone,
SkipBlanks:= _
        False, Transpose:=False
260        Application.CutCopyMode = False
        Selection.Sort    Key1:=Range("BA6"),    Order1:=xlAscending,
Key2:=Range("BE6" _
        ), Order2:=xlDescending, Header:=xlGuess, OrderCustom:=1,
MatchCase:= _
265        False, Orientation:=xlTopToBottom

MsgBox " Checked for signals with multiple assigned formulas. " &
_
270 Range("BI5").Value & " multiple assignments remain and have to be
manually checked."

        Sheets("Export").Range("A4:IV30000").Clear
        Sheets("Sort4").Range("BA6:BI2030").Select
        Selection.Copy
275        Sheets("Export").Select
        Range("A4").Select
        Selection.PasteSpecial    Paste:=xlValues,    Operation:=xlNone,
SkipBlanks:= _

```

```
False, Transpose:=False
280
    Sheets("Sort4").Select
    Range("BN6:BO2030").Select
    Selection.Copy
    Sheets("Export").Select
285    Range("J4").Select
        Selection.PasteSpecial    Paste:=xlValues,    Operation:=xlNone,
SkipBlanks:= _
        False, Transpose:=False

290    Sheets("Sort4").Select    'Not    Assigned    Signals    are
transported to sheet EXPORT and sorted.
    Range("BJ6:BJ2030").Select
    Selection.Copy
    Sheets("Export").Select
295    Range("M4").Select
        Selection.PasteSpecial    Paste:=xlValues,    Operation:=xlNone,
SkipBlanks:= _
        False, Transpose:=False

300    Sheets("Sort4").Select
    Range("BK6:BK2030").Select
    Application.CutCopyMode = False
    Selection.Copy
    Sheets("Export").Select
305    Range("O4").Select
        Selection.PasteSpecial    Paste:=xlValues,    Operation:=xlNone,
SkipBlanks:= _
        False, Transpose:=False

310    Sheets("Sort4").Select
    Range("BL6:BL2030").Select
    Application.CutCopyMode = False
    Selection.Copy
    Sheets("Export").Select
315    Range("T4").Select
        Selection.PasteSpecial    Paste:=xlValues,    Operation:=xlNone,
SkipBlanks:= _
```

```
False, Transpose:=False

320     Range("M4:T2028").Select
        Application.CutCopyMode = False
        Selection.Sort      Key1:=Range("M4"),      Order1:=xlAscending,
Header:=xlGuess, _
        OrderCustom:=1,      MatchCase:=False,
325 Orientation:=xlTopToBottom
    MsgBox "Results are listed in sheet EXPORT. Parameters for
calculation are on sheet: SETTINGS. There are " &
Sheets("Sort4").Range("BI5").Value & " signals with two or more
assingnments. Please check those manually."
330 End Sub
```


Code for Worksheet: "MWCsort"

```

=WENN(LINKS(F3;5)="; FF ";I2+1;I2)
=WENN(I3=I2;" ";I3)
=WENN(ISTFEHLER(WERT(RECHTS(F4;2)))=WAHR;" ";WERT(RECHTS(F4;2)))
335 =WENN(K3>0;F5;" ")
=WENN(ISTFEHLER(ABS(WERT(WENN(K3>0;WECHSELN(WECHSELN(H5;"dm=";" ";1)
;"ppm";"";1);"")))=WAHR;" ";ABS(WERT(WENN(K3>0;WECHSELN(WECHSELN(H5
;"dm=";" ";1);"ppm";"";1);""))))
=SVERWEIS($B5;RawData!$J$2:$AE$25000;L$1;FALSCH)
340 =SVERWEIS($B5;RawData!$J$2:$AE$25000;V$1;FALSCH)
=INDEX(L5:AE5;;VERGLEICH(KKLEINSTE(V5:AE5;1);V5:AE5;0))
=AL5+AM5-Settings!$C$18
=WENN(ISTFEHLER(WERT(TEIL(AF5;FINDEN("H";AF5;1)+1;3)))=WAHR;WERT(TE
IL(AF5;FINDEN("H";AF5;1)+1;2)))-
345 Settings!$C$17;WERT(TEIL(AF5;FINDEN("H";AF5;1)+1;3))-
Settings!$C$17)
=WENN(ISTFEHLER(FINDEN("O";AF5;1))=WAHR;0;WENN(ISTFEHLER(WERT(TEIL(
AF5;FINDEN("O";AF5;1)+1;2)))=WAHR;WENN(ISTFEHLER(WERT(TEIL(AF5;FIND
EN("O";AF5;1)+1;1)))=WAHR;1;WERT(TEIL(AF5;FINDEN("O";AF5;1)+1;1)))
350 WERT(TEIL(AF5;FINDEN("O";AF5;1)+1;2))))
=WENN(ISTFEHLER(FINDEN("S";AF5;1))=WAHR;0;WENN(ISTFEHLER(WERT(TEIL(
AF5;FINDEN("S";AF5;1)+1;2)))=WAHR;WENN(ISTFEHLER(WERT(TEIL(AF5;FIND
EN("S";AF5;1)+1;1)))=WAHR;1;WERT(TEIL(AF5;FINDEN("S";AF5;1)+1;1)))
WERT(TEIL(AF5;FINDEN("S";AF5;1)+1;2))))
355 =WENN(ISTFEHLER(FINDEN("C2_";AF5;1))=WAHR;0;1)
=WENN(ISTFEHLER(FINDEN("C3_";AF5;1))=WAHR;0;1)
=WENN(ISTFEHLER(FINDEN("Ag";AF5;1))=WAHR;0;1)
=(AH5*2+2)-AI5
=WENN(ODER(AN5=1;AO5=1);"Cluster";WENN(AP5<0;FALSCH;WENN(ISTUNGERAD
360 E(AP5);"NoMethyl";WAHR)))
=WENN(ISTFEHLER(WENN(AQ3=FALSCH;AG3*1000000;WENN(AQ3="cluster";AG3*
1000;AG3)))=WAHR;1000000;WENN(AQ3=FALSCH;AG3*1000000;WENN(AQ3="clu
ster";AG3*1000;AG3)))
=WENN(ISTFEHLER(WAHL(VERGLEICH(KKLEINSTE((EV5:FE5);1);(EV5:FE5);0);
365 AF5;AR5;BD5;BP5;CB5;CN5;CZ5;DL5;DX5;EJ5))=WAHR;" ";WAHL(VERGLEICH(KK
LEINSTE((EV5:FE5);1);(EV5:FE5);0);AF5;AR5;BD5;BP5;CB5;CN5;CZ5;DL5;D
X5;EJ5))

```

10 Spreadsheet Code “HP2000”

Worksheet: “Sort1”

```

370 =WENN(ISTFEHLER(KKLEINSTE($AU4:$BD4;BF$3))=WAHR;" ";KKLEINSTE($AU4:$
BD4;BF$3))
=WENN(BF4=" "; " "; INDEX($AI4:$AR4;;VERGLEICH(BF4;$AU4:$BD4;0)))
=WENN(CE4=1;VERKETTEN("*S";CC4;"Z";CD4);VERKETTEN("S";CC4;"Z";CD4))
375 =WENN(ISTFEHLER(WERT(TEIL(BQ4;FINDEN("S";BQ4)+1;1)))=WAHR;" ";WERT(T
EIL(BQ4;FINDEN("S";BQ4)+1;1)))
=WENN(ISTFEHLER(WERT(TEIL(BQ4;FINDEN("Z";BQ4)+1;2)))=WAHR;" ";WERT(T
EIL(BQ4;FINDEN("Z";BQ4)+1;2)))
=WENN(ISTFEHLER(FINDEN("*";BQ4))=WAHR;0;1)
=WENN(ISTFEHLER(FINDEN("M";BQ4))=WAHR;0;1)
380 =WENN(CC4=" "; " "; WENN(REST(RUNDEN(KF*WENN(CF4=1;$C4-Methylated;$C4)-
KF*INDEX(KMDTable!$E$8:$H$38;(CD4+4)/2;CC4+1);2);14)=0;(KF*WENN(CF4
=1;$C4-Methylated;$C4)-
KF*INDEX(KMDTable!$E$8:$H$38;(CD4+4)/2;CC4+1))/14;" "))
=WENN($CH4<>" "; CC4;WENN($CO4<>" "; CJ4;WENN($CV4<>" "; CQ4;" ")))
385 "(=SUMME(WENN($CX$4:$CX$1500=CX4;WENN($CY$4:$CY$1500=CY4;1;0))))"
=WENN(CW4=" "; " "; DD4)
=WENN(ISTFEHLER(SVERWEIS(L83;Sort1!$CW$4:$DE$2003;8;FALSCH))=WAHR;0
;SVERWEIS(L83;Sort1!$CW$4:$DE$2003;8;FALSCH))

```

Worksheet: “Sort3”

```

390 =Sort1!DC4                                Carbon number (number of methylen groups)
=INDEX(U$4:U$34;(G3+4)/2;)
                                C atoms in base molecule (defines class & type)
=INDEX(V$4:V$34;(G3+4)/2;)
                                H atoms in base molecule (defines class & type)
395 =2*O3-G3                                H atoms in elemental composition
=WENN(Sort1!DC4=" "; " "; Sort1!B4)                                take Z

=WENN(Sort1!DC4=" "; " "; WENN(Sort1!DA4=1;Sort1!C4-
Methylated;Sort1!C4))                                Check methylation
400 =WENN(F3=" "; " "; WENN(K3=1;VERKETTEN("*C";O3;"H";P3;WENN(H3>0;VERKETT
EN("S";H3);" "));VERKETTEN("C";O3;"H";P3;WENN(H3>0;VERKETTEN("S";H3)
;" "))))                                compose elemental composition
=WENN(L3=" "; " "; WENN(Sort1!DA4=1;VERKETTEN("M";L3);L3))
                                Add methylation/protonation marker to elemental composition

```



```

=WENN(AL5="";"";SVERWEIS($AL5;$U$5:$Y$104;4;FALSCH)*1000)
445                                     difference calc. - measured mass
=WENN(AL5="";"";$I$2)                   number of initial assignments
=WENN(AL5="";"";$C$2)                   Z
=WENN(AL5="";"";$D$2)                   class
=WENN(AL5="";"";SVERWEIS(AL5;$AA$5:$AC$2003;3;FALSCH))
450                                     relativ intensity

```

All data is then combined with that for all other series and transferred to Worksheet "Sort4".

Worksheet: "Sort4"

```

455 =WENN(B6="";"";WENN(B6=B7;"ALARMMD";WENN(B6=B5;"ALARMU";"")))
                                     check for multiple assignments for one signal
=WENN(J6="";B6;WENN(J6="ALARMMD";WENN(UND(G6=G7;H6=H7);B6;WENN(F6>=F
7*MemFac;B6;""));WENN(J6="ALARMU";WENN(UND(G6=G5;H6=H5);"";WENN(F6>
=F5*MemFac;B6;"")))))
460     decide which signal fits better, criteria: Member factor
=WENN($K6="";"";C6)                   transfer data from best assignment
=WENN($K6="";"";D6)
..
=WENN(ISTFEHLER(SVERWEIS(A6;BA$1:BG$2030;1;FALSCH))=WAHR;SVERWEIS(A
465 6;Sort1!$B$4:$D$2003;1;FALSCH);"")
find signals without assignment and sort them according to signal
no.
=WENN(ISTFEHLER(BJ6)=WAHR;"";WENN(BJ6="";"";SVERWEIS(A6;Sort1!$B$4:
$D$2003;2;FALSCH)))
470                                     transfer accurate mass for unassigned signals
=WENN(BK6="";"";SVERWEIS(A6;Sort1!$B$4:$D$2003;3;FALSCH))
                                     transfer relative intensity for unassigned signals

```

1. Whitehurst, D.D., T. Isoda, and I. Mochinda, *Present state of the art and future challenges in the hydrodesulfurization of polyaromatic sulfur compounds*. Adv. Catal., 1998. **42**: p. 345-471.
2. Marshall, A.G. and R.P. Rodgers, *Petroleomics: The next grand challenge for chemical analysis*. Acc. Chem. Res., 2004. **37**(1): p. 53-59.
3. Czogalla, C.D. and F. Boberg, *Sulfur Compounds in Fossil Fuels*. Sulfur Reports, 1983. **3**(4): p. 121-167.
4. Kleinjan, W.E., A.d. Keizer, and A.J.H. Janssen, *Topics in Current Chemistry 230*, ed. R. Streudel. Vol. Berlin. 2003, Berlin: Springer Verlag. 167-188.
5. Damste, J.S.S., et al., *The Occurrence and Identification of Series of Organic Sulfur-Compounds in Oils and Sediment Extracts .2. Their Presence in Samples from Hypersaline and Non-Hypersaline Paleoenvironments and Possible Application as Source, Palaeoenvironmental and Maturity Indicators*. Geochim. Cosmochim. Acta, 1989. **53**(6): p. 1323-1341.
6. Damste, J.S.S., et al., *The Occurrence and Identification of Series of Organic Sulfur-Compounds in Oils and Sediment Extracts .1. A Study of Rozel Point Oil (USA)*. Geochim. Cosmochim. Acta, 1987. **51**(9): p. 2369-2391.
7. Cyr, T.D., et al., *A Homologous Series of Novel Hopane Sulfides in Petroleum*. Org. Geochem., 1986. **9**(3): p. 139-143.
8. Payzant, J.D., D.S. Montgomery, and O.P. Strausz, *Novel Terpenoid Sulfoxides and Sulfides in Petroleum*. Tetrahedron Lett., 1983. **24**(7): p. 651-654.
9. Schmid, J.C., J. Connan, and P. Albrecht, *Occurrence and Geochemical Significance of Long-Chain Dialkylthiacyclopentanes*. Nature, 1987. **329**(6134): p. 54-56.
10. Brassell, S.C., et al., *Isoprenoid Thiophenes - Novel Products of Sediment Diagenesis*. Nature, 1986. **320**(6058): p. 160-162.
11. Damste, J.S.S., et al., *Origin of Organic Sulfur Compounds and Sulphur-containing High Molecular Weight Substances in Sediments and Immature Crude Oils*. Adv. Org. Geochem., 1987. **13**(4-6): p. 593-606.
12. Barakat, A.O. and J. Rullkotter, *Origin of organic sulfur compounds in sediments from the Nordlinger Ries (Southern Germany)*. J. Petrol. Sci. Eng., 1999. **22**(1-3): p. 103-119.
13. Damste, J.S.S. and J.W. Leeuw, *Analysis, Structure and Geochemical Significance of Organically-Bound Sulfur in the Geosphere - State-of-the-Art and Future-Research*. Org. Geochem., 1990. **16**(4-6): p. 1077-1101.
14. Andersson, J.T., *Schwefel in Erdöl - ein giftiges Thema?* ChiuZ, 2004. **in Press**.
15. Asaoka, S., et al., *Asphaltene Cracking in Catalytic Hydrotreating of Heavy Oils .2. Study of Changes in Asphaltene Structure During Catalytic Hydroprocessing*. Ind. Eng. Chem. Proc. Dd, 1983. **22**(2): p. 242-248.
16. Babich, I.V. and J.A. Moulijn, *Science and technology of novel processes for deep desulfurization of oil refinery streams: A review*. Fuel, 2003. **82**(6): p. 607-631.
17. Environmental Protection Agency (EPA), <http://www.epa.gov/earth1/r6/6en/xp/lppapp6a.pdf>. 2004: USA.
18. Yung, K.Y., et al., *Catalytic solutions to new challenges in Residue Fluid Catalytic Cracking*, in *Catalysts Courier* - 53. 2003. p. -.
19. Boduszynski, M.M., *Composition of Heavy Petroleums .2. Molecular Characterization*. Energ. Fuels, 1988. **2**(5): p. 597-613.

20. Ma, X.L., K.Y. Sakanishi, and I. Mochida, *Hydrodesulfurization Reactivities of Various Sulfur-Compounds in Diesel Fuel*. Ind. Eng. Chem. Res., 1994. **33**(2): p. 218-222.
21. Houalla, M., et al., *Hydrodesulfurization of Methyl-Substituted Dibenzothiophenes Catalyzed by Sulfided Co-Mo-Gamma-Al₂O₃*. J. Catal., 1980. **61**(2): p. 523-527.
22. Macaud, M., A. Milenkovic, and E. Schulz, *Hydrodesulfurization of alkyl dibenzothiophenes: Evidence of highly unreactive aromatic sulfur compounds*. J. Catal., 2000. **193**(2): p. 255-263.
23. Ma, X.L., K. Sakanishi, and I. Mochida, *Hydrodesulfurization reactivities of various sulfur compounds in vacuum gas oil*. Ind. Eng. Chem. Res., 1996. **35**(8): p. 2487-2494.
24. Sapre, A.V., et al., *Hydrodesulfurization of Benzo[b]naphtho[2,3-d]thiophene Catalyzed by Sulfided CoO-MoO₃-Gamma-Al₂O₃ - the Reaction Network*. Aiche Journal, 1980. **26**(4): p. 690-694.
25. Ancheyta, J., et al., *Individual Hydrotreating of FCC Feed Components*. Energ. Fuels, 2004. **18**(4): p. 1001-1004.
26. Ostvold, G., *Characterization of Petroleum Residues by High-Performance Liquid-Chromatography*. J. Chromatogr., 1983. **282**(DEC): p. 413-422.
27. Sharma, B.K., S.L.S. Sarowha, and S.D. Bhagat, *Chromatographic characterization of high-boiling petroleum fractions*. J. Sep. Sci., 2003. **26**(18): p. 1657-1664.
28. IFP, *Petroleum Products separation of saturates, aromatics, resins and asphaltenes fractions liquid adsorption chromatography*. Inst. Francais Petrole, 2002. **Method IFP 9305**: p. 1-8.
29. Ramaswamy, V., et al., *Rapid Hydrocarbon Type Separation of Vacuum Residues*. Fres. Z. Anal. Chem., 1988. **332**(4): p. 358-361.
30. Artok, L., et al., *Structure and reactivity of petroleum-derived asphaltene*. Energ. Fuels, 1999. **13**(2): p. 287-296.
31. Artok, L., et al., *Structural characterization of asphaltene fraction from vacuum residue of Arabian crude mixture by spectroscopic and pyrolytic methods*. Sekiyu Gakkashi-J. Jap. Petrol. Inst., 1999. **42**(4): p. 206-214.
32. Herod, A.A., Y.Q. Zhuo, and R. Kandiyoti, *Size-exclusion chromatography of large molecules from coal liquids, petroleum residues, soots, biomass tars and humic substances*. J. Biochem. Bioph. Meth., 2003. **56**(1-3): p. 335-361.
33. Suelves, I., et al., *Chromatographic separations enabling the structural characterisation of heavy petroleum residues*. Fuel, 2003. **82**(1): p. 1-14.
34. Fujii, M., et al., *Measurements of asphaltenes in vacuum residues by laser desorption ionization mass spectroscopy*. Sekiyu Gakkaishi J. Jap. Petr. Inst., 2000. **43**(2): p. 149-156.
35. Deelchand, J.P., et al., *Planar chromatographic separation of petroleum residues and coal-derived liquids*. J. Chromatogr. A, 1999. **830**(2): p. 397-414.
36. Li, W., et al., *Thin-layer chromatography of pitch and a petroleum vacuum residue - Relation between mobility and molecular size shown by size-exclusion chromatography*. J. Chromatogr. A, 2004. **1024**(1-2): p. 227-243.
37. Karaca, F., et al., *The calibration of size exclusion chromatography columns: Molecular mass distributions of heavy hydrocarbon liquids*. Energ. Fuels, 2004. **18**(3): p. 778-788.

38. Herod, A.A., et al., *Size exclusion chromatography of soots and coal-derived materials with 1-methyl-2-pyrrolidinone as eluent: Observations on high molecular mass material*. *Energ. Fuels*, 2000. **14**(5): p. 1009-1020.
39. Buuhoi, N.P. and P. Jacquignon, *Sur Une Nouvelle Methode Chromatographique Pour La Separation De Composes Polycycliques Aromatiques Ou Heterocycliques*. *Experientia*, 1957. **13**(9): p. 375-376.
40. Diack, M., et al., *Analysis of Coal Hydroliquefaction Products (Semiaromatic Compounds) on a Picric Acid Column by Charge-Transfer Chromatography*. *Fuel Process. Tech.*, 1990. **24**: p. 151-156.
41. Felix, G. and C. Bertrand, *Hplc on Normal-Propyl Picryl Ether Silica-Gel*. *J. High Res. Chromatog.*, 1984. **7**(12): p. 714-715.
42. Kershaw, J.R. and K.J.T. Black, *Structural Characterization of Coal-Tar and Petroleum Pitches*. *Energ. Fuels*, 1993. **7**(3): p. 420-425.
43. Zander, M., *On the Nitrogen Containing Constituents of Coal-Tar Pitch*. *Fuel*, 1991. **70**(4): p. 563-565.
44. Nondek, L. and J. Malek, *Liquid-Chromatography of Aromatic-Hydrocarbons on a Chemically Bonded Stationary Phase of Charge-Transfer Type*. *J. Chromatogr.*, 1978. **155**(1): p. 187-190.
45. Jewell, D.M., *Preparative Trinitrofluorenone Charge-Transfer Chromatography of Petroleum Aromatics*. *Anal. Chem.*, 1975. **47**(12): p. 2048-2050.
46. Diack, M., et al., *Catalytic-Hydrogenation of Benzo(a) and Benzo(e)pyrenes - Analysis of the Hydrogenated Products by Charge-Transfer Chromatography and HPLC on Amino Bonded Phase*. *Chromatographia*, 1990. **30**(1-2): p. 24-34.
47. Holstein, W., *Donor-Acceptor Complex Chromatography - Tetrachlorophthalimidopropyl Silica, a New Bonded Stationary Phase for Separation of Coal-Liquefaction Products and Other Aromatic Mixtures by HPLC*. *Chromatographia*, 1981. **14**(8): p. 468-477.
48. Holstein, W. and H. Hemetsberger, *Donor-Acceptor Complex Chromatography (Dacc) 1. Introduction and Nomenclature*. *Chromatographia*, 1982. **15**(3): p. 186-190.
49. Holstein, W. and H. Hemetsberger, *Donor-Acceptor Complex Chromatography (Dacc) 2. Review of Papers*. *Chromatographia*, 1982. **15**(4): p. 251-258.
50. Wise, S.A., L.C. Sander, and W.E. May, *Determination of Polycyclic Aromatic-Hydrocarbons by Liquid-Chromatography*. *J. Chromatogr.*, 1993. **642**(1-2): p. 329-349.
51. Sander, L.C., M. Pursch, and S.A. Wise, *Shape selectivity for constrained solutes in reversed-phase liquid chromatography*. *Anal. Chem.*, 1999. **71**(21): p. 4821-4830.
52. Ternan, M., et al., *Coprocessing - Elemental and Molecular-Weight Distributions in Unconverted Vacuum Residues*. *Energ. Fuels*, 1995. **9**(6): p. 1011-1022.
53. Friedman, L., D.L. Fishel, and H. Shechter, *Oxidation of Alkylarenes with Aqueous Sodium Dichromate . A Useful Method for Preparing Mono- and Polyaromatic Carboxylic Acids*. *J. Org. Chem.*, 1965. **30**(5): p. 1453-&.
54. Barakat, A.O. and J. Rullkotter, *Product distribution from oxidative degradation of sulphur-rich kerogens from the Nordlinger Ries (southern Germany)*. *Fuel*, 1998. **77**(1-2): p. 85-94.
55. Kasai, M. and H. Ziffer, *Ruthenium Tetroxide Catalyzed Oxidations of Aromatic and Heteroaromatic Rings*. *J. Org. Chem.*, 1983. **48**(14): p. 2346-2349.

56. Carlsen, P.H.J., et al., *A Greatly Improved Procedure for Ruthenium Tetraoxide Catalyzed Oxidations of Organic-Compounds*. J. Org. Chem., 1981. **46**(19): p. 3936-3938.
57. Winans, R.E., et al., *Characterization of Heteroaromatics in Coals and Coal Products*. Abstr. Pap. Am. Chem. Soc., 1980. **179**(MAR): p. 11-Petr.
58. Warton, B., R. Alexander, and R.I. Kagi, *Characterisation of the ruthenium tetroxide oxidation products from the aromatic unresolved complex mixture of a biodegraded crude oil*. Org. Geochem., 1999. **30**(10): p. 1255-1272.
59. Schluter, E.C., E.P. Parry, and G. Matsuyama, *Determination of Sulfur in Petroleum Products by Hydrogenation*. Anal. Chem., 1960. **32**(3): p. 413-417.
60. Curtis, J.L.S. and M.O. Baker, *Determination of Unsaturation in Sulfur-Containing Petroleum Fractions by Quantitative Hydrogenation*. Anal. Chem., 1970. **42**(2): p. 278-&.
61. Thomson, J.S., J.B. Green, and T.B. McWilliams, *Determination of sulfides and thiols in petroleum distillates using solid-phase extraction and derivatization with pentafluorobenzoyl chloride*. Energ. Fuels, 1997. **11**(4): p. 909-914.
62. Green, T.K., et al., *Structural Characterization of Sulfur-Compounds in Petroleum by S-Methylation and C-13 Nmr-Spectroscopy*. Energ. Fuels, 1994. **8**(1): p. 244-248.
63. Pailer, M. and V. Hlozek, *Studies on High-Sulfur Shale Oils*, .7. Monatsh. Chem., 1975. **106**(6): p. 1259-1284.
64. Rullkotter, J. and W. Michaelis, *The Structure of Kerogen and Related Materials - a Review of Recent Progress and Future-Trends*. Org. Geochem., 1990. **16**(4-6): p. 829-852.
65. Kelemen, S.R., G.N. George, and M.L. Gorbaty, *Direct Determination and Quantification of Sulfur Forms in Heavy Petroleum and Coals .1. The X-Ray Photoelectron-Spectroscopy (Xps) Approach*. Fuel, 1990. **69**(8): p. 939-944.
66. Gorbaty, M.L., G.N. George, and S.R. Kelemen, *Direct Determination and Quantification of Sulfur Forms in Heavy Petroleum and Coals .2. The Sulfur-K Edge X-Ray Absorption-Spectroscopy Approach*. Fuel, 1990. **69**(8): p. 945-949.
67. George, G.N., et al., *Direct Determination and Quantification of Sulfur Forms in Coals from the Argonne Premium Sample Program*. Energ. Fuels, 1991. **5**(1): p. 93-97.
68. Artoc, L.S., Y.; Hirose, Y.; Murata, S.; Nomura, M., *Structural characterization of asphaltene fraction from vacuum residues of Arabian crude mixture by spectroscopic and pyrolytic methods*. Sekiyu Gakkashi-J. Jap. Petrol. Inst., 1999. **42**(4): p. 206-14.
69. Larsen, B.S., et al., *Evaluations of Heavy Constituents in Fractions of Petroleum Residues Using Gel-Permeation and Field Desorption Mass-Spectrometry*. Anal. Chem., 1986. **58**(6): p. 1088-1091.
70. Hsu, C.S. and K. Qian, *High-Boiling Aromatic-Hydrocarbons Characterized by Liquid-Chromatography Thermospray Mass-Spectrometry*. Energ. Fuels, 1993. **7**(2): p. 268-272.
71. Pace, C.M. and L.D. Betowski, *Measurement of High-Molecular-Weight Polycyclic Aromatic Hydrocarbons in Soils by Particle-Beam High-Performance Liquid-Chromatography Mass*. J. Am. Soc. Mass Spectr., 1995. **6**(7): p. 597-607.
72. Anacleto, J.F., et al., *Comparison of Liquid-Chromatography Mass-Spectrometry Interfaces for the Analysis of Polycyclic Aromatic Compounds*. Anal. Chem., 1995. **67**(22): p. 4145-4154.

73. Lafleur, A.L., et al., *Characterization of flame-generated C-10 to C-160 polycyclic aromatic hydrocarbons by atmospheric-pressure chemical ionization mass spectrometry with liquid introduction via heated nebulizer interface*. J. Am. Soc. Mass Spectr., 1996. **7**(3): p. 276-286.
74. Marvin, C.H., et al., *Multi-dimensional liquid chromatography coupled with atmospheric pressure chemical ionization LC-MS for profiling high molecular mass polycyclic aromatic hydrocarbons*. Polycyclic Aromatic Compounds, 1996. **9**(1-4): p. 193-200.
75. Thomas, D., et al., *Application of Reversed-Phase Liquid-Chromatography with Atmospheric-Pressure Chemical-Ionization Tandem Mass-Spectrometry to the Determination of Polycyclic Aromatic Sulfur Heterocycles in Environmental-Samples*. J. Mass Spec., 1995. **30**(7): p. 1034-1040.
76. Rudzinski, W.E., K. Zhou, and X.M. Luo, *Mass spectrometric characterization of organosulfur compounds using palladium(II) as a sensitivity-enhancing reagent*. Energ. Fuels, 2004. **18**(1): p. 16-21.
77. Rudzinski, W.E., L. Oehlers, and Y. Zhang, *Tandem mass spectrometric characterization of commercial naphthenic acids and a Maya crude oil*. Energ. Fuels, 2002. **16**(5): p. 1178-1185.
78. Fenn, J.B., et al., *Electrospray Ionization - Principles and Practice*. Mass Spectrom. Rev., 1990. **9**(1): p. 37-70.
79. Roussis, S.G. and R. Proulx, *Molecular weight distributions of heavy aromatic petroleum fractions by Ag⁺ electrospray ionization mass spectrometry*. Analytical Chemistry, 2002. **74**(6): p. 1408-1414.
80. Van Berkel, G.J. and K.G. Asano, *Chemical Derivatization for Electrospray-Ionization Mass-Spectrometry .2. Aromatic and Highly Conjugated Molecules*. Anal. Chem., 1994. **66**(13): p. 2096-2102.
81. Rudzinski, W.E., Y. Zhang, and X.M. Luo, *Mass spectrometry of polyaromatic sulfur compounds in the presence of palladium(II)*. J. Mass Spec., 2003. **38**(2): p. 167-173.
82. Lumpkin, H.E. and B.H. Johnson, *Identification of Compound Types in a Heavy Petroleum Gas Oil*. Anal. Chem., 1954. **26**(11): p. 1719-1722.
83. Lumpkin, H.E., *Determination of Saturated Hydrocarbons in Heavy Petroleum Fractions by Mass Spectrometry*. Anal. Chem., 1956. **28**(12): p. 1946-1948.
84. Lumpkin, H.E., *Use of Low Voltage Techniques in High-Molecular-Weight Mass Spectrometry*. Anal. Chem., 1957. **29**(9): p. 1379-1379.
85. Lumpkin, H.E., *Analysis of Trinuclear Aromatic Petroleum Fraction by High Resolution Mass Spectrometry*. Anal. Chem., 1964. **36**(13): p. 2399-&.
86. Rodgers, R.P., et al., *Resolution, elemental composition, and simultaneous monitoring by Fourier transform ion cyclotron resonance mass spectrometry of organosulfur species before and after diesel fuel processing*. Anal. Chem., 1998. **70**(22): p. 4743-50.
87. Guan, S.H., A.G. Marshall, and S.E. Scheppele, *Resolution and chemical formula identification of aromatic hydrocarbons and aromatic compounds containing sulfur, nitrogen, or oxygen in petroleum distillates and refinery streams*. Anal. Chem., 1996. **68**(1): p. 46-71.
88. Hughey, C.A., R.P. Rogers, and A.G. Marshall, *Resolution of 11 000 compositionally distinct components in a single Electrospray ionization Fourier transform ion cyclotron resonance mass spectrum of crude oil*. Anal. Chem., 2002. **74**(16): p. 4145-4149.

89. Schaub, T.M., et al., *High-resolution field desorption/ionization Fourier transform ion cyclotron resonance mass analysis of nonpolar molecules*. Anal. Chem., 2003. **75**(9): p. 2172-2176.
90. Qian, K.N., et al., *Resolution and identification of elemental compositions for more than 3000 crude acids in heavy petroleum by negative-ion microelectrospray high-field Fourier transform ion cyclotron resonance mass spectrometry*. Energ. Fuels, 2001. **15**(6): p. 1505-1511.
91. Wu, Z.G., et al., *Resolution of 10,000 compositionally distinct components in polar coal extracts by negative-ion electrospray ionization Fourier transform ion cyclotron resonance mass spectrometry*. Energ. Fuels, 2003. **17**(4): p. 946-953.
92. Qian, K., et al., *Reading chemical fine print: Resolution and identification of 3000 nitrogen-containing aromatic compounds from a single electrospray ionization Fourier transform ion cyclotron resonance mass spectrum of heavy petroleum crude oil*. Energ. Fuels, 2001. **15**(2): p. 492-498.
93. Miyabayashi, K., et al., *Structure characterization of petroleum vacuum residues by in-beam EI Fourier transform ion cyclotron resonance mass spectrometry*. Int. J. Mass Spec., 2002. **221**(2): p. 93-105.
94. Kressmann, S., *personal communication*, H. Müller, Editor. 2001: Muenster. p. Meeting.
95. Later, D.W., et al., *Chemical Class Separation and Characterization of Organic-Compounds in Synthetic Fuels*. Anal. Chem., 1981. **53**(11): p. 1612-1620.
96. Kressmann, S. and F.X. Haulle, *Elements on refractory sulfur compounds after hydrotreatment of vacuum residue*. Abstr. Pap. Am. Chem. Soc., 2001. **221**: p. U529-U529.
97. Andersson, J.T., et al., *Synthesis of seven trimethyldibenzothiophenes*. Polycyclic Aromatic Compounds, 2001. **18**(3): p. 351-360.
98. Djerassi, C. and C.R. Scholz, *Brominations with Pyridine Hydrobromide Perbromide*. J. Am. Chem. Soc., 1948. **70**(1): p. 417-418.
99. Jackson, S.N. and K.K. Murray, *Infrared matrix-assisted laser desorption/ionization of polycyclic aromatic hydrocarbons with a sulfolane matrix*. Rap. Com. Mass Spec., 2001. **15**(16): p. 1448-1452.
100. Balasanmugam, K., S.K. Viswanadham, and D.M. Hercules, *Characterization of Polycyclic Aromatic-Hydrocarbons by Laser Mass-Spectrometry*. Anal. Chem., 1986. **58**(6): p. 1102-1108.
101. Sullivan, R.F., M.M. Boduszynski, and J.C. Fetzer, *Molecular-Transformations in Hydrotreating and Hydrocracking*. Energ. Fuels, 1989. **3**(5): p. 603-612.
102. McKinney, D.E., et al., *High-Performance Liquid-Chromatography (Hplc) of Coal-Liquefaction Process Streams Using Normal-Phase Separation with Diode-Array Detection*. Energ. Fuels, 1995. **9**(1): p. 90-96.
103. Godlewicz, M., *A New Method for the Separation of Hydrocarbons by Selective Adsorption*. Nature, 1949. **164**(4183): p. 1132-1133.
104. Jadaud, P., M. Caude, and R. Rosset, *Main Parameters Governing the Retention of Polynuclear Aromatic-Hydrocarbons on Tetrachlorophthalimidopropyl-Bonded Silica*. J. Chromatogr., 1988. **439**(2): p. 195-211.
105. Eppert, G. and I. Schinke, *Liquid-Chromatographic Separation of Classes of Higher Boiling Aromatic Compounds by Means of Compact Phases That Form Charge-Transfer Complexes*. J. Chromatogr., 1983. **260**(2): p. 305-327.

106. Grizzle, P.L. and J.S. Thomson, *Liquid-Chromatographic Separation of Aromatic-Hydrocarbons with Chemically Bonded (2,4-Dinitroanilinopropyl)Silica*. Anal. Chem., 1982. **54**(7): p. 1071-1078.
107. Welch, K.J. and N.E. Hoffman, *Physicochemical Properties of Electron-Acceptor Stationary Phases in Liquid-Chromatography*. J. Chromatogr., 1992. **591**(1-2): p. 75-88.
108. Müller, H., *Gel Permeation Chromatographic Separation of Three-Ring Sulfur Aromatics*, in *Department of Analytical Chemistry*. 2000, Westfälische Wilhelms-Universität: Muenster. p. 85.
109. Andersson, J.T., *Polycyclic Aromatic Sulfur Heterocycles .I. Use of Hydrogen-Peroxide Oxidation for the Group Separation of Polycyclic Aromatic Hydrocarbons and Their Sulfur Analogs*. Int. J. Environ. Anal. Chem., 1992. **48**(1): p. 1-15.
110. Andersson, J.T., *Retention Properties of a Palladium Chloride Silica Sorbent for the Liquid-Chromatographic Separation of Polycyclic Aromatic Sulfur Heterocycles*. Anal. Chem., 1987. **59**(17): p. 2207-2209.
111. Pyell, U., S. Schober, and G. Stork, *Ligand-exchange chromatographic separation of polycyclic aromatic hydrocarbons and polycyclic aromatic sulfur heterocycles on a chelating silica gel loaded with palladium(II) or silver(I) cations*. Fres. Z. Anal. Chem., 1997. **359**(7-8): p. 538-541.
112. Schade, T., B. Roberz, and J.T. Andersson, *Polycyclic aromatic sulfur heterocycles in desulfurized diesel fuels and their separation on a novel palladium(II)-complex stationary phase*. Polycyclic Aromatic Compounds, 2002. **22**(3-4): p. 311-320.
113. Andersson, J.T. and T. Schade, *Separation of sulfur heterocycles*. Abstr. Pap. Am. Chem. Soc., 2001. **221**: p. U517-U518.
114. Andersson, J.T., T. Schade, and H. Muller, *Separation of aromatic sulfur heterocycles from aromatic hydrocarbons by use of a palladium ion complex*. Abstr. Pap. Am. Chem. Soc., 2002. **224**: p. U574-U575.
115. Popl, M., J. Fahnrich, and M. Stejskal, *Adsorption Effect in GPC Separation of Polycyclic Aromatic Hydrocarbons*. J. Chromatogr. Sci., 1976. **14**(11): p. 537-540.
116. Ehring, H., et al., *Photochemical versus thermal mechanisms in matrix-assisted laser desorption/ionization probed by back side desorption*. Rap. Com. Mass Spec., 1996. **10**(7): p. 821-824.
117. Zenobi, R. and R. Knochenmuss, *Ion formation in MALDI mass spectrometry*. Mass Spec. Rev., 1998. **17**(5): p. 337-366.
118. Takino, M., et al., *Determination of polycyclic aromatic hydrocarbons by liquid chromatography-electrospray ionization mass spectrometry using silver nitrate as a post-column reagent*. J. Chromatogr. A, 2001. **928**(1): p. 53-61.
119. Hughey, C.A., et al., *Kendrick mass defect spectrum: A compact visual analysis for ultrahigh-resolution broadband mass spectra*. Anal. Chem., 2001. **73**: p. 4676.
120. Kendrick, E., *A Mass Scale Based on CH₂=14.0000 for High Resolution Mass Spectrometry of Organic Compounds*. Anal. Chem., 1963. **35**(13): p. 333-40.
121. Qian, K.N. and C.S. Hsu, *Molecular-Transformation in Hydrotreating Processes Studied by Online Liquid-Chromatography Mass-Spectrometry*. Anal. Chem., 1992. **64**(20): p. 2327-2333.
122. Hsu, C.S., K.N. Qian, and Y.N.C. Chen, *An Innovative Approach to Data-Analysis in Hydrocarbon Characterization by Online Liquid-Chromatography Mass-Spectrometry*. Anal. Chim. Acta, 1992. **264**(1): p. 79-89.

123. Andersson, J.T., *Liquid-Chromatographic Determination of Planar Aromatic Sulfur-Compounds in Crude Oil - Comment*. J. Chromatogr., 1991. **585**(2): p. 376-377.
124. Acheson, R.M. and D.R. Harrison, *Synthesis, Spectra, and Reactions of Some S-Alkylthiophenium Salts*. J. Chem. Soc. C, 1970. **13**: p. 1764-1784.
125. Boberg, F.B., W.; Mußhoff, D., *Schwefelverbindungen des Erdöls XVI Dibenzothiophene mit einem unverzweigten C1-C5-Alkylrest*. Phosphorus sulfur Silicon, 1992. **72**: p. 13-31.
126. Pailer, M. and H. Begutter, *Studies of Shale Oils with High Sulfur Content .4*. Monatsh. Chem., 1973. **104**(1): p. 297-311.
127. Pailer, M. and Bernerfe.L, *Studies of Sulfur-Rich Shale Oils .6*. Monatsh. Chem., 1973. **104**(2): p. 339-351.
128. Ma, X.L., et al., *Determination of sulfur compounds in non-polar fraction of vacuum gas oil*. Fuel, 1997. **76**(4): p. 329-339.
129. Pailer, M. and H. Grunhaus, *Studies of Shale Oils with High Sulfur Content .5*. Monatsh. Chem., 1973. **104**(1): p. 312-337.
130. Coleman, H.J., et al., *Compositional Studies of a High-Boiling 370-535 Degrees C Distillate from Prudhoe-Bay, Alaska, Crude Oil*. Anal. Chem., 1973. **45**(9): p. 1724-1737.
131. Charrie-Duhaut, A., et al., *Terpenoid-derived sulfides as ultimate organic sulfur compounds in extensively desulfurized fuels*. Angew. Chem.- Int. Ed., 2003. **42**(38): p. 4646-4649.
132. Ehrenberger, F., *Quantitative Elementaranalyse*. XXI ed. 1991, Weinheim: VCH Verlag Chemie. 436-440.

Lebenslauf

Hendrik Müller

geboren am 29.10.1974 in Freiburg i. Brg.

ledig

Eltern:

Harald Müller,

Ursula Breer, geb. Korndörfer

Schulbildung: Mariengrundschohle von 1981 bis 1985 in Senden
Wilhelm Hittorf Gymnasium von 1985 bis 1994 in Münster

Hochschulreife: Abitur am 16.5.1994 in Münster

Studium: Chemie auf Diplom
an der Westfälischen Wilhelms-Universität Münster von
10.1994 bis 11.2000

Diplom: Diplom im Fach Chemie am 23.11.2000 an der Westfälischen
Wilhelms-Universität

Promotionsstudiengang: Chemie

Tätigkeiten: studentische Hilfskraft vom 7.6.2000 bis 31.10.2000
wissenschaftliche Hilfskraft vom 1.11.2000 bis 30.6.2001
wissenschaftlicher Mitarbeiter von 1.7.2001 bis 30.9.2004

Beginn der Dissertation: 1.2001, Institut für Anorganische und Analytische Chemie
unter Betreuung von Prof. Dr. J. T. Andersson

.....